

CHAPTER

7

Abutments

7.1 TOP OF ABUTMENT DETAILS AND TREATMENT

Various types of abutments are discussed in section 1.3, and are illustrated in Figures 1–7 through 1–10. Abutment configurations and details for integral and semi-integral construction are shown in Figures 1–11 and 1–12, and are discussed further in subsequent sections.

Top of abutment details are influenced by the conditions of the approach pavement, the type of superstructure, and the expansion length, including the type of bearings used at this location. The top of the abutment backwall that supports the approach slab may be constructed level, unless excessive skew and superelevated roadway make this impracticable. A standard 20 foot long approach pavement 14½ inches thick will induce a dead load reaction of approximately 3 kips per foot of width. This reaction should not be included in the design if its effect is to reduce the load on the piles.

Figure 7–1 shows section through top of abutment. This detail may be used when the approach roadway is a nonrigid type, such as gravel, crushed stone, or low type bituminous mix, and the expansion length is less than about 150 feet. The one-half-inch premoulded joint filler allows free movement of the superstructure, and allows end rotation as the structure is deflected under load. A sealed joint also excludes deck drainage through the opening.

When the approach surface is a rigid type (concrete slab), the end-of-slab treatment at an expansion abutment may be as shown in Figure 7–2, which shows abutment details for superstructures of steel framing with concrete slab. For all concrete superstructures or precast prestressed decks, the abutment configuration at the top is as shown in detail A.

Future approach pavement: When constructed, premoulded joint filler shall be placed between approach pavement & structure.

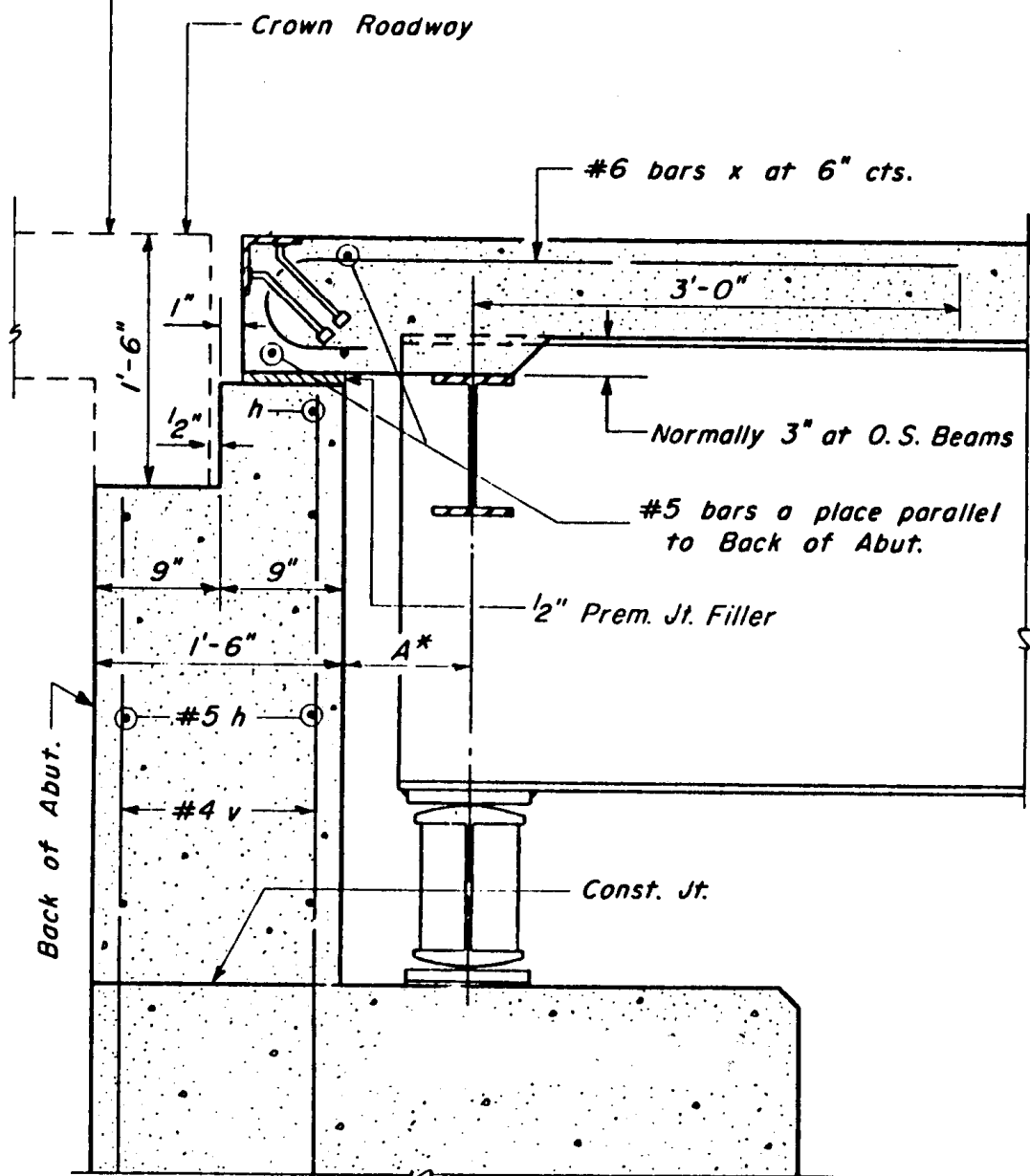


Figure 7-1 Details of abutment top, nonrigid approach roadway (Illinois DOT).

As shown in Figure 7-2, a preformed joint seal is usually inserted between the two expansion angles to seal the joint and inhibit drainage through the opening. The limitations and practical range of open joints formed with steel angles are dictated by the expansion length and the skew angle of the bridge. Where these criteria are exceeded, the joint may be formed with a sliding plate or a finger plate. State standards usually cover these aspects in detail.

When a neoprene expansion joint is placed at the opening formed by the steel angles, an anchorage load will be exerted against the abutment. This thrust is induced as

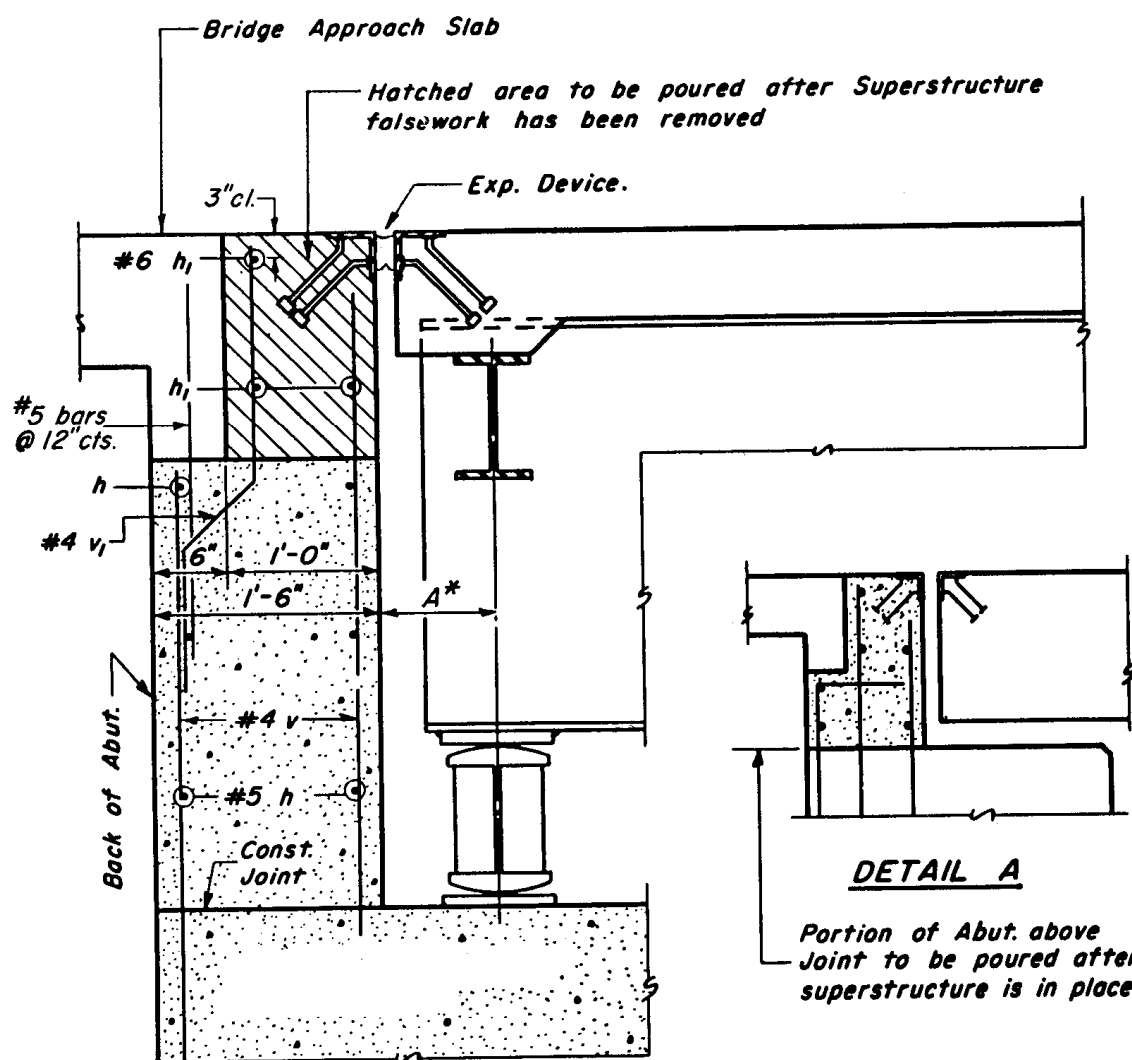


Figure 7-2 Details of abutment top, rigid approach roadway (Illinois DOT).

the bridge expands, and should be applied at the point of connection to the abutment wall. The manner in which this lateral force is resisted is open to conjecture, and consideration should be given to the type of approach pavement as well as to the type of expansion bearing. The most logical theory is that this force is created as the neoprene seal is squeezed between the two steel angles when the bridge expands. It may be resisted by friction between the approach slab and the soil underneath, but until this assumption is warranted it may continue to act against the abutment wall. The following guideline is provided for the magnitude of this force:

Size of neoprene joint: 2 to 4 inches

Force (kips/ft) = 1.3

$6\frac{1}{2}$ inches

1.8

When a neoprene expansion joint is specified at one abutment or at one end of the superstructure unit, it should also be specified at the other abutment or end of the same unit, in order to balance the thermal forces acting on the fixed pier. If this arrangement is not provided, the thermal forces specified above should be applied to the fixed bearing.

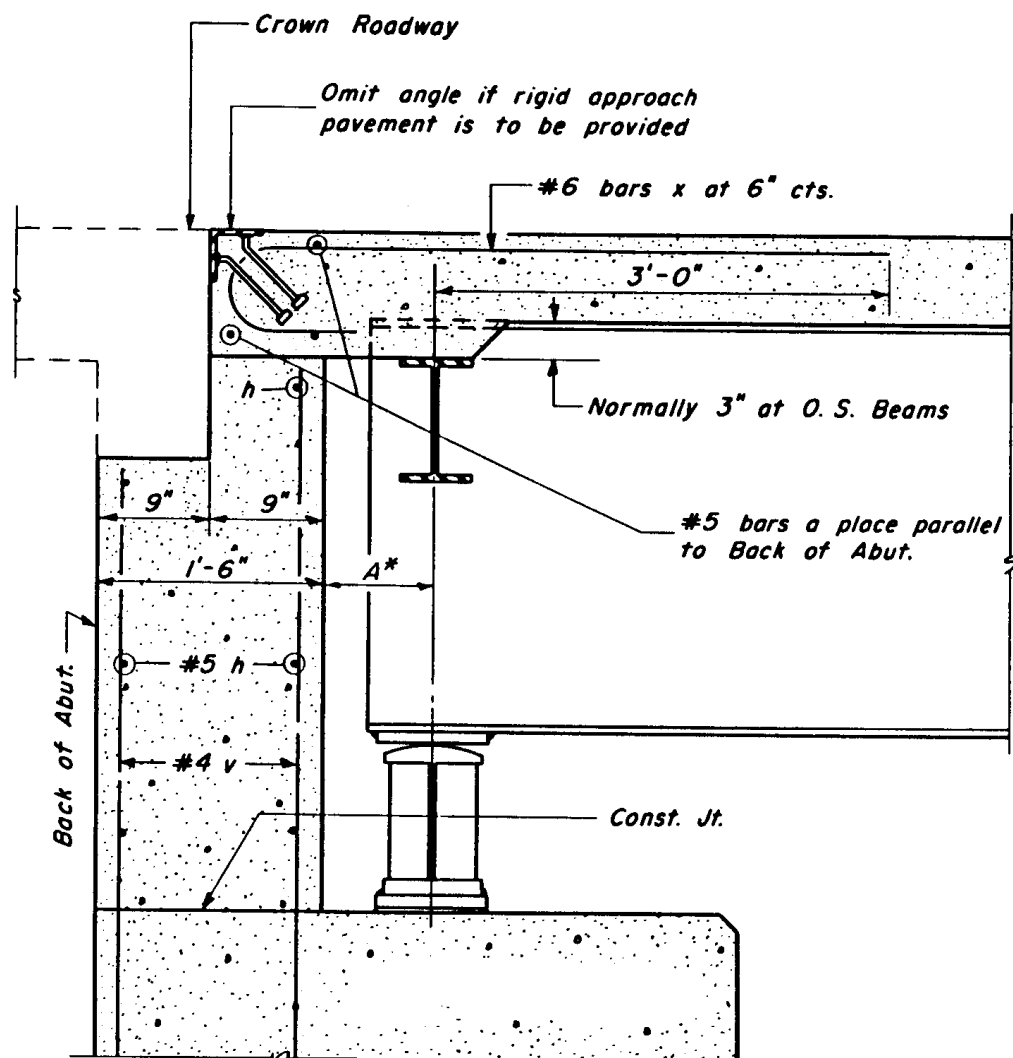


Figure 7-3 Detail of abutment top, fixed bearing (Illinois DOT).

With fixed bearings at the abutment, expansion joints in the deck are not necessary. In this case the top of the abutment can be detailed as shown in Figure 7-3. This detail is suitable with all types of approach surfaces, but it should be noted that it does not constitute an integral abutment.

The dimension A^* depends mainly on the skew angle and the width of the bottom flange plate, which also determines the width of the bearing plate. An edge distance of 4 inches between the corner point of the steel beam flange and the front face of the abutment wall usually is specified and provides the additional criterion. These considerations determine the bridge seat width, hence the dimensions of the abutment.

7.2 PILE BENT (STUB) ABUTMENTS, DESIGN CONSIDERATIONS

A typical pile bent abutment is shown in Figure 1-8. The dimensions of the height and width are minimum and may be increased to satisfy the layout criteria. A berm is provided in front of the bent, with a minimum clearance 1.75 feet below the underside of

the superstructure. Note that this layout will accommodate bearing devices 13 to 14 inches high, usually of the rocker or roller type.

Pile spacing. As a rule of thumb, and for preliminary estimates, the design may select n piles in the front row (R_2) and $n+1$ piles in the back row (R_1) at 8-foot maximum alternate centers. The dimensions B and C are established after the overall bent width is known, and are proportioned so that the pile loads between the back and front row are as equal as possible.

Design loads. The following loads should be applied to produce maximum effects.

1. Dead load of pile bent.
2. Dead load reaction from superstructure.
3. Dead load of approach slab (if an approach slab is to be provided).
4. Earth pressure on the back of the pile bent. This should have a pattern and magnitude compatible with the expected movement, or it may be stipulated by applicable standards as an equivalent fluid pressure. This pressure should be used with all combinations of loading.
5. Live load (HS truck or lane loading). This may be placed either on the bridge (reaction transmitted through the bearing) or on the approach slab (reaction transmitted through the backwall).
6. Live load surcharge, to be added on the lateral earth pressure if an approach slab is not provided, and coincident with live load reaction from the superstructure. Usually local standards stipulate a surcharge of 2 feet (about 230 lb/ft²), which is substantially close to the surcharge of 0.21 kips/ft² used in the design example of section 6.9 by taking the tributary area of a truck load.
7. Thermal forces. These may be as specified in other sections where applicable. There may also be a temperature force applied as rolling friction at the expansion bearing, but may be neglected since it will act opposite to the earth pressure.

Referring to Figure 1-8, the total load carried by each row of piles may be assumed to be the static reactions R_1 and R_2 acting on the bottom of the cap. Hence, the load on piles is

$$\text{Back Row Pile Load} = \frac{R_{1(\max)}}{n+1} \quad (7-1)$$

$$\text{Front Row Pile Load} = \frac{R_{2(\max)}}{n} \quad (7-2)$$

Deflections or lateral movement of pile bents may be critical if joints can close, causing unwarranted forces to be induced in the superstructure and eventually transferred to the end bent as additional passive resistance. Although the pile bent shown in Figure 1-8 does not have a high degree of stiffness, resistance to deflection or translation is helped by the end wing walls and the battered piles. Pile bents with fixed bearings should also be designed for longitudinal forces.

7.3 CLOSED (FULL) ABUTMENTS, DESIGN CONSIDERATIONS

A typical section of a closed abutment is shown in Figure 1–9. Reinforcement details and design pressures represent applicable local standards. For this condition, the superstructure is anchored as shown. By placing the top dowels near the front face of the abutment, the end restraint is essentially removed and the superstructure can rotate at the ends with minimum resistance. The abutment wall is therefore assumed to have pinned top. The base of the abutment wall may be designed as pinned, partially fixed, or fixed. The two most usual conditions are shown in Figure 7–4(a) and (b) for free and fixed bottom, respectively. The main wall is subjected to the same forces as the pile bent, discussed in the foregoing section. Note that lateral earth pressure and surcharge load pressure are combined into one diagram.

If p and p_1 is the unit earth pressure at the top and bottom of the wall, respectively, and h is the wall height as shown, bending moment equations may be derived for the free and the fixed bottom condition.

Both Ends Free. From Figure 7–4 (a), the reactions are obtained as

$$R_u = \frac{1}{6}(p_1 + 2p)h \quad \text{and} \quad R_1 = \frac{1}{6}(2p_1 + p)h \quad (7-3)$$

The point of zero shear is also the point of maximum moment, and is located at distance x_1 from the top given by

$$x_1 = \frac{p}{p_1 - p} \left[-1 + \sqrt{1 + \frac{1}{3} \left(\frac{p_1}{p} + 2 \right) \left(\frac{p_1}{p} - 1 \right)} \right] h \quad (7-4)$$

The maximum bending moment at distance x_1 is

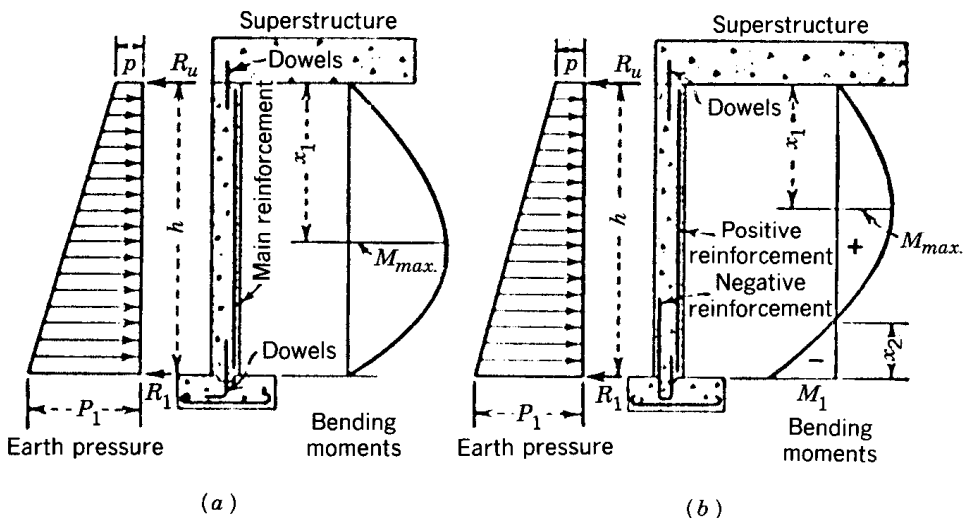


Figure 7-4 Abutment wall supported at top; (a) wall freely supported at bottom; (b) wall fixed at bottom.

$$M_{\max} = \frac{1}{18} \frac{\frac{x_1}{h} \left(3 \frac{p}{p_1 - p} + 2 \frac{x_1}{h} \right)}{2 \frac{p}{p_1 - p} + \frac{x_1}{h}} (p_1 + 2p) h^2 \quad (7-5)$$

Both Ends Fixed. Referring to Figure 7-4(b), the reactions are computed as

$$R_u = \frac{1}{40} (4p_1 + 11p)h \quad \text{and} \quad R_1 = \frac{1}{40} (16p_1 + 9p)h \quad (7-6)$$

Likewise, the point of zero shear is the point of maximum (positive) moment, and is located at distance x_1 from the top given by

$$x_1 = \frac{p}{p_1 - p} \left[-1 + \sqrt{1 + \frac{1}{20} \left(11 + 4 \frac{p_1}{p} \right) \left(\frac{p_1}{p} - 1 \right)} \right] h \quad (7-7)$$

The maximum positive moment at distance x_1 is

$$M_{\max} = \frac{1}{120} \frac{\frac{x_1}{h} \left(3 \frac{p}{p_1 - p} + 2 \frac{x_1}{h} \right)}{2 \frac{p}{p_1 - p} + \frac{x_1}{h}} (11p + 4p_1)h^2 \quad (7-8)$$

The negative moment at the bottom (fixed end) may be computed from

$$M_1 = -\frac{1}{120} (7p + 8p_1)h^2 \quad (7-9)$$

and the point of contraflexure is at distance x_2 from the bottom, given by

$$x_2 = \frac{p}{p_1 - p} \left[\left(5 + \frac{p_1}{p} \right) - 6 \sqrt{1 + \frac{1}{240} \left(11 + 4 \frac{p_1}{p} \right) \left(\frac{p_1}{p} - 1 \right)} \right] h \quad (7-10)$$

Wall footing. For the abutment wall supported freely at the bottom, the footing is subject to vertical reactions from the superstructure, the weight of the structure and its footing, and the weight of fill placed on the interior part of the footing. The horizontal reaction due to lateral loads at the bottom is resisted by friction at the footing-soil interface and by a partial passive pressure, if certain conditions are satisfied (see also foregoing sections).

When the wall is fixed at the bottom, in addition to the loads and forces mentioned above, the footing is subjected to a moment M_1 transferred to it by the fixity of the abutment wall. Since overturning is not a design condition for either case (a) or (b) of Figure 7-4, the footing dimensions and projection beyond the wall face are determined to best balance the resulting soil pressure.

Earth pressure. Simple spans supported on closed abutments may be fixed at both supports when the back-to-back of abutment dimension does not exceed 45 feet. With both supports fixed, the abutments should be designed as restrained top and bottom. This implies that both top and bottom are restrained against movement either into or away from the backfill. Therefore, the at-rest pressure is the type suitable for this condition. For a well-compacted backfill of granular material it is reasonable to use $K_o = 0.5$, and unit weight $\gamma = 120 \text{ lb/ft}^3$. The pressure p at the top of the wall, shown in Figure 7-4, is the result of a surcharge (usually 2 feet) with the live load placed on the approach pavement. Friction and cohesion behind the wall may be disregarded for simplicity. The foregoing assumptions result in an equivalent fluid pressure $0.5 \times 120 = 60 \text{ lb}$. The reinforcement requirements shown in Figure 1-9 are based on a wall with both ends free (simple span) and an equivalent 50 lb fluid pressure.

An adequate drainage system should be provided behind the abutment wall, its function being to prevent water pressures from developing behind the wall.

7.4 GRAVITY AND THE SEMI-GRAVITY ABUTMENTS, DESIGN CONSIDERATIONS

When the bridge length exceeds the span for which expansion provisions are not needed (usually 40 to 45 ft), the abutments may have a fixed bearing at one end and an expansion bearing at the other. For this situation, both closed abutments must be designed as free cantilevers.

The design requirements of full abutments with unrestrained tops are essentially the same as for gravity and semi-gravity walls, discussed in detail in section 6.6. The abutment structure must be designed to resist overturning ($FS \geq 2.0$), and sliding ($FS \geq 1.5$). Dead and live loads are assumed uniformly distributed over the length of the abutment between expansion joints.

Except for gravity abutments, at least 1/8-inch of horizontal reinforcement per foot of height should be provided near exposed surfaces not otherwise reinforced to resist the formation of temperature and shrinkage cracks.

Drainage and backfilling. The backfill materials behind abutments should be free draining, nonexpansive soil, properly drained by a suitable system. Cohesive backfills are difficult to compact. Walls backfilled with cohesive soils should not be designed for active earth pressures, even if large movements are tolerable, because cohesive soils tend to creep. Thus, walls with cohesive backfills designed for active earth pressure will continue to move gradually and indefinitely, especially when the backfill is soaked by rain or by rising groundwater. In this case, the abutments must be designed for pressures between active and at rest.

In addition to the loads mentioned for gravity walls, abutments must be designed to withstand wind, longitudinal forces, centrifugal forces, and earthquake loads according to AASHTO Art. 3.2.1 or to LRFD Article 11.6.

7.5 ABUTMENTS ON MECHANICALLY STABILIZED EARTH WALLS

Abutment footings are proportioned to meet sliding and overturning criteria discussed in the foregoing sections. These members should also be designed to satisfy the maximum uniform bearing pressures using an effective width of foundation ($B - 2e$) where

B = width of retaining wall foundation, and e = eccentricity of load from center line of foundation (see also Figure 7-5).

Below the abutment footing, the MSE wall must be designed for any additional loads imposed by the footing pressure and supplemental earth pressure resulting from lateral loads applied at the bridge seat and from the backwall. The footing load may be assumed to be uniformly distributed over the effective foundation width ($L - 2e$) at the base of the footing, and to be distributed with depth using a slope 2:1 with the vertical. The supplemental loads may be applied as shears along the bottom of the footing, diminishing uniformly with depth to a point on the face of the wall equal to twice the effective width of the abutment footing.

Horizontal stresses in abutment reinforced zones may be computed by superposition as follows (see also Figure 7-5):

$$\sigma_{H(\max)} = \gamma_p (\sigma_{v1} K + \sigma_{v2} K_a + \sigma_H) \quad (7-11)$$

where σ_H = lateral pressure due to surcharge; σ_{v1} = vertical (overburden) soil stress; σ_{v2} = vertical soil stress due to footing load; K = earth pressure coefficient; K_a = active earth pressure coefficient; and γ_p = load factor for earth pressure.

The factored horizontal force P_i acting on the reinforcement at any reinforcement level may be computed as

$$P_i = \sigma_{H(\max)} h_1 \quad (7-11a)$$

where $\sigma_{H(\max)}$ = factored horizontal stress as determined from Eq. (7-11)

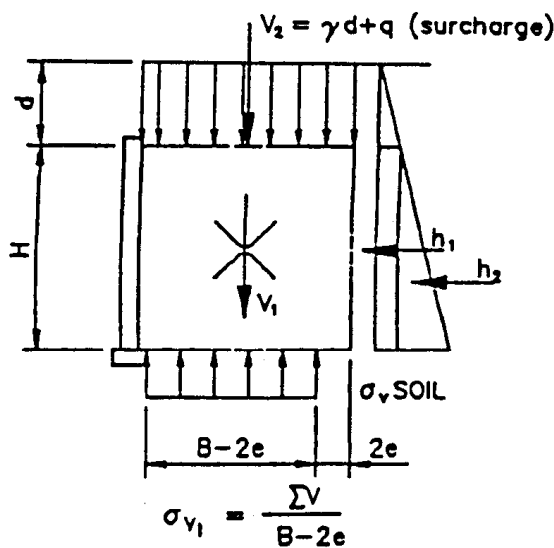
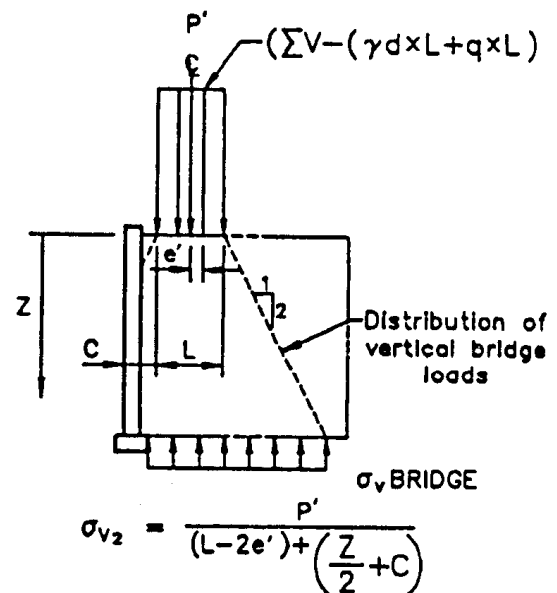
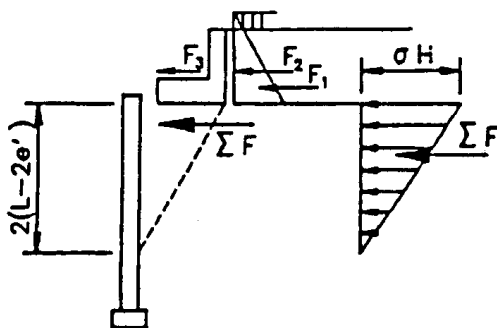
h_1 = height of reinforced soil zone contributing horizontal load to the reinforcement, computed as the vertical distance from the midpoint between the layer under consideration and the next overlying layer to the mid-point between the layer under consideration and the next underlying layer.

The effective length used for analyzing internal stability under the abutment footing should be the greater of either the length beyond the end of the footing or a distance from the facing equal to 30 percent of the wall height.

Abutments should not be constructed on mechanically stabilized embankments if the anticipated differential settlement between abutments or between piers and abutments is greater than about one-half the limiting differential angular distortion discussed in section 3.12. This criterion is a general guideline, and where conditions warrant, a more detailed analysis will be required to assess the effects of differential settlement.

Where abutments are supported by piles, the horizontal force transmitted to the piles may be assumed to be resisted by the lateral capacity of the piles, or by the horizontal component of the batter piles. If necessary, additional reinforcement may be placed in the upper portion of the structure.

The mass equilibrium of the system should be checked at each level of reinforcement below the bridge seat. Moments should be taken at each level under consideration about the center line of the reinforced mass to determine the eccentricity of load at each level. A uniform vertical stress is then computed using a fictitious width ($B - 2e$), and the corresponding horizontal stress is determined by multiplying by the appropriate earth pressure coefficient.

SOIL LOADSFOOTING LOADSSUPPLEMENTAL LOADS

$$\sigma_H \text{ supplemental max.} = \frac{\Sigma F}{L-2e'}$$

$$H \text{ max.} = \sigma_{v1} \cdot K + \sigma_{v2} \cdot K_A + \sigma_H$$

Figure 7-5 Horizontal stresses in abutments.

7.6 ABUTMENTS ON MODULAR SYSTEMS

Abutment seats may be constructed on modular units. In this case they must be designed for earth pressures and supplemental horizontal pressures from the abutment seat beam and earth pressure on the backwall. The top module should be checked for stability under the combined action of normal and supplemental earth pressures.

AASHTO stipulates minimum top module width as 6 feet. The center line of bearing should be at least 2 feet from the outside face of the top module, and the abutment beam seat should be supported and cast integrally to the top module.

The front face thickness of the top module must be designed for bending action developed by supplemental earth pressures. The loads on the abutment beam seat should be carried to the foundation level and considered acting on the footing. Differential settlement provisions should be considered.

7.7 WING WALLS

Wing walls may be placed parallel to the roadway, at some angle, or placed on the same alignment as the abutment wall. Possible configurations and structural solutions for wing walls of closed abutments are discussed in section 1.3.

Certain standards require the wing walls to be separated from the abutment wall with an open joint. AASHTO, however, allows the wing walls to be built as monolithic structures with the main abutment. In the latter case, reinforcing bars should be spaced across the junction between wing walls and abutment wall to tie them together. These bars should extend into the concrete on each side of the joint far enough to develop the strength of the bar, and should be varied in length in order to avoid planes of weakness.

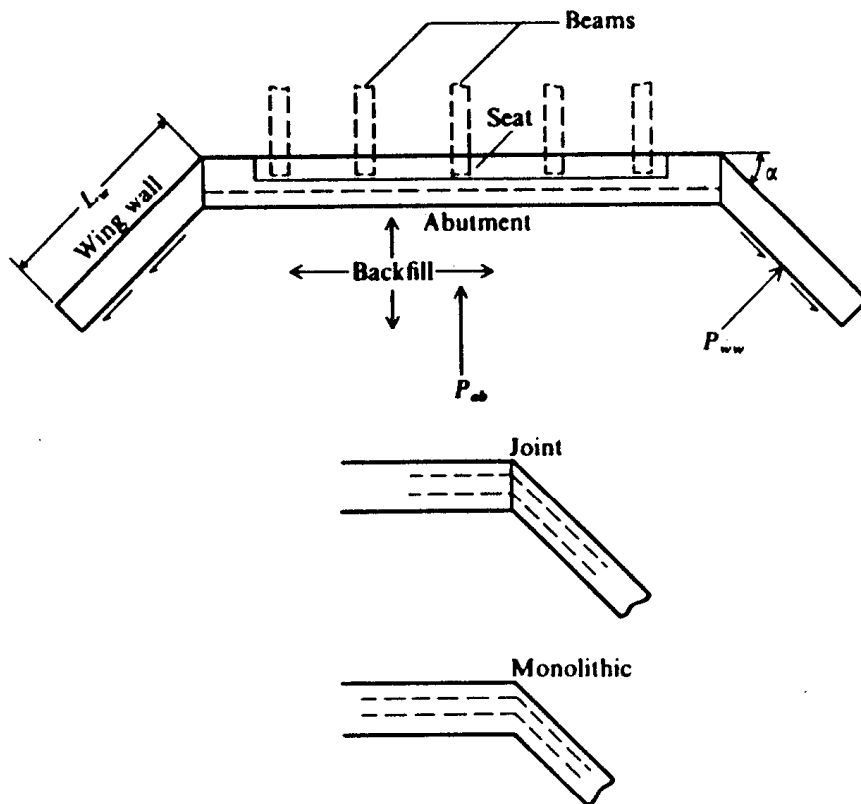


Figure 7-6 Bridge abutment and wing wall earth pressure and methods of construction. As abutment tilts forward, friction develops on wing walls as shown if wall is rigidly attached.

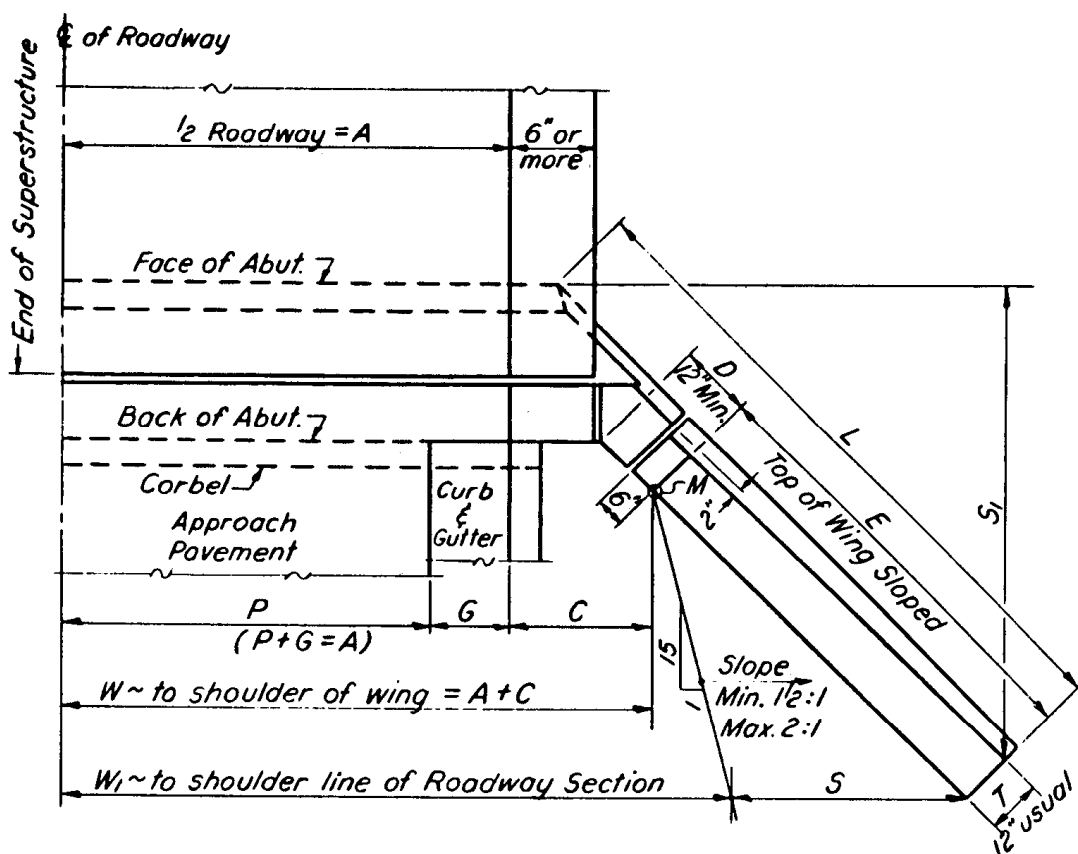


Figure 7-7 Layout of wing walls, closed abutment.

There appears to be some question as to how much design force (shear, tension, and moment) is produced at the junction of the abutment and the wing wall. Referring to Figure 7-6, it may appear that if the abutment wall carries the forces P_{ab} and P_{WW} , there is little left for the junction to carry, and in this case shrinkage and temperature reinforcement is all that is needed. However, it is more likely that wing walls respond as horizontal cantilevers near the top and close to the junction with the abutment, and as vertical cantilevers if they rest on spread footing and near the end.

Figure 7-7 shows a simple procedure to be followed for the dimensional layout of wing walls for a closed abutment. The wing wall makes an angle of 45° with the abutment wall. The following steps are necessary.

1. Select dimension W to an even 6-inch dimension so that D (the level portion of the wing wall) is 12 inches or more.
2. Establish wing wall length L as follows: (a) if the approach roadway slopes are 1½:1, calculate L to the nearest 6 inches to allow a slope 1½:1 along $S + T + S_1$ from actual shoulder elevation to toe of slope; (b) if the roadway slopes are 2:1 or flatter, calculate wing lengths for 2:1 slope along $S + T + S_1$.
3. Establish wing height and drop: (a) top of wing to be at top of curb or sidewalk along distance D to M ; (b) calculate drop to nearest 3 inches so that inside face at the end is the same distance above earth slope as M is exposed above the ground.

7.8 ABUTMENTS FOR SEGMENTAL BRIDGES

Abutments for segmental bridges should conform to the general design requirements and loading conditions stipulated in AASHTO Art. 7.5.2. In addition, consideration must be given to erection loads, moments, and shears imposed by the construction methods. Besides the normal loads, there may be random and accidental loads that have their origin in unusual natural events and construction incidents. In most cases, the abutment types discussed in the foregoing sections will be found suitable and structurally adequate. Hence, this section reviews abutment configurations for special conditions.

Abutment types. Figure 7–8 shows an abutment for a nominal-height segmental bridge, classified as Type I. This abutment may be considered where poor quality of the soil makes it difficult to resist the horizontal thrusts due to earth pressures combined with braking and thermal forces. The abutment is essentially a gravity system founded on vertical piles or drilled shafts. At the base, the entire horizontal loads are resisted by embedded prestressed concrete ties anchored in the back into a continuous dead-man structure as shown. This arrangement ensures stability against sliding. Resistance to overturning is still provided by a resisting couple of forces in the front and back row of piles.

Separate End Support and Retaining Wall. In this case, the two main functions of superstructure support and retaining wall are articulated in two separate structures. A front wall supported on spread footing or piles provides the superstructure end

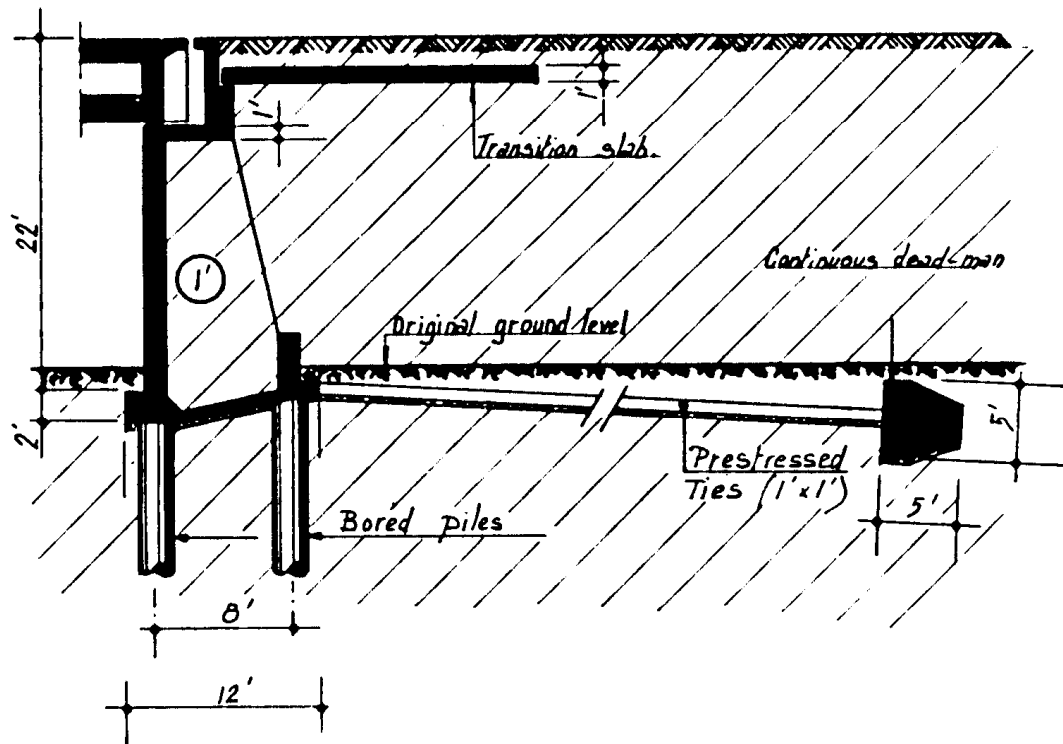


Figure 7–8 Abutment Type I, segmental bridges.

bearing. Behind this wall a separate MSE wall contains the approach fill. This scheme is designated as Type II.

Hollow Box Abutment. With relatively high bridges generating high levels of earth pressure behind the abutment wall, and where it is not possible or expedient to extend the approach fill under the deck, a suitable solution is an abutment built as a box, as shown in Figure 7-9, designated as Type III. A box with a front wall supports the superstructure and the approach roadway slab between the deck and the adjacent pavement. This structure may also be founded on piles or on spread footing. A hollow box abutment is essentially a derivative of the vaulted type shown in Figure 1-10.

Abutments Designed for Uplift. An example of segmental bridge with end uplift is the Tricastin Bridge over the Rhone River, France (Podolny and Muller, 1982). Piers were not desired in the waterway area, and this dictated a three-span structure

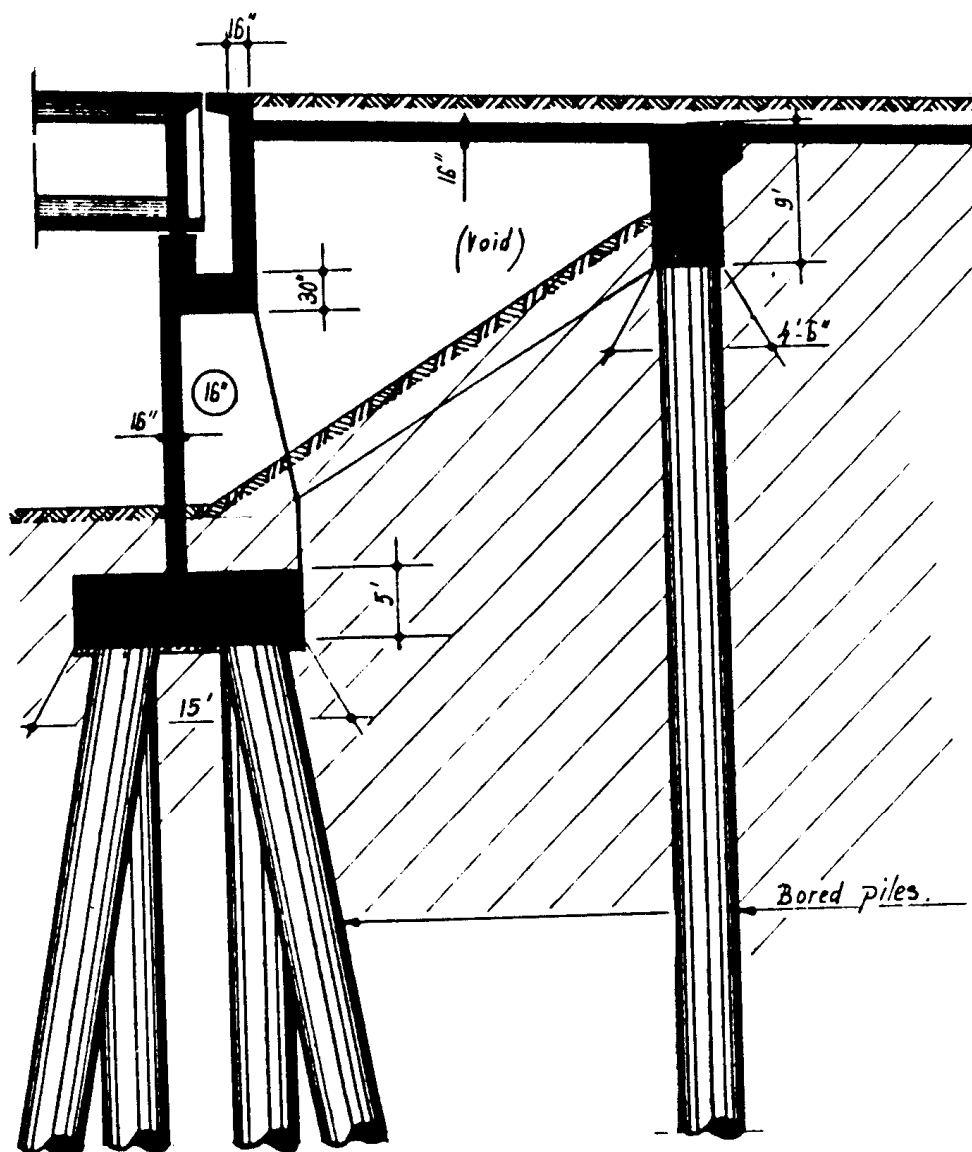


Figure 7-9 Hollow box abutment Type III, segmental bridges.

with a main span 467 feet and two short spans 83 feet each. The uplift is in this case transferred to the abutments.

An abutment designed and built to resist uplift is shown in Figure 7-10, designated as Type IV. A large caisson is open-dredged and filled with tremie concrete after completion of the excavation to the required foundation level to provide a total weight sufficient to balance the uplift reaction from the deck.

The abutment types shown in Figures 7-8 through 7-10 are not necessarily unique to segmental construction. The same or similar structures may be designed and built for medium-range bridges with truss and steel-box girder superstructures.

Commentary on abutment movement. A consideration relevant to the amount of horizontal movement that bridges in general can tolerate is the movement of abutments necessary to reduce the earth pressures to the design value. If an abutment, irrespective of its type, does not move, the earth pressure acting behind the structure is close to the at-rest value. If the abutment moves away from the backfill, the earth pressure will be reduced below the at-rest value. If this movement is large enough the earth pressure may be reduced to the active level.

If the backfill is a clean mix of sand and gravel, the earth pressure may be assumed to reduce to active values, if the horizontal movement of the abutment away from the backfill is about 0.004 times the height of the abutment wall. This criterion translates to 0.5-inch movement for a 10-foot high wall, 1.0 inch for a 20-foot wall, and 1.5 inches for a 30-foot high wall. These values may be used as a general guideline for sand and gravel backfill in a loose condition. In dense sand and gravel, the movement

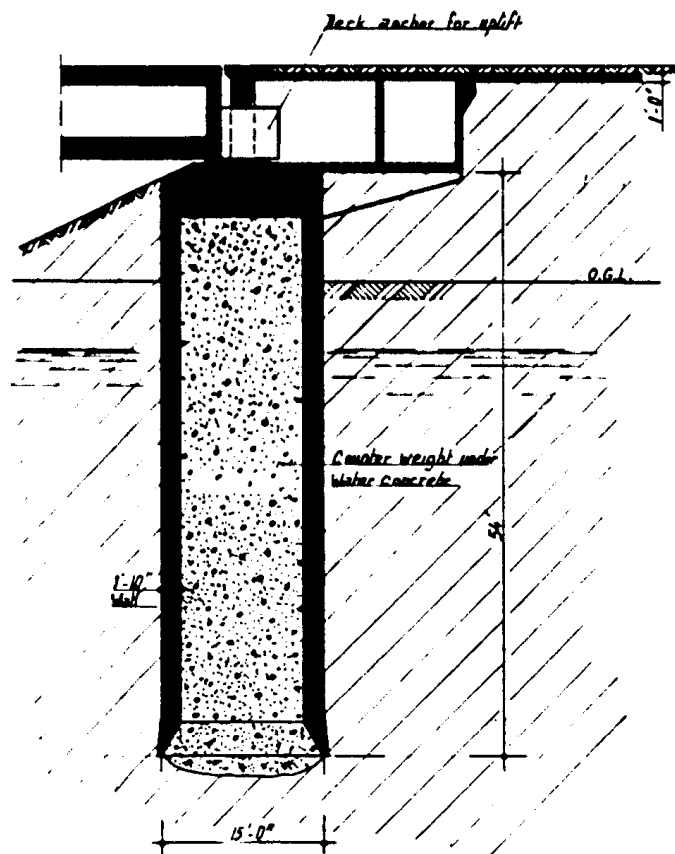


Figure 7-10 Abutment Type IV to resist uplift, segmental bridges.

necessary to reduce the earth pressure to active values is smaller than 0.004 times the wall height.

If the backfill consists of clay, or if it contains enough clay or plastic silt to impart cohesion and plasticity to the system, the movement necessary to bring the earth pressure to the active condition is much larger than for sand and gravel. Furthermore, cohesive soils have creep characteristics. Even though the wall may move enough to reduce the earth pressure to the active value, the pressure will begin to increase again as creep takes effect. Continuous movement has been demonstrated where active pressures were used to design walls backfilled with cohesive soils. Hence, where these materials provide the backfill, it is essential and structurally consistent to select pressures at rest.

It is apparent that the selection of earth pressures for the design of abutments will have certain implications regarding wall movement. If active pressures are introduced, the design should check how much movement will be necessary to develop these pressures. These considerations should be included in the design of expansion joints that will allow for temperature expansion and abutment movement.

Frost Effects

Water in soil expands when it freezes so that ice lenses may form, resulting in frost heave in the frozen soil. Foundation for closed abutments should be built below the frost line to prevent frost damage. This problem is less severe with pile bents built in embankments, unless the water level can rise to unexpected levels.

The maximum frost depth is usually available from local experience, or may be determined from frost-depth contour maps. The data shown in Figure 7-11 give an alternate procedure for estimating frost depth using a freezing index proposed by the U.S. Corps of Engineers (1949) and Brown (1964). According to this,

$$\text{Freezing Index} = N_{32^\circ\text{F}} \times (32^\circ\text{F} - T) \quad (7-12)$$

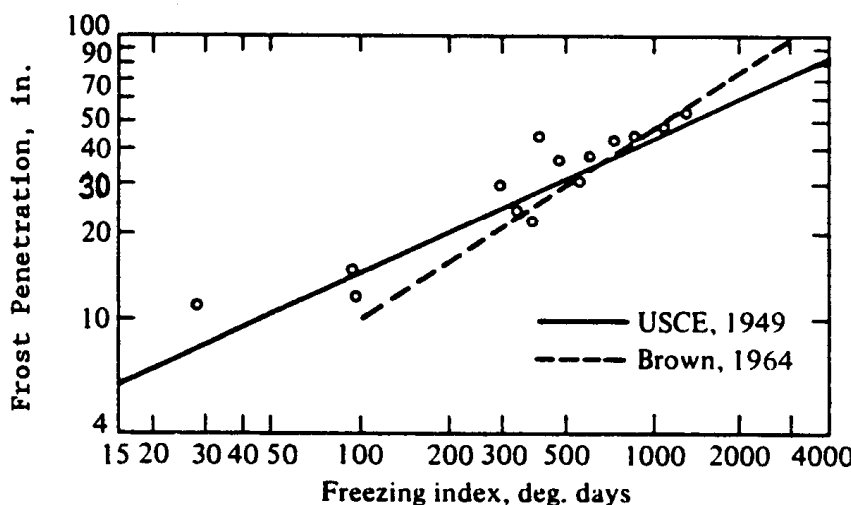


Figure 7-11 Design curves for maximum frost penetration based on the freezing index (from U.S. Corps of Engineers, 1949; and Brown 1964).

where $N_{32^{\circ}\text{F}}$ = number of days below 32°F , and T = average daily temperature. For example, if $N_{32^{\circ}\text{F}} = 25$ days, and $T = 22^{\circ}\text{F}$ for a particular site, the freezing index is $(25)(32 - 22) = 250$. From the graph of Figure 7-11 the corresponding frost depth is obtained as about 20 inches.

7.9 SEISMIC DESIGN OF ABUTMENTS

General Principles

Certain basic principles are discussed in section 3.10 in conjunction with the two approaches used to formulate the current AASHTO philosophy in seismic design. The relative displacement effects are of particular importance. As mentioned, these may arise from out-of-phase motion of different parts of the bridge, from lateral displacement or rotation of the foundations, and differential displacement of abutments. This makes it necessary to stipulate minimum support lengths.

Numerous case histories of damage or failure of bridges attributed to abutment failure or displacement during earthquakes have demonstrated the need to address the seismic factor in abutment design. Damage may be associated with excessive settlement or slumping of the backfill, excessive displacement caused by high seismically induced lateral earth pressure, or the transfer of large longitudinal or transverse inertia forces from the bridge superstructure. Settlement of abutment backfill, and abutment or deck damage resulting from abutment movement may lead to loss of bridge access, and hence abutments must be regarded as an important parameter in the overall seismic design process.

The pattern of abutment movement or damage during past earthquakes has been documented in case histories. Evans (1971) has examined the abutments of 39 bridges within 30 miles of the 1968 M7 Inangahua earthquake in New Zealand. Of these, 23 showed measurable movement and 15 suffered some form of damage. Movement of free-standing abutments followed the general pattern of outward motion and rotation about the top after contact with the superstructure induced a corresponding restraint. Fill settlement was observed to be 10 to 15 percent of the fill height. Similar damage effects were documented on bridge abutments in the M7.1 Madang earthquake in New Guinea (Ellison, 1971); abutment movement was as much as 20 inches. Damage to abutments in the 1971 San Fernando earthquake is reported by Fung, LeBeau, Klein, Belvedere, and Goldschmidt (1971). Numerous instances of abutment displacement and associated damage have been reported on the Niigata and Alaska earthquakes, but these failures were primarily related to soil liquefaction.

As is evident from sections 7.1 through 7.8, abutment types vary and their main features are influenced by the characteristics of the bridge site, foundation conditions, bridge geometry, and loads from superstructure. For the wide variety of abutments discussed in the foregoing sections, the foundation may consist of spread footings, vertical or battered piles, and drilled shafts. Connection details to the superstructure may be structural joints, roller supports, or elastomeric bearings. Given the large number of design variables and relevant parameters combined with the complex abutment-superstructure-soil interaction, the analysis of abutment response during earthquakes is a complex problem.

Seismic Earth Pressures

Free-standing abutment walls. In this category are gravity or cantilever-type abutments that can yield laterally during an earthquake (i.e., by supporting superstructures through bearings that are free to rotate or slide). For these abutments, the earth pressures induced during an earthquake can be computed using the Mononobe-Okabe pseudo-static approach.

In highly seismic areas, the design of these abutments to provide zero displacement under peak ground acceleration is grossly unrealistic, and should be replaced by an approach where a small lateral displacement is acceptable. A method recently developed to estimate the magnitude of relative wall displacement during a seismic incident is included in this section. Based on a simplified approach, suggested guidelines are introduced for selecting a pseudo-static seismic coefficient and the corresponding displacement level for a given peak ground acceleration.

Mononobe-Okabe theory. This is essentially a static approach developed by Mononobe (1929) and Okabe (1926). Essentially the analysis is an extension of the Coulomb sliding wedge theory considering horizontal and vertical inertia forces acting on the soil. Complete details of the associated methodologies are given by Seed and Whitman (1970), and Richards and Elms (1979). The following assumptions are made:

1. The abutment is free to yield sufficiently to mobilize the soil strength and active pressure conditions. If the abutment is rigidly fixed and thus unable to move, the soil forces will be much greater than those predicted by this analysis.
2. The backfill is cohesionless material, with a definite friction angle ϕ .
3. The backfill is unsaturated so that liquefaction does not occur.

Equilibrium conditions of the active soil wedge behind the abutment are shown in Figure 7–12. These considerations lead to a value E_{AE} of the active force imposed on the soil mass by the abutment (and vice versa) when the latter is at the point of failure. The following expression gives E_{AE}

$$E_{AE} = \frac{1}{2} \gamma H^2 (1 - k_v) K_{AE} \quad (7-13)$$

where the seismic active pressure coefficient K_{AE} is given by

$$K_{AE} = \frac{\cos^2(\phi - \theta - \beta)}{\cos \theta \cos^2 \beta \cos(\delta + \beta + \theta)} \times \left[1 + \sqrt{\frac{\sin(\phi + \delta) \sin(\phi - \theta - i)}{\cos(\delta + \beta + \theta) \cos(i - \beta)}} \right]^2 \quad (7-14)$$

and where γ = unit weight of soil; H = height of soil face (as shown in Figure 7–12); ϕ = angle of friction of soil; θ = $\arctan[k_h/(1 - k_v)]$; δ = wall friction angle; k_h = horizontal acceleration coefficient; k_v = vertical acceleration coefficient; i = backfill slope angle; and β = slope of soil face.

If the abutment is moved towards the backfill, the equivalent expression for the passive force is

$$E_{PE} = \frac{1}{2} \gamma H^2 (1 - k_v) K_{PE} \quad (7-15)$$

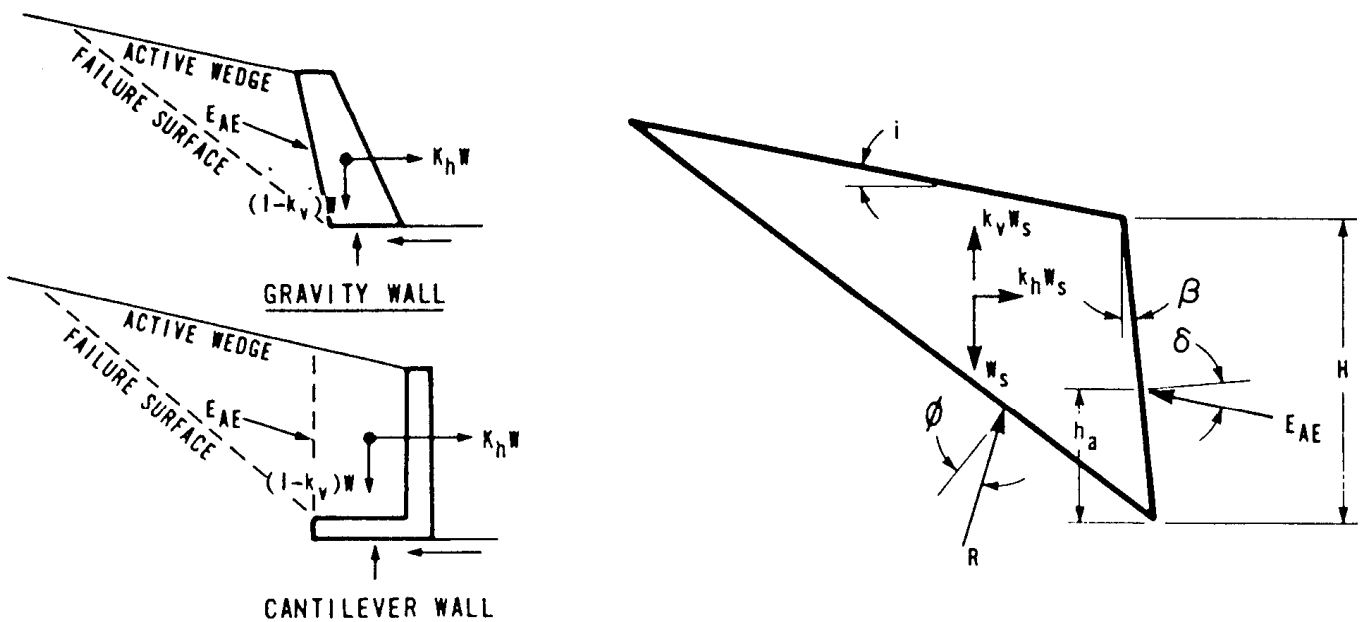


Figure 7-12 Active wedge force diagram.

where the seismic passive pressure coefficient K_{PE} is given by

$$K_{PE} = \frac{\cos^2(\phi - \theta + \beta)}{\cos \theta \cos^2 \beta \cos(\delta - \beta + \theta)} \times \left[1 - \sqrt{\frac{\sin(\phi - \delta) \sin(\phi - \theta + i)}{\cos(\delta - \beta + \theta) \cos(i - \beta)}} \right]^2 \quad (7-16)$$

As the seismic inertia angle θ increases, the values of K_{AE} and K_{PE} approach each other, and for a vertical backfill they become equal when $\theta = \phi$.

This approach has a relative simplicity. Its accuracy, however, has been confirmed by model tests (Franklin and Chang, 1977) and by back calculations from observed failures of flood channel walls (Elms and Martin, 1979). In the latter case, however, the displacements were larger, and this could modify the effective value of k_h at which failure occurs.

The arm h_a that defines the point of application of the resultant soil pressure is usually taken as $H/3$ for the static conditions without earthquake effects. This arm becomes greater, however, when earthquake effects are present. This has been shown theoretically by Wood (1973), who determined that the resultant of the dynamic pressure is located approximately at the midheight, and confirmed by tests. Seed and Whitman (1970) have suggested that the static component of the soil force (computed from Eq. 7-13 with $\theta = k_v = 0$) acts at a height $H/3$, but the additional dynamic effect should be taken at height $0.6 H$ (see also section 6.13). For simplicity, most engineers will assume $h = H/2$ for the composite effect, with a uniformly distributed pressure. Taking the location of the total resultant at midheight is also suggested by AASHTO (Elms and Martin, 1979).

The Mononobe-Okabe expression for active thrust is readily estimated for a given geometry and friction angle. The significance and the effects of the various parameters are not, however, directly obvious. Very useful data on these effects are included in AASHTO commentary on seismic design.

The effects of abutment inertia are not taken into consideration in the foregoing analysis. One approach is to neglect the inertia forces due to the mass of the abutment, but this is not a conservative assumption, and where the design must rely on the mass of the abutment for stability it is also an unreasonable assumption.

Design for displacement. If peak ground accelerations are used in the Mononobe-Okabe analysis, the size of gravity structures will often be too excessive. Alternatively, a more economical structure may be provided if the design accepts a small tolerable displacement rather than no displacement at all.

Test show that a gravity retaining wall will fail incrementally in an earthquake. For a given earthquake ground motion, the total relative displacement may be computed using the sliding block method proposed by Newmark (1965). A displacement pattern is assumed similar to that of a block resting on a plane rough horizontal surface subjected to an earthquake, with the block being free to move against frictional resistance in one direction only. Figure 7-13 shows relationship of the relative displacement to the acceleration and velocity time histories of soil and wall. At a critical value of k_h the wall is assumed to begin sliding; relative motion will continue until wall and soil velocities are equal.

Newmark computed the maximum displacement response for four earthquake records, and the results were plotted after scaling the earthquakes to a common maximum acceleration and velocity. Franklin and Chang (1977) repeated the analysis for a large number of both natural and synthetic records and added the results to the same plot. Upper bound envelopes are shown in Figure 7-14. All records are scaled to a maximum acceleration coefficient 0.5 and a maximum velocity $V = 30$ in/sec. The maximum

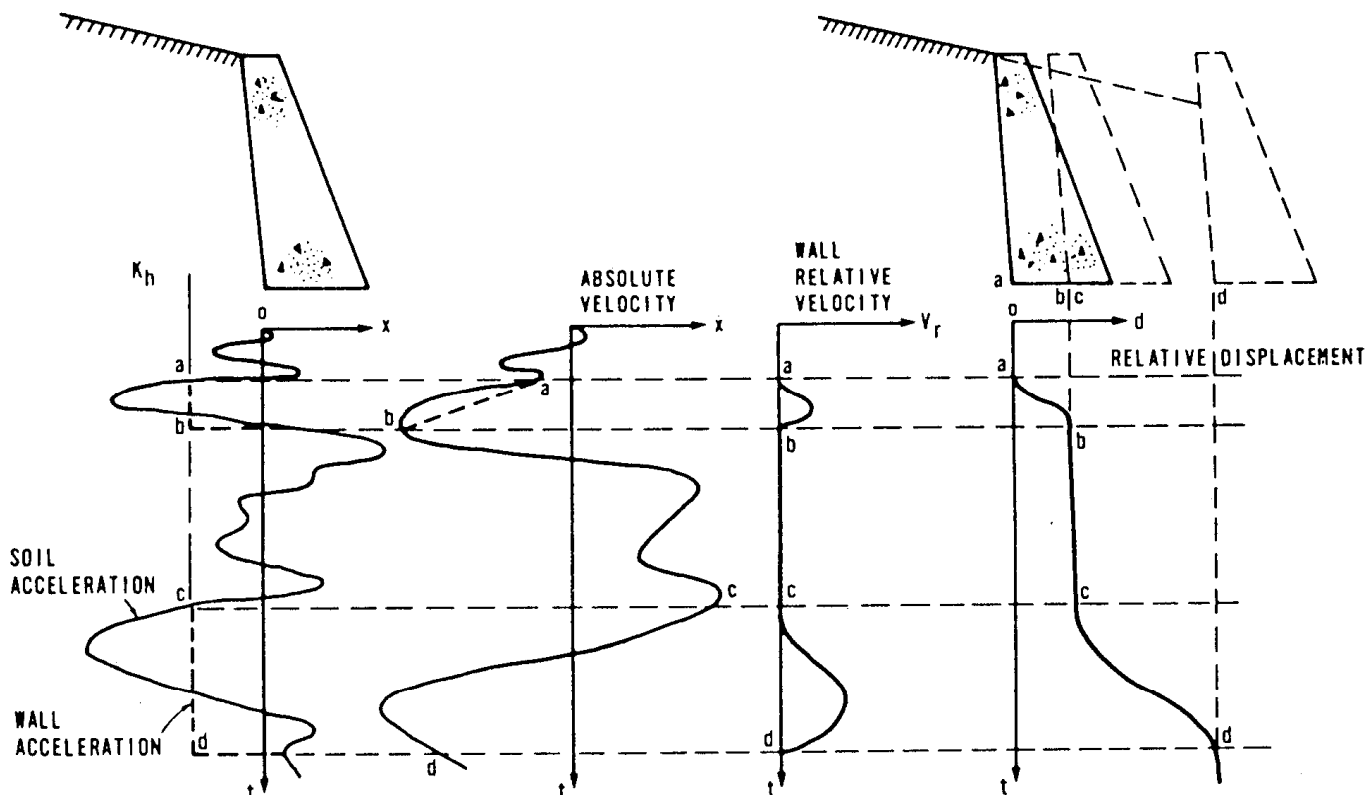


Figure 7-13 Relation between relative displacement and acceleration and velocity time histories of soil and wall.

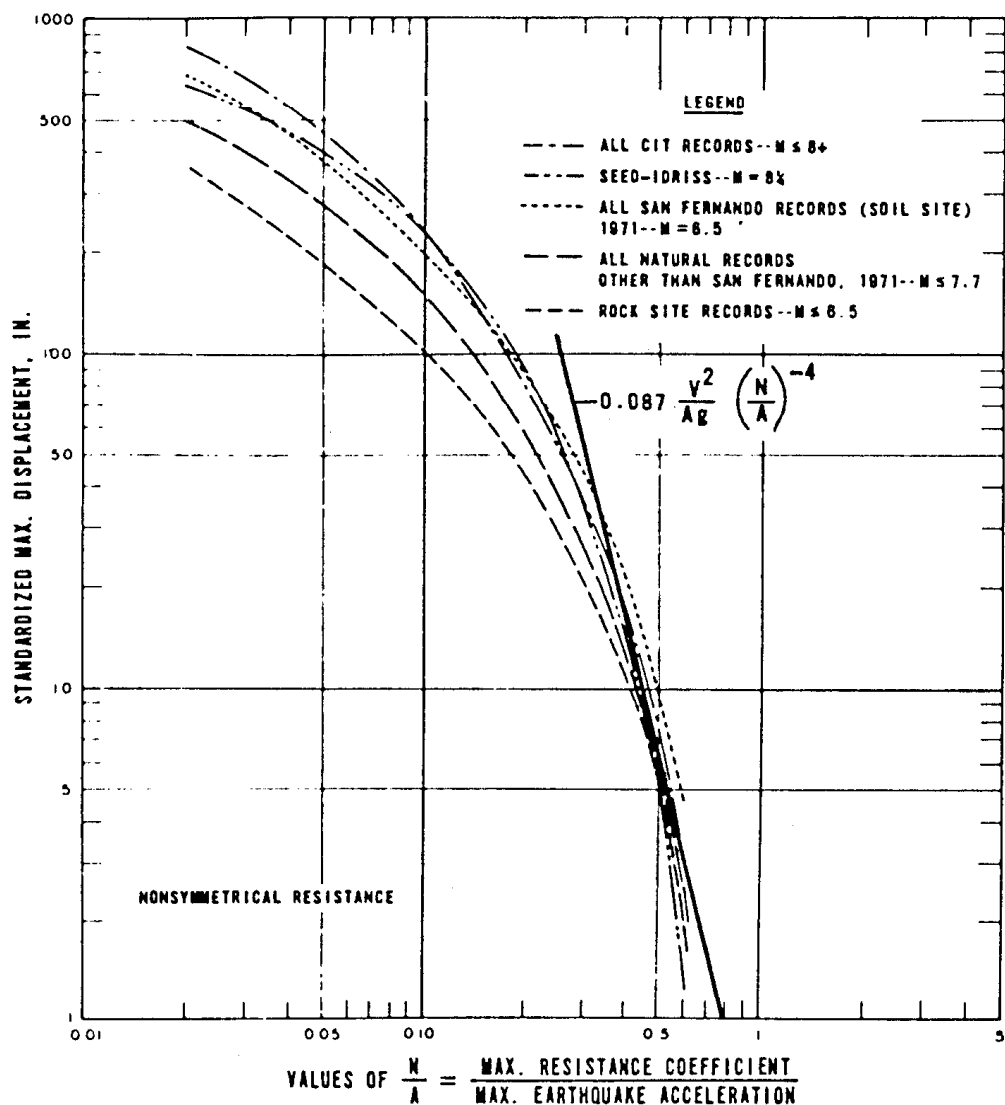


Figure 7-14 Upper bound envelope curves of permanent displacements for all natural and synthetic records analyzed by Franklin and Chang (1 inch = 25.4 mm).

resistance of coefficient N is the maximum acceleration coefficient sustainable by a sliding block before it slides. For a wall designed using the M-O method, the maximum coefficient is k_h .

Figure 7-14 shows that the displacement envelopes for all the scaled records have the same basic shape. For relatively low displacements, an approximation to the curves gives the following relation:

$$d = 0.087 \frac{V^2}{A g} \left(\frac{N}{A} \right)^{-4} \quad (7-17)$$

where V = maximum velocity; A = acceleration coefficient; and g = acceleration of gravity = 32.2 ft/sec². The parameter d is the total relative displacement of a wall subjected to the ground motion. On Figure 7-14 a straight line is fitted, and since Equation (7-17) is derived from envelope curves it will tend to overestimate d for most earthquakes.

A suggested design approach is to choose a desired value for the maximum wall

displacement d together with appropriate earthquake parameters, and then use Equation (7-17) to determine the seismic acceleration coefficient for which the wall should be designed. The superstructure connections should be detailed to accommodate this displacement.

Elms and Martin (1979) applied this procedure to several examples and concluded that a value of $k_n = A/2$ should be adequate for most design purposes, provided that allowance is made for an outward displacement of the abutment of up to $10A$ inches.

For bridges with SPC C and D, more detailed analysis is necessary to articulate the transfer of structural inertia forces through bearings to free-standing abutments, particularly for category D, because of the continued bridge accessibility required after a major earthquake.

Figure 7-15 shows force diagrams for sliding steel bearings or pot bearings, describing limiting equilibrium conditions for a simple abutment. Where the bearings consist of unconfined elastomeric pads, the forces transferred to the abutment become more complex because these bearings are capable of transmitting significant force. This force initially depends on the relative movement between superstructure and abutment and can become quite large before slip occurs.

For bridges with SPC D classification, provisions should be made to connect superstructure and abutment using bolts and buffers, such as the detail shown in Figure 7-16. Linkage bolts are used to prevent spans dropping off supports. The rubber rings act as buffers to prevent damage due to impact. The knock-off section of the backwall will accommodate differential displacement between superstructure and abutment beyond the scope of the expansion device and will thus minimize impact damage. A typical detail provision used in the United States is to seal the gap between superstructure and abutment with bituminous material. Irrespective of these measures, some form of damage with possible abutment rotation should be expected in strong earthquakes.

The same guidelines suggest also the use of a settlement approach slab tied to the abutment. This will provide bridge access in the event of backfill settlement as well as additional abutment friction anchorage against lateral movement.

Non-yielding abutments. The M-O analysis assumes that the abutment is free to yield laterally enough to mobilize peak soil strength in the backfill. For granular backfills, the criteria of movement discussed in the foregoing sections translate into a deflection at the top of about 0.5 percent of the height. If an abutment is restrained against lateral movement (i.e., by ground anchors, batter piles, etc.), the lateral pressures will be greater than those computed from the M-O analysis (Wood, 1973). Where doubt exists, a factor of 1.5 should be applied to the peak ground acceleration to account for the lateral restraint of the abutment.

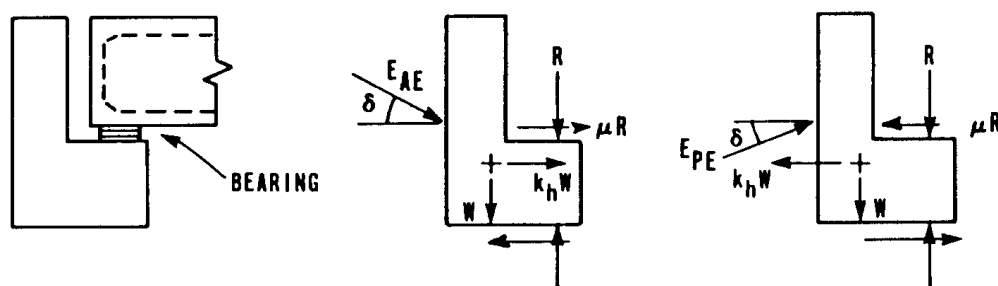


Figure 7-15 Force diagrams including bearing friction.

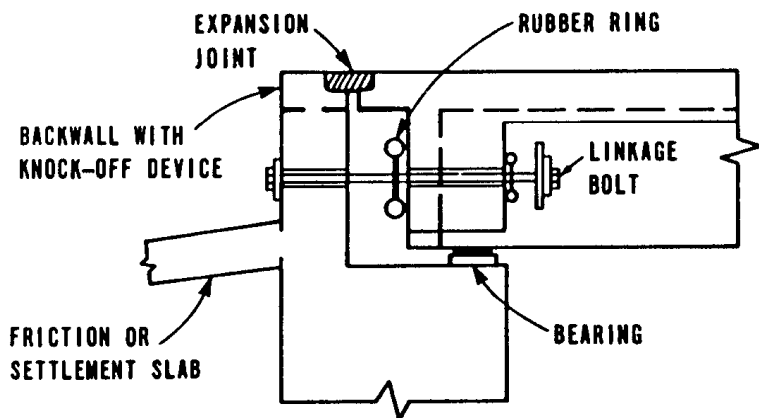


Figure 7-16 Abutment support detail.

Monolithic abutments. Figure 7-17 shows a monolithic or end diaphragm abutment commonly used for single and for two-span bridges in California. The end diaphragm is cast monolithically with the superstructure and may be supported directly on piles. The diaphragm acts as a retaining wall while the superstructure functions as a prop between abutments.

Monolithic abutments of this type have performed well during earthquakes, since they avoid problems related to backwall and bearing damage as the abutment yields; they also reduce the lateral load carried by columns or piers. On the other hand, the di-

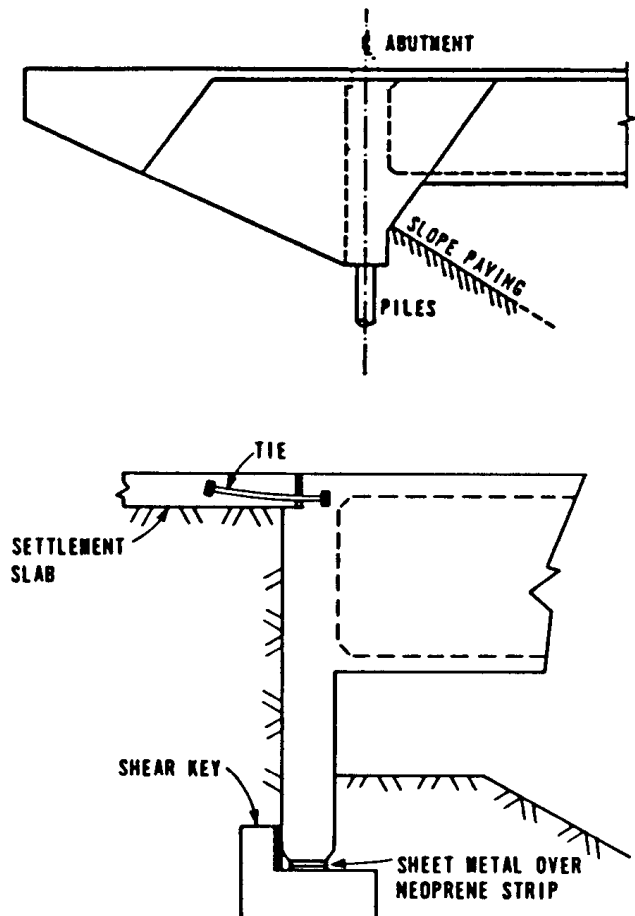


Figure 7-17 Typical monolithic abutments.

rect connection with the superstructure implies that higher longitudinal and transverse inertia forces are transmitted directly into the backfill, and provisions must be made for adequate passive resistance.

Free-standing or seat-type abutments are more compatible with the development of soil forces and with better control. However, the added joint introduces a potential collapse mechanism into the entire structure. Thus, monolithic abutments are viable alternatives and particularly suitable for bridges in SPC D. The response in this case may be heavier damage than for the free-standing abutment because of the higher forces transferred to the backfill, but the bridge as a whole has a lower collapse potential. When making estimates of monolithic abutment stiffness and associated longitudinal displacements during transfer of peak earthquake forces from the structure, a recommendation is to have the abutments proportioned to restrict displacements to 0.3 feet (9.1 cm) or less in order to minimize damage.

AASHTO Requirements

The foregoing criteria form the basis for the requirements of seismic design stipulated in the current AASHTO standard specifications.

Seismic performance category B. For free-standing abutments or retaining walls that can displace horizontally without major restraint, the M-O method of analysis is recommended, using $k_h = A/2$ and ignoring the effect of vertical acceleration. Abutments should be proportioned to slide rather than tilt, and thus they should be designed to accommodate displacements up to 10A inches. The seismic design should consider forces due to seismically induced lateral earth pressures, additional forces arising from wall inertia effects, and the transfer of seismic forces from the superstructure where bearing supports are not free to slide. For free-standing abutments restrained against horizontal movement by anchors or batter piles, the maximum lateral earth pressure may be computed using $k_h = 1.5A$ in conjunction with the M-O analysis.

For monolithic abutments (integrally formed with the superstructure), maximum earth pressures acting on the abutment may be assumed to be the maximum longitudinal earthquake force transferred from the superstructure. To minimize abutment damage, the abutment should be designed to resist the passive pressure that can be mobilized by the abutment backfill, which should be greater than the maximum computed longitudinal earthquake force transferred to the abutment. However, it may be assumed that the lateral active earth pressure during an earthquake is less than the superstructure earthquake load. When longitudinal seismic forces are also resisted by piers, the portion of earthquake load transferred to the abutment should be proportioned to each substructure stiffness.

Seismic performance category C. In addition to the foregoing provisions, the design should consider the mechanism of transfer of superstructure transverse inertial forces. Adequate resistance to lateral pressure should be provided by wing walls or abutment keys to minimize lateral displacement of the abutment.

Seismic performance category D. In addition to the requirements for Categories B and C, the design should consider the transfer mechanism of superstructure longitudinal and transverse inertia forces to the abutments as well as the associated abutment-soil interaction. In order to prevent the potential loss of bridge access due to abutment

damage, monolithic and end diaphragm construction is strongly recommended for short span bridges. Settlement or approach slabs linked to abutments by flexible ties should be mandatory.

7.10 DESIGN EXAMPLE 7-1, PILE BENT ABUTMENTS, ASD METHOD

Figure 7-18 shows the elevation and span lengths for a 7-span bridge with simple and continuous units as shown. Hinges are located in spans 1, 4, and 7, and the resulting superstructure configuration is three simple spans, and two-span continuous units with cantilever over the end supports. Both end bents are provided with fixed bearings. Because of severe geometric restrictions, the bridge is placed on a rather unusual skew angle, where all substructure elements form an angle of 65° with the vertical to the bridge axis.

The superstructure consists of a concrete deck on steel plate girders (72-inch web plate). There are 6 steel girders spaced at 7 feet 4 inches. The concrete slab is 8 inches thick, and the deck accommodates three lanes in the same direction. The bridge site is in a region of low seismic activity (Category A), and hence earthquake requirements do not apply. Referring to Figure 7-18, span 1 is 106 feet long, but because of the hinge, the actual design span is 95 feet. The severe skew angle of the bridge results in abutment lengths of about 100 ft. We will design End Bent 1 (fixed bearing) using ASD method.

A typical (initial) section of the bent is shown in Figure 7-19, together with the pile layout and spacing. Design lateral earth pressures have been established by the supervising authority, and are articulated as 35 lb equivalent fluid pressure. Since a structural approach slab is provided and supported on the back wall, live load surcharge from the fill is omitted.

Group I. This includes dead load, live load, and earth pressure.

1. Dead load from superstructure.

From Superstructure design $DL_s = 418$ kips

2. Dead load, weight on bent.

Referring to Figure 7-19(a), we calculate the following

$$\text{Section } ① = (5.00)(5.00)(100)(0.15) = 375 \text{ kips}$$

$$② = (9.00)(1.50)(100)(0.15) = 203 \text{ kips}$$

$$③ = (2.50)(1.67)(100)(0.15) = 63 \text{ kips}$$

$$\text{Total} \quad DL_b = 641 \text{ kips}$$

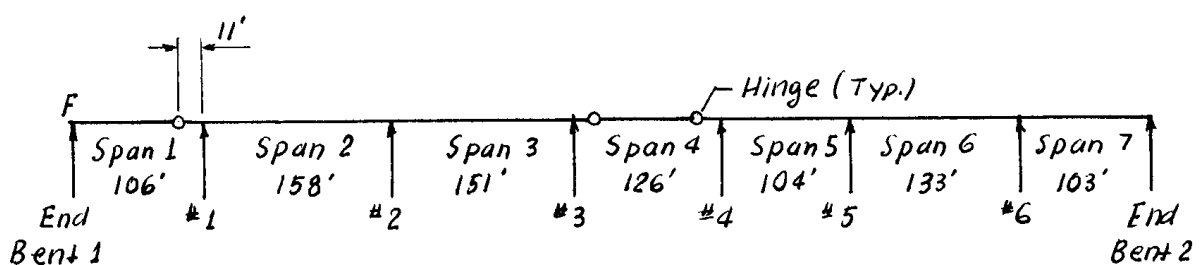


Figure 7-18 Bridge elevation, Design Example 7.1.

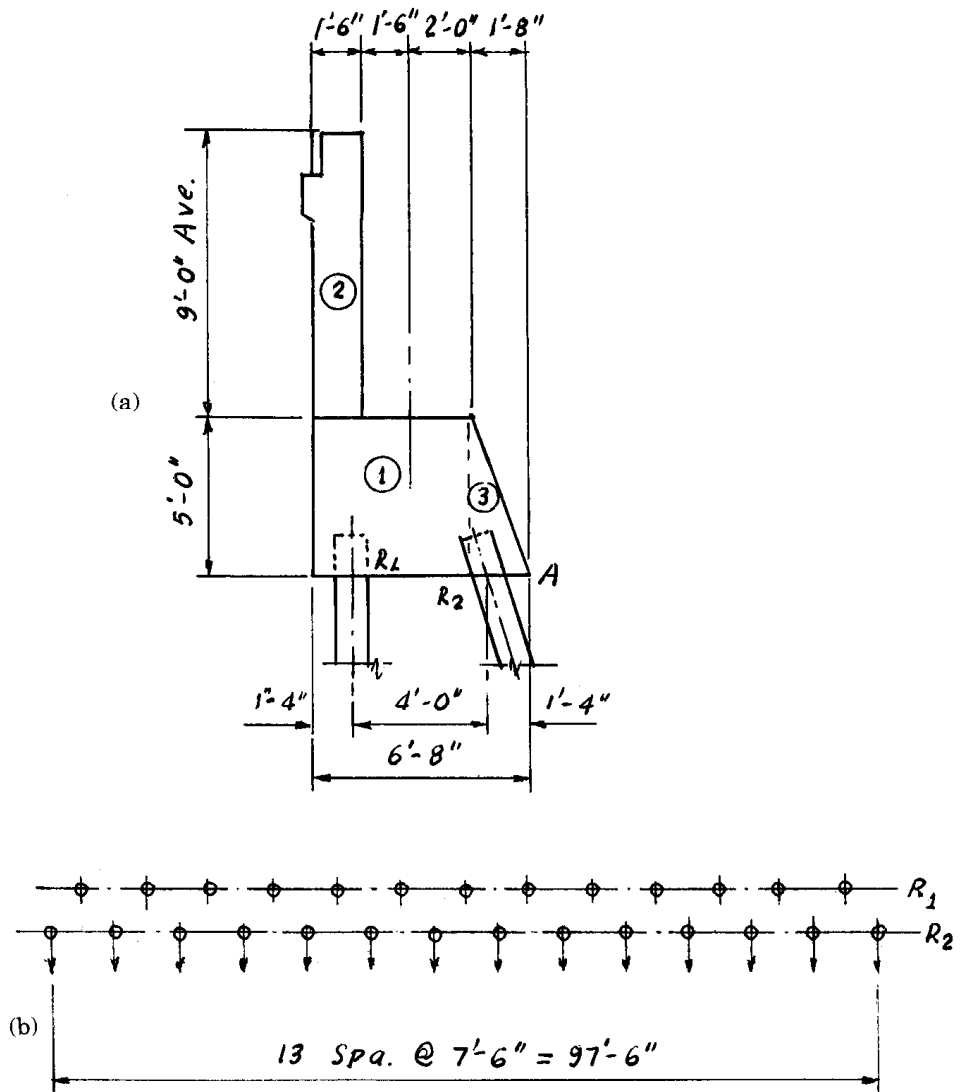


Figure 7-19 Bent of Design Example 7.1 (a) Preliminary section; (b) pile layout.

3. Dead load, weight of approach slab (24 feet wide) ✓
This is computed as (36)(1.875), or $DL_{as} = 68 \text{ kips}$
4. Live load from bridge (HS 20 without impact)
3 lanes load $LL = (3)(0.9)(64.9)$ or $LL = 175 \text{ kips}$
5. Lateral earth pressure (lin. ft).
For a height $h = 14'$, $P_e = (0.035)(\frac{14^2}{2}) = 3.43 \text{ kips/lin. ft}$

Case A. Dead load plus earth pressure (check conditions necessary to balance lateral loads). Referring to Figure 7-19(a), we take moments about point A.

$$\begin{aligned}
 M_{DL_s} &= 418 \times 3.67 = 1534 \text{ ft-kips} & \curvearrowleft \\
 M_b &= 375 \times 4.17 = 1564 \text{ ft-kips} & \curvearrowleft \\
 203 \times 5.92 &= 1202 \text{ ft-kips} & \curvearrowleft \\
 63 \times 1.11 &= 70 \text{ ft-kips} & \curvearrowleft
 \end{aligned}$$

$$\begin{aligned}
 M_{as} &= 68 \times 6.17 = 420 \text{ ft-kips} \\
 \text{Earth pressure, total force} &= (3.43)(96) = 329 \text{ kips} \\
 M_e &= (329)(4.67) = -1536 \text{ ft-kips} \\
 \text{Total} &\quad 1127 \text{ kips} \quad 3254 \text{ ft-kips}
 \end{aligned}$$

From point A to resultant $= x = 3254/1127 = 2.88$ ft. Referring to Figure 7-20 the dimension e is computed as the difference $5.33 - 2.88 = 2.45$ ft.

The total load of 1127 kips is distributed to the front and back rows as follows:

$$\begin{aligned}
 R_1 &= (1127)(1.55)/4.00 = 436 \text{ kips} \\
 R_2 &= \quad \quad \quad 691 \text{ kips}
 \end{aligned}$$

Horizontal component of front row $= 691/3 = 230$ kips.

Unbalanced horizontal force $= 329 - 230 = 99$ kips.

This would give a lateral force of $99/27 = 3.7$ kips per pile, which is excessive. An allowable horizontal force per pile is for this case 2 kips. The initial bent design must, therefore, be revised.

Figure 7-21 shows the revised (final) cross section of the bent. The intent of this revision is to increase the overall dead load, and further increase the load transferred to the front row by moving the bearing line closer to this row, and by placing the back row further away from the front row. The new loads are as follows.

1. Dead load from superstructure $DL_s = 418$ kips

2. Dead load, weight of bent

$$\begin{aligned}
 \text{Section ①} &= (3.50)(4.50)(100)(0.15) = 236 \text{ kips} \\
 ② &= 203 \text{ kips} \\
 ③ &= (8.00)(2.50)(100)(0.15) = \underline{\underline{300}} \text{ kips}
 \end{aligned}$$

$$\text{Total} \quad DL_b = 739 \text{ kips}$$

3. Dead load, approach slab $DL_{as} = 68$ kips

4. Live load from bridge = same as before

5. Lateral earth pressure (lin. ft)

$$\text{For } p_e = (0.035)\left(\frac{15^2}{2}\right) = 3.94 \text{ kips/lin. ft}$$

6. Dead load, weight of earth

$$⑦ = (12.50)(2)(100)(0.12) = 300 \text{ kips}$$

$$⑧ = (1.50)(2.00)(100)(0.12) = 36 \text{ kips}$$

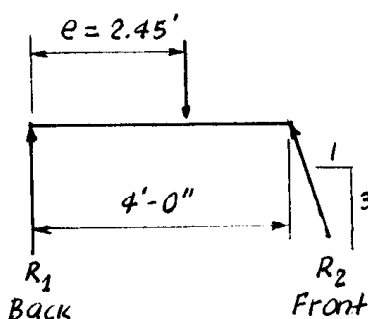


Figure 7-20 Pile details and batter.

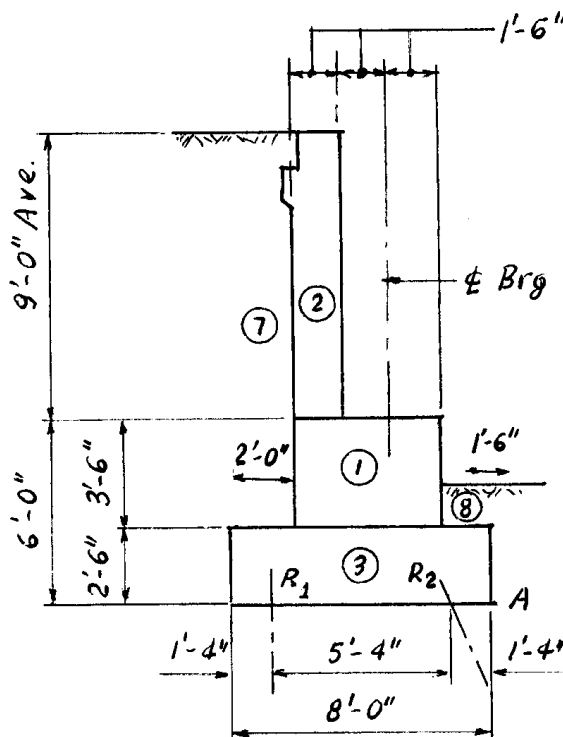


Figure 7-21 Final bent section, Design Example 7.1.

Case A (Revised). Dead load plus earth pressure. Taking moments about point A in Figure 7-21, we obtain

$$\begin{aligned}
 M_{DL_s} &= 418 \times 3.00 = & 1254 \text{ ft-kips} & \curvearrowleft \\
 M_b &= 236 \times 3.75 = & 885 \text{ ft-kips} & \curvearrowleft \\
 & 300 \times 4.00 = & 1200 \text{ ft-kips} & \curvearrowleft \\
 & 203 \times 5.25 = & 1066 \text{ ft-kips} & \curvearrowleft \\
 M_{as} &= 68 \times 6.00 = & 408 \text{ ft-kips} & \curvearrowleft \\
 M_7 &= 300 \times 7.00 = & 2100 \text{ ft-kips} & \curvearrowleft \\
 M_8 &= 36 \times 0.75 = & 27 \text{ ft-kips} & \curvearrowleft \\
 M_e &= 378 \times 5 = -1890 \text{ ft-kips} & & \curvearrowleft \\
 \text{Total} &= 1561 \text{ kips} & 5050 \text{ ft-kips} & \curvearrowleft
 \end{aligned}$$

Distance from point A to resultant = $5050/1561 = 3.23$ ft, giving $e = 6.67 - 3.23 = 3.44$ ft (see Figure 7-22). Therefore

$$\begin{aligned}
 R_1 &= (1561)(1.89)/5.33 = 554 \text{ kips} \\
 R_2 &= 1007 \text{ kips}
 \end{aligned}$$

Horizontal component of front row = $1007/3 = 336$ kips

Unbalanced horizontal force = $378 - 336 = 42$ kips, giving a horizontal force per pile = $42/27 = 1.6$ kips, OK.

The stability against overturning about the front row of piles is checked next. The resultant of vertical loads gives a moment about point A = 6940 ft-kips, for a moment arm $6940/1561 = 4.45$ ft, or $4.45 - 1.33 = 3.12$ ft from R_2 . The balancing moment is

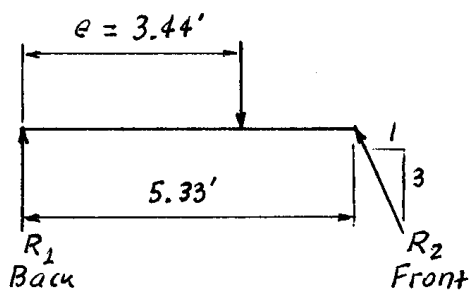


Figure 7-22 Pile details and batter.

therefore $M_b = (1561)(3.12) = 4870$ ft-kips, giving a factor of safety against overturning $4870/1890 = 2.58$, or adequate.

Note: The analysis of piles subjected to lateral load involves certain assumptions. Methods for calculating lateral resistance are broadly divided into two categories: (1) initially calculate ultimate lateral resistance, and then obtain a working lateral load by applying a factor of safety; and (2) determine acceptable deflections at working lateral load (the allowable lateral load corresponds to an acceptable lateral deflection). The lateral load in either case is also a function of the top pile condition, free-head or fixed head. For a complete review of this subject, reference is made to Prakash and Sharma (1990), and to chapter 9.

Case B. (Case A plus live load on bridge)

Live load moment about point A,

$$\begin{aligned} M_{LL} &= (175)(3.00) = 525 \text{ ft-kips} \\ \text{Total} &= 1736 \text{ kips} \quad 5575 \text{ ft-kips} \end{aligned}$$

Distance of resultant from point A, $= (5575)/1736 = 3.21$ ft.

Eccentricity $e = 6.67 - 3.21 = 3.46$ ft. Therefore

$$\begin{aligned} R_1 &= (1736)(1.87)/5.33 = 609 \text{ kips} \\ R_2 &= 1736 - 609 = 1127 \text{ kips} \end{aligned}$$

Horizontal component of front row $= 1127/3 = 376$ kips

Unbalanced force $= 378 - 376 = 2$ kips, OK.

Case C. (Case A plus live load on approach slab)

For a 22-foot long approach slab, the live load reaction per lane is 43.6 kips.

Total reaction (3 lanes) $= 43.6 \times 3 \times 0.9 = 118$ kips

Moment $= 118 \times 6.00 = 702$ ft-kips

Total vertical load $= 1561 + 118 = 1679$ kips

Total moment $= 5050 + 702 = 5752$ ft-kips

Distance of resultant from point A $= 5752/1679 = 3.43$ ft

Eccentricity $e = 6.67 - 3.43 = 3.24$ ft. Therefore

$$\begin{aligned} R_1 &= (1679)(2.09)/5.33 = 658 \text{ kips} \\ R_2 &= 1679 - 658 = 1021 \text{ kips} \end{aligned}$$

Horizontal component of front row $= 1021/3 = 340$ kips

Unbalanced force $= 378 - 340 = 38$ kips, per pile $= 38/27 = 1.41$ kips, OK.

Pile Load. From Case B, $R_2 = 1127$ kips, or per pile

$$R_2 = 1127/14 = 80.5 \text{ kips}$$

$$\text{Horizontal component} = 80.5/3 = 26.8 \text{ kips}$$

$$\text{Resultant axial load per pile } R = \sqrt{80.5^2 + 26.8^2} = 85 \text{ kips}$$

Use 45-ton piles

Load factor (strength design) method. The lateral load capacity of a pile under strength design approach would involve an estimation of the ultimate resistance. Since the most severe condition occurs under Case A (dead load and earth pressure), the comparison of factored effects and factored resistance reduces to these two loads. Because the dead load provides the resisting force, it should be factored by applying a load factor less than 1. Since the earth pressure represents the load effects, it should be factored by applying a load factor greater than 1. The two methods, load factor approach and ASD, become compatible and equivalent in this case merely by calibrating load and resistance factors to correspond to the factor of safety used in ASD.

Group II. This includes dead load, earth pressure, and wind on superstructure, and the design may consider an allowable stress 125 percent. Referring to Figure 7-23, the wind direction (lateral and longitudinal) is taken as shown, so that the component N normal to the abutment acts in the same direction as the lateral earth pressure.

The exposed depth of superstructure is computed as 11.66 feet, and includes parapet, concrete floor depth, plate girder, and superelevation. The span length exposed to wind is 96 feet. One-half of the lateral wind force is applied to the abutment, but the entire longitudinal wind must be resisted at this location. For wind computations, we use the simplified loading suggested in AASHTO Art. 3.15.2.1.3.

$$\text{Lateral wind} = (0.5)(96)(11.66)(0.05) = 28 \text{ kips} \quad N = 25.5 \text{ kips}$$

$$\text{Longitudinal wind} = (96)(11.66)(0.012) = 13.4 \text{ kips} \quad N = 5.6 \text{ kips}$$

$$\text{Total } N = 31.1 \text{ kips normal to the bent}$$

This force acts about 7.5 feet above bridge seat, or 13.5 feet above bottom of footing.

$$\text{Moment due to } N, M_N = (31.1)(13.5) = -420 \text{ ft-kips}$$

$$\text{Total moment } M = 5050 - 420 = 4630 \text{ ft-kips}$$

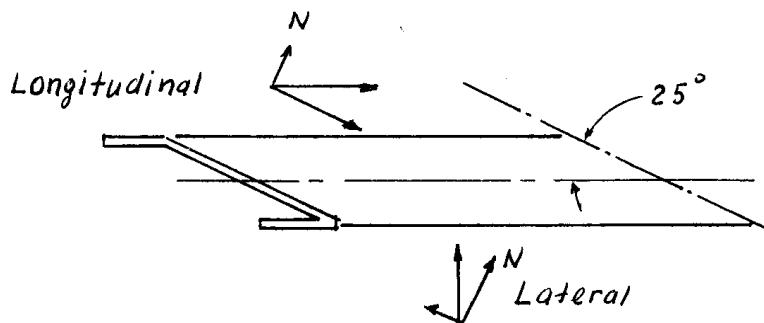


Figure 7-23 Wind forces, longitudinal and lateral.

Distance from point A to resultant = $4630/1561 = 2.97$ ft, giving $e = 6.67 - 2.97 = 3.70$ ft.
Therefore

$$R_1 = (1561)(1.63)/5.33 = 478 \text{ kips}$$

$$R_2 = 1561 - 478 = 1083 \text{ kips}$$

Horizontal component of front row = $1083/3 = 361$ kips

Unbalanced horizontal force = $(378 + 31) - 361 = 48$ kips

Per pile, horizontal force = $48/27 = 1.78$ kips, or for 125 percent stress $1.78/1.25 = 1.42$ kips, OK.

Summary and conclusions. The foregoing analysis shows that a basic problem in designing pile bents supporting deep plate-girder superstructures is how to balance the lateral earth pressures behind the abutment wall. The earth pressure of 35 lb equivalent fluid should be the minimum to be used, and is warranted if clean sand is used as backfill and the bent is allowed to move to mobilize the active state. For this example, the movement is $15 \times 0.004 \times 12 = 0.72$ inch, say 3/4 inch.

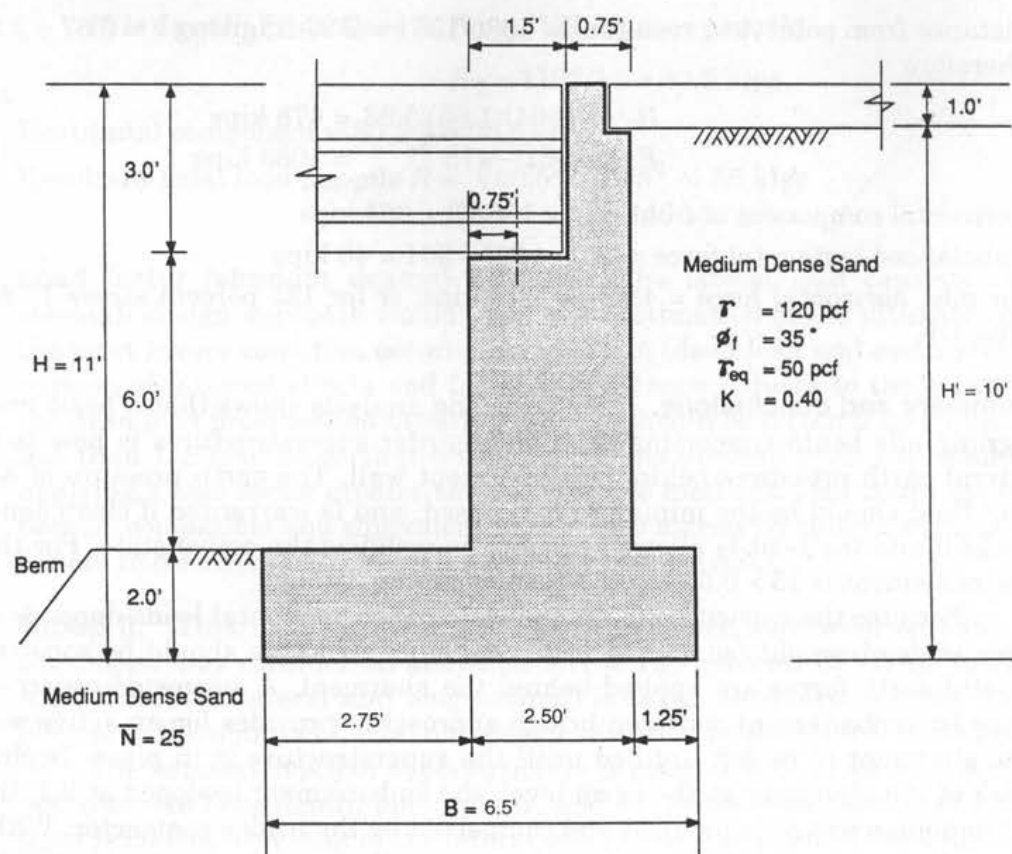
Because the capacity of batter piles to resist horizontal loads depends on the presence of dead weight (sustained load), the superstructure should be constructed before lateral earth forces are applied behind the abutment. A suggested construction procedure for embankment cones on bridge approaches provides for an active wedge behind the abutment to be left unfilled until the superstructure is in place. Beginning at the back of the abutment at the berm level, the embankment is sloped at 2:1, thus creating a triangular wedge to be filled and compacted by the bridge contractor. With heavy static or dynamic compaction used to minimize settlement, the increase in the lateral earth forces should be considered. Passive resistance in the berm in front of the bent should be ignored. If a predetermined abutment movement is to be induced, it may be superimposed on the requirements of the expansion device.

7.11 DESIGN EXAMPLE 7-2, FULL ABUTMENT

Figure 7-24 shows a full abutment cross section supporting a bridge across a waterway. The abutment has spread footing on sandy gravel with index properties as shown. The value of $K = 0.40$ approaches the at rest condition, and the ultimate bearing capacity of the foundation soil is estimated as 30.0 kips/ft². The friction angle δ between the footing and the soil has been determined to be 29°. The stability of the abutment will be checked using ASD and load factor (strength design) method.

The passive pressure in front of the abutment is neglected. A live load surcharge of 2 feet is placed on the backfill, and the weight of the approach slab is also a surcharge load. If the approach slab is supported on the abutment wall at one end and spans across the backfill, both surcharges should be omitted and the live load applied on the backwall as in Design Example 7.1. An equivalent fluid pressure is obtained as $0.40 \times 120 = 48$, use 50 lb/ft.

For conformity, we will use AASHTO designation of loads and load factors (AASHTO Table 3-22.1A), with the general group N expressed by AASHTO Equation (3-10). The application of these loads is shown in Figure 7-25. Note that this abutment provides the expansion bearing in a simple bridge span, with the other abutment fixed.



where \bar{N} = average standard penetration test blow count

T = unit weight of soil

ϕ_f = internal friction angle

T_{eq} = equivalent fluid pressure

K = horizontal earth pressure coefficient

Figure 7-24 Bridge abutment of Design Example 7-2; configuration and dimensions.

The design philosophy is to apply one-half of the longitudinal forces acting on the bridge to the expansion bearing, provided that this force does not exceed the frictional resistance of the bearing, estimated as 10 percent of the dead load. Alternatively, many designers will also check the fixed abutment using 100 percent of the longitudinal forces assuming that the expansion bearings may become frictionless at some point during the service life of the bridge. Under these assumptions, loads and forces are computed as follows (reference to Figure 7-25).

- Dead load $DL = 7.50 \text{ kips/ft}$ (dead load from superstructure)
- Live load $LL = 6.50 \text{ kips/ft}$ (live load from superstructure)
- Wind $W = 0.25 \text{ kips/ft}$ (wind load on structure)
- $WL = 0.05 \text{ kips/ft}$ (wind load on live load)
- $LF = 0.25 \text{ kips/ft}$ (braking force)

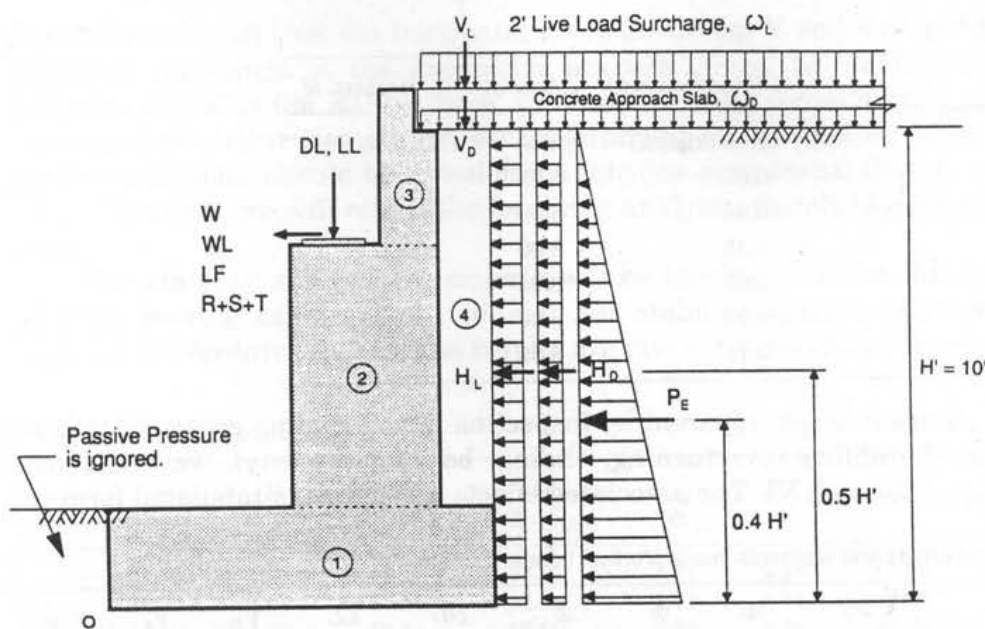


Figure 7-25 Abutment of Design Example 7-2; loads and forces.

- $R+S+T = 10\% \text{ of } DL \text{ (mainly shrinkage and temperature forces)}$
- Surcharge LL $W_L = (2)(120) = 0.24 \text{ kips/ft}^2$
 $W_D = (1)(150) = 0.15 \text{ kips/ft}^2$
 $P_E = \left(\frac{1}{2}\right)(50)(10) = 2.50 \text{ kips/ft}$
 $H_L = (0.40)(0.24)(10) = 0.96 \text{ kips/ft}$
 $H_D = (0.40)(0.15)(10) = 0.60 \text{ kips/ft}$
 $V_L = (0.24)(1.25) = 0.30 \text{ kips/ft}$
 $V_D = (0.15)(1.25) = 0.19 \text{ kips/ft}$

ASD method. For ASD analysis, the foregoing unfactored loads are used to compute moments about point 0. These effects are shown in a tabulated form as follows (see also Figure 7-25)

Vertical Loads

Item	V (unfactored)	Arm (ft)	Moment M_o
① (6.5)(2.0)(0.15)	1.95 (kips/ft)	3.25	6.34
② (6.0)(2.50)(0.15)	2.25	4.00	9.00
③ (0.75)(3.0)(0.15)	0.34	4.88	1.66
④ (1.25)(8.0)(0.12)	1.20	5.88	7.06
DL	7.50	3.50	26.25
LL	6.50	3.50	22.75
V_D	0.19	5.88	1.12
V_L	0.30	5.88	1.76

Horizontal Loads

Item	H (unfactored)	Arm (ft)	Moment M_o
P_E	2.50 (kips/ft)	4.00	10.00
H_D	0.60	5.00	3.00
H_L	0.96	5.00	4.80
W	0.25	8.00	2.00
WL	0.05	8.00	0.40
LF	0.25	8.00	2.00
$R+S+T$	0.75	8.00	6.00

Since it is not apparent by inspection which loading group controls the various aspects of stability (overturning, sliding, bearing capacity), we will consider AASHTO groups I through VI. The associated effects are shown in tabulated form.

Vertical Loads and Moments due to Vertical Loads

Item	①	②	③	④	DL	LL	V_D	V_L	Sum	%	Sum%
V (unfact.)	1.95	2.25	0.34	1.20	7.50	6.50	0.19	0.30			
I	1.95	2.25	0.34	1.20	7.50	6.50	0.19	0	19.93	100	19.93
II	1.95	2.25	0.34	1.20	7.50	0	0.19	0	13.43	125	10.74
III	1.95	2.25	0.34	1.20	7.50	6.50	0.19	0	19.93	125	15.94
IV	1.95	2.25	0.34	1.20	7.50	6.50	0.19	0	19.93	125	15.94
V	1.95	2.25	0.34	1.20	7.50	0	0.19	0	13.43	140	9.59
VI	1.95	2.25	0.34	1.20	7.50	6.50	0.19	0	19.93	140	14.24
M_v (unfact.)	6.34	9.00	1.66	7.06	26.25	22.75	1.12	1.76	Sum	%	Sum%
I	6.34	9.00	1.66	7.06	26.25	22.75	1.12	0	74.18	100	74.18
II	6.34	9.00	1.66	7.06	16.25	0	1.12	0	51.43	125	41.14
III	6.34	9.00	1.66	7.06	26.25	22.75	1.12	0	74.18	125	59.34
IV	6.34	9.00	1.66	7.06	26.25	22.75	1.12	0	74.18	125	59.34
V	6.34	9.00	1.66	7.06	26.25	0	1.12	0	51.43	140	36.74
VI	6.34	9.00	1.66	7.06	26.25	22.75	1.12	0	74.18	140	52.99

Horizontal Forces and Moments due to Horizontal Loads

Item	P_E	H_D	H_L	W	WL	LF	$R+S+T$	Sum	%	Sum%
H (unfact.)	2.50	0.60	0.96	0.25	0.05	0.25	0.75			
I	2.50	0.60	0	0	0			3.10	100	3.10
II	2.50	0.60	0	0.25	0			3.35	125	2.68
III	2.50	0.60	0	0.075	0.05	0.25	0	3.47	125	2.78
IV	2.50	0.60	0	0	0	0	0.75	3.85	125	3.08
V	2.50	0.60	0	0.25	0	0	0.75	4.10	140	2.93
VI	2.50	0.60	0	0.07	0.05	0.25	0.75	4.22	140	3.01
M_H (unfact.)	10.00	3.00	4.80	2.00	0.40	2.00	6.00	Sum	%	Sum%
I	10.00	3.00	0	0	0	0	0	13.00	100	13.00
II	10.00	3.00	0	2.00	0	0	0	15.00	125	12.00
III	10.00	3.00	0	0.60	0.40	2.00	0	16.00	125	12.80
IV	10.00	3.00	0	0	0	0	6.00	19.00	125	15.20
V	10.00	3.00	0	2.00	0	0	6.00	21.00	140	15.00
VI	10.00	3.00	0	0.60	0.40	2.00	6.00	22.00	140	15.71

It should be noted that the horizontal loads for Group V and VI should not exceed the frictional resistance of the expansion bearing. Since, by definition, this resistance has been taken as the R+S+T force, wind and braking forces should not be included in these groups. Otherwise stated, all longitudinal forces applied to an expansion substructure element should be consolidated into one component, that is, a frictional resistance. However, we will retain the foregoing analysis, merely to demonstrate the design steps.

The stability and bearing criteria will be checked now for three conditions: overturning, bearing capacity, and sliding. For stability against overturning, a check is made on the eccentricity, and the results are given in a tabulated form.

Eccentricity Check (Overturning)

Item	V (kips)	H (kips)	M_V (ft-kips)	M_H (ft-kips)	x_o ft	e ft	e_{max}	q_t (ksf)	q_{unit} (ksf)
I	19.93	3.10	74.18	13.00	3.07	0.18	<1.08	3.58	3.24
II	10.74	2.68	41.14	12.00	2.71	0.54	<1.08	2.47	1.98
III	15.94	2.78	59.34	12.80	2.92	0.33	<1.08	3.20	2.73
IV	15.94	3.08	59.34	15.20	2.78	0.47	<1.08	3.51	2.87
V	9.59	2.93	36.74	15.00	2.27	0.98	<1.08	2.81	2.11
VI	14.24	3.01	52.99	15.71	2.62	0.63	<1.08	3.46	2.72

where x_o = location of resultant from point 0 = $(M_V - M_H)/V$

e = eccentricity of resultant = $(B/2) - x_o$

e_{max} = $B/6 = 6.5/6.00 = 1.08$ ft

q_t = trapezoidal bearing pressure at toe (see Figure 6-32a), kips/ft²

q_{unit} = uniformly distributed bearing pressure at toe (see Figure 6-32c), kips/ft²

Bearing Capacity Assessment

Item	V	H	H/V	D_f/B_e	R_1	q_{ult}^v	q_{ult}^i	q_{ult}^i/FS	q_{max}
I	19.83	3.10	0.16	0.33	0.58	30.00	17.40	4.35	>3.24
II	10.74	2.68	0.25	0.37	0.43	30.00	12.90	3.22	>1.98
III	15.94	2.78	0.17	0.34	0.59	30.00	17.70	4.42	>2.73
IV	15.94	3.08	0.19	0.36	0.53	30.00	15.90	3.97	>2.87
V	9.59	2.93	0.31	0.44	0.37	30.00	11.10	2.77	>2.11
VI	14.24	3.01	0.21	0.38	0.52	30.00	15.60	3.90	>2.72

where D_f = depth from ground surface to bottom of footing = 2.0 ft

B_e = effective base width = $2x_o$

R_1 = reduction factor due to inclined load

q_{ult}^v = vertical (ultimate) bearing capacity (kips/ft²)

q_{ult}^i = inclined ultimate bearing capacity = $R_1 q_{ult}^v$ (kips/ft²)

FS = factor of safety for SPT method = 4.0

q_{max} = maximum bearing pressure = q_{unif}

(Note: the reduction factor R_1 for inclined loading is discussed in detail in chapter 8).

Resistance to sliding. Since the pressures are assumed to be uniformly distributed (Figure 6-32 c), the effective base width B_e for calculating resistance to sliding will be taken as $2x_o$. The results of the analysis are tabulated as follows:

Item	V (kips)	$\tan\delta$	F_r (kips)	FS	F_r/FS	H
I	19.83	0.554	10.99	1.5	7.33	> 3.10
II	10.74	0.554	5.95	1.5	3.97	> 2.68
III	15.94	0.554	8.83	1.5	5.55	> 2.78
IV	15.94	0.554	8.83	1.5	5.55	> 3.08
V	9.59	0.554	5.31	1.5	3.54	> 2.93
VI	14.24	0.554	7.89	1.5	5.26	> 3.01

where $F_r = V\tan\delta$

Summary. For ASD analysis, Group V gives most severe results with respect to eccentricity criteria. Group I results in the largest bearing pressure. Groups I and IV give about the least (almost the same) margin of safety in the bearing capacity pressure. These conclusions, however, cannot be generalized.

Strength design method. For this analysis, we will consider Groups I, II, and IV. The load factors γ and load coefficients β_i will be taken from AASHTO Table 3.22.1A, so that for each load type the two parameters are lumped into a single load factor $\gamma\beta_i$. This factor is as follows: DL = 1.3; LL = 2.17; $E_v = 1.3$; $E_h = 1.69$; $E_{hd} = 1.69$; $E_{hL} = 2.17$; W = 1.3; WL = 1.3; LF = 1.3 or 1.25; and R+S+T = 1.30 or 1.25. Using these factors we tabulate factored loads and moments due to factored loads.

Factored Vertical Loads V

Item	① D	② D	③ D	④	DL D	LL L	V_D D	V_L L	V_u Total
(unf.)	1.95	2.25	0.34	1.20	7.50	6.50	0.19	0	19.93
I	2.54	2.93	0.44	1.56	9.75	14.11	0.24	0	31.57
II	2.54	2.93	0.44	1.56	9.75	0	0.24	0	17.46
IV	2.54	2.93	0.44	1.56	9.75	8.45	0.24	0	25.91

Factored Moments M_v

Item	① D	② D	③ D	④ E_v	DL D	LL L	V_D D	V_L L	$M\mu_u$
M_v (unf.)	6.34	9.00	1.66	7.06	26.25	22.75	1.12	0	Total
I	8.24	11.70	2.16	9.18	34.13	49.37	1.46	0	116.24
II	8.24	11.70	2.16	9.18	34.13	0	1.46	0	66.87
IV	8.24	11.70	2.16	9.18	34.13	29.58	1.46	0	96.45

Horizontal Forces H

Item	P_E E_h	H_D E_{hD}	H_L E_{hL}	W	WL	LF	$R+S+T$	H_u
H (unf.)	2.50	0.60	0.96	0.25	0.05	0.25	0.75	Total
I	4.23	1.01	0	0	0	0	0	5.24
II	4.23	1.01	0	0.33	0	0	0	5.57
IV	4.23	1.01	0	0	0	0	0.98	6.22

Factored Moments due to Horizontal Forces, M_H

Item	P_E E_h	H_D E_{hD}	H_L E_{hL}	W	WL	LF	$R+S+T$	M_{Hu}
M (unf.)	10.00	3.00	4.80	2.00	0.40	2.00	6.00	Total
I	16.90	5.07	0	0	0	0	0	21.97
II	16.90	5.07	0	2.60	0	0	0	24.57
IV	16.90	5.07	0	0	0	0	7.80	29.77

Stability Against Overturning (Eccentricity Check)

Item	V_u (kips)	H_u (kips)	M_{Vu} (ft-kips)	M_{hL} (ft-kips)	x_o ft	e ft	e_{max} ft	q_t (ksf)	$q_{(unif)}$ (ksf)
I	31.57	5.24	116.24	21.97	2.99	0.26	<1.62	6.03	5.37
II	17.46	5.57	66.87	24.57	2.42	0.83	<1.62	4.75	3.61
III	25.91	6.22	96.45	29.77	2.60	0.65	<1.62	6.32	4.93

where x_o = location of resultant (distance from 0) = $(M_{vu} - M_{hL})/V_u$

e = eccentricity = $B/2 - x_o$

e_{max} = $B/4 = 6.50/4 = 1.62$ ft

$q_{(unif)}$ = uniformly distributed bearing pressure at toe (Figure 6-32c)

q_t = triangular or trapezoidal bearing pressure at toe (Figure 6-32)

(In this case, the resultant is in the middle third, and hence the trapezoidal diagram applies).

Bearing Capacity Check

Item	R_1	q_{ult}^u (ksf)	q_{ult}^i (ksf)	ϕq_{ult}^i (ksf)	q_{max} (ksf)
I	0.58	30.0	17.40	7.83	> 5.37
II	0.48	30.0	14.40	6.48	> 3.61
IV	0.53	30.0	15.90	7.16	> 4.93

where R_1 = reduction factor (the same as in ASD)

B_e = $2x_o$

q_{ult}^i = inclined bearing capacity = $R_1 q_{ult}^u$

ϕq_{ult}^i = factored bearing capacity

ϕ = performance factor = 0.45

q_{max} = maximum bearing pressure = q_{unif}

Resistance to Sliding. Since the uniformly distributed pressures are used, the effective width for calculating resistance to sliding is taken as $2x_o$, as in ASD analysis.

Item	V_u (kips)	$\tan\delta$	F_{ru} (kips)	ϕ_s	$\phi_s F_{ru}$	H_u
I	31.57	0.554	17.49	0.80	13.99	> 5.24
II	17.46	0.554	9.67	0.80	7.74	> 5.57
IV	25.91	0.554	14.18	0.80	11.34	> 6.22

where $F_{ru} = V_u \tan\delta$; and ϕ_s = sliding performance factor for SPT data.

Serviceability limit state criteria. Procedures for estimating the settlement of abutments under service conditions are discussed in subsequent sections. Tolerable movement criteria are discussed in section 8.9. The minimum average SPT blow count N within the range of depth from the footing base to depth B below that level is taken as 25.

Calculation of Settlement. For Group I (producing the largest bearing pressures), the effective base width is $B_e = 2x_o = 2 \times 3.07 = 6.14$ ft, and the uniform pressure is 3.24 kips/ft².

According to the Terzaghi and Peck (1967) method, reference is made to Figure 8–12 giving bearing pressures for one-inch of settlement of footings in sand. Using $N = 25$ and $B_e = 6.14$ ft, the bearing pressure corresponding to 1-inch settlement is interpolated from the graphs as 2.7 tons/ft² = 5.4 kips/ft². If the water table below the abutment foundation is assumed at least $2B$ precluding any effects on the bearing capacity, the calculated settlement of the footing is

$$\Delta = 3.24 / 5.40 = 0.60 \text{ inch}$$

From Table 5–9, the adjusted settlement using 90 percent reliability is

$$\Delta' = (1.05)(0.60) = 0.63 \text{ inch}$$

This settlement satisfies the tolerable movement criteria discussed in section 8.9.

Design of footing, ASD method. Since this is a conventional reinforced concrete substructure, the specified concrete strength is 3000 lb/in², and the reinforcing steel is Grade 40. Hence, $f_c = (0.40)(3000) = 1200$ lb/in², and $f_s = 20,000$ lb/in². The maximum bending moment for the toe section of the footing is taken at the face of the abutment wall, and is computed for a maximum uniform bearing pressure for Group I, $q_{unif} = 3.24$ kips/ft². Thus $M = (3.24 - 0.30)(2.75)^2/2 = 11.11$ ft-kips. Using $n = 9$, compute $k = 1/(1+20/9 \times 1.2) = 0.35$, $j = 1 - k/3 = 0.88$, and $a = (20,000)(0.88)/12,000 = 1.46$.

For a 3-inch cover, $d = 20.5$ in, and

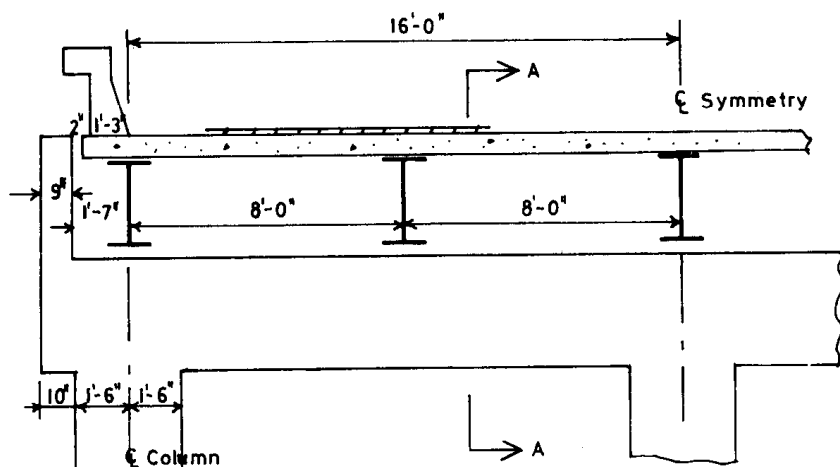
$$A_s = \frac{11.11}{(1.46)(20.5)} = 0.37 \text{ in}^2/\text{ft}, \text{ Use } \#5 @ 10 \text{ in} = 0.37 \text{ in}^2/\text{ft}$$

For maximum shear, we will take the critical section also at the wall face. Shear $V = (2.94)(2.75) = 8.08$ kips

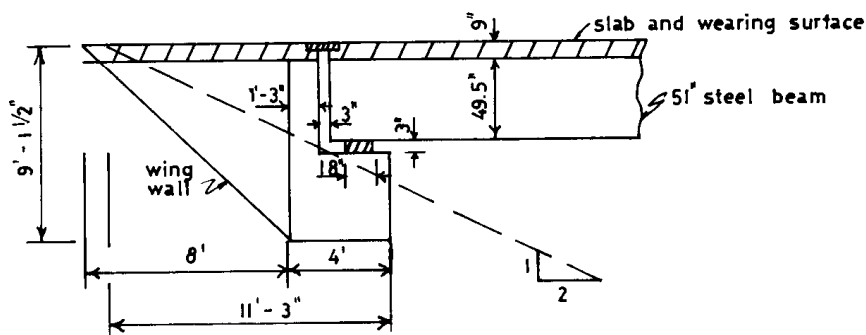
$$v = (8.08) / (20.5 \times 12) = 32 \text{ lb/in}^2 < 0.9\sqrt{f'_c} = 49 \text{ lb/in}^2$$

7.12 DESIGN EXAMPLE 7–3, SPILL-THROUGH ABUTMENT

Spill-through abutments may be selected where shallow foundations are feasible and economical. As shown in Figure 1–7, they have three main components: the footing, tapered columns, and the bridge seat. A spill-through abutment for this design example is shown in Figure 7–26 that includes a partial longitudinal elevation (transverse section) and the abutment seat. The configuration of this structure accommodates a two-lane



(a) Transverse section



(b) Section A-A

Figure 7-26 Spill-through abutment; (a) partial longitudinal elevation; (b) abutment cross section A-A.

bridge deck supported on steel beams. The bridge has two simple equal spans, each 85 feet long. Three columns are used to support the beam seat and transfer the loads to the common footing. Three of the steel beams are set directly on the columns, and the other two between columns producing bending moments in the bridge seat.

Loads and Forces.

The abutment receives loads from the superstructure as well as loads and forces applied directly to it.

Dead load from superstructure. These are as follows:

Interior Beams	$R_{DL} = 46.8 \text{ kips/beam}$
Exterior Beams	$R_{DL} = 50.2 \text{ kips/beam}$

Live load from superstructure. For maximum moment in the beam seat the live load (HS 20) is placed as shown in Figure 7-27, centered over the interior beams. However, the trucks can be placed in different positions across the roadway to give maximum load effects on the abutment elements. For maximum live load reaction, one rear axle is placed directly over the bearing line, giving a reaction

$$P = 16(1 + 71/85) + 4(57/85) = 32.1 \text{ kips (conservative).}$$

Dead load, weight of abutment. An end view of the abutment is shown in Figure 7-28. The dead load is computed as follows:

Beam Seat	= 2.4 kips/ft
Back Wall	= 0.82 kips/ft
Wing Wall (each)	= 10.2 kips
Column (each)	= 21.6 kips
Footing	= 40.5 kips (each)

Longitudinal forces. These are taken as 5 percent of two lanes of live load, or $F_L = 2(0.64 \times 85 + 18)(0.05) = 7.3$ kips, say 8 kips.

Friction. This is mobilized by temperature expansion and contraction. The abutment has teflon sliding bearings with a coefficient of friction taken as 0.06. Since the longitudinal forces due to expansion oppose each other at the fixed pier, they are transferred through the beams to the abutment bearings. Total friction

$$F_f = (46.8 \times 3 + 50.2 \times 2)(0.06) = 14.5 \text{ kips.}$$

Earth pressures. For a spill-through abutment pressures act on the beam seat and behind the columns, but they are partially offset by the earth pressure in front of the abutment. For simplicity, the earth pressure is assumed as 35-lb equivalent fluid, and since there is an approach slab a live load surcharge is not considered. The lateral pressure diagram is shown in Figure 7-29.

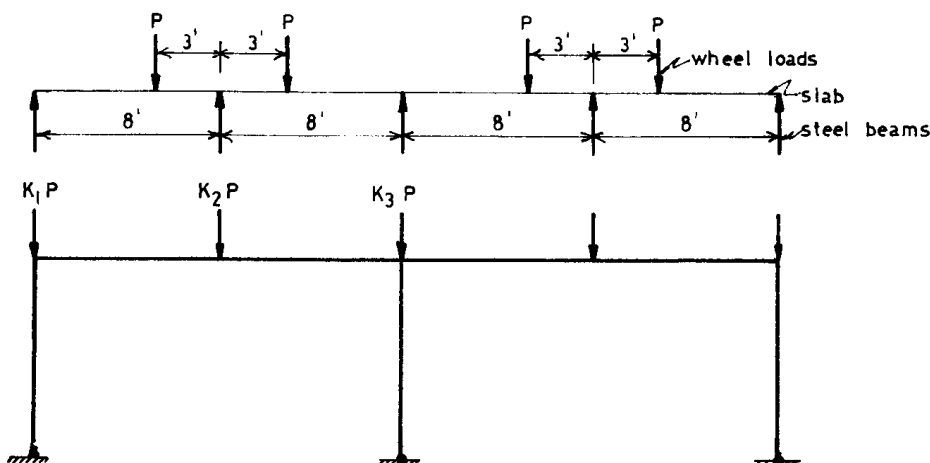


Figure 7-27 Live load arrangement, abutment of Figure 7-26.

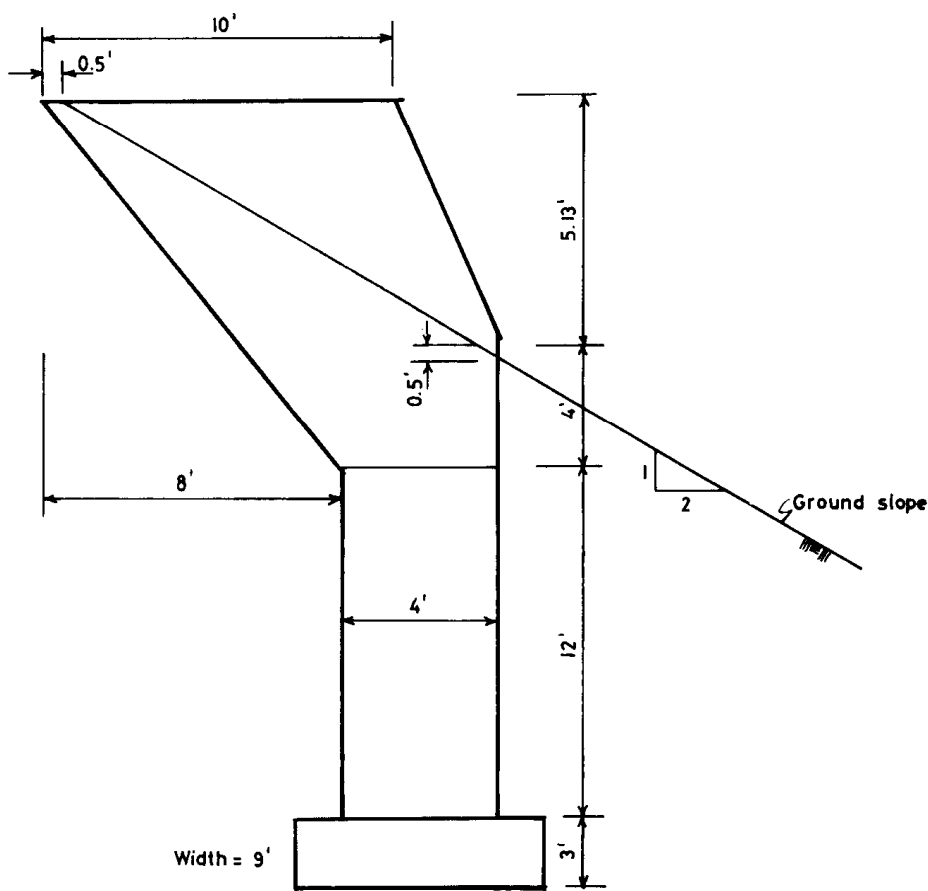


Figure 7-28 End view, abutment of Figure 7-26.

Base Stability

The abutment must be stable against sliding and overturning. The total dead load (superstructure plus abutment) and the lateral earth pressures are tabulated in Table 7-1. Also shown in this table are the longitudinal and transverse forces.

The longitudinal force 84.8 kips must be resisted by friction at the footing-soil interface. The coefficient of friction $\tan \delta$ varies widely in the range 0.25 – 0.55 (in design example 2, $\tan \delta = 0.55$). For this example, we will use $\tan \delta = 0.35$. Then the factor of safety against sliding is

$$FS = \frac{(0.35)(560.7)}{84.8} = 2.3 > 1.5$$

The factor of safety against overturning is

$$FS = 2776/1149 = 2.4 > 2 \text{ (AASHTO Article 5.5.5)}$$

Footing and Bearing Pressure

The longitudinal overturning moment about the three footings is the total overturning moment given in Table 7-1 adjusted by the moment caused by the weight of the wing wall and back wall, and the heavy reactions. The resulting moment is

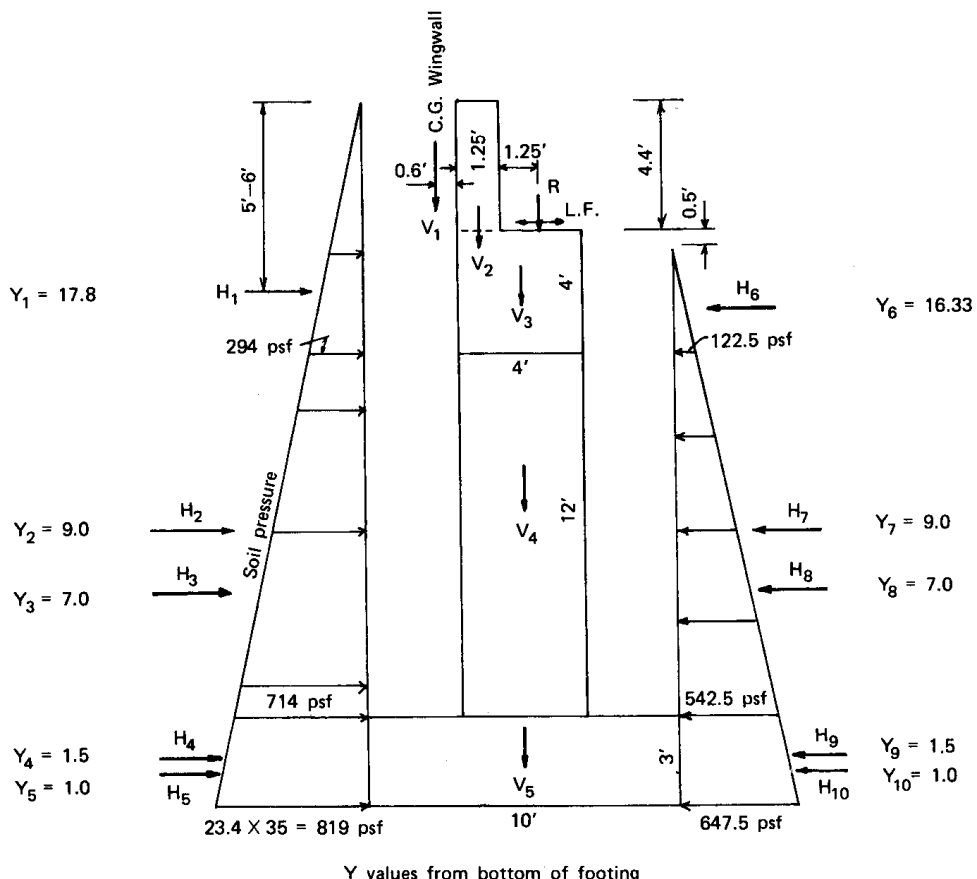


Figure 7-29 Loads on forces acting on abutment, example of Figure 7-26.

$$M_L = -1149 - 20.4(2.6) - 28.8(1.37) + 241(0.5) = 1175 \text{ ft-kips}$$

The overturning moment for one footing is, therefore

$$M_L = 1175/3 = 392 \text{ ft-kips}$$

Referring to Figure 7-27, the reactions at each column are calculated for $P = 32.1$ kips treating the beam seat as a continuous beam on rigid supports. The coefficients k_1 , k_2 and k_3 are calculated as follows:

$$k_1 = 0.24 \quad k_2 = 1.50 \quad k_3 = 0.52$$

giving $k_1P = 7.8$ kips, $k_2P = 48.8$ kips, and $k_3P = 16.9$ kips.

The vertical loads and transverse moments on footings caused by frame action are obtained from frame analysis and are as follows:

Outside Columns =	$P = 200.3$ kips	$M_T = 40$ ft-kips
Inside Columns =	$P = 290.0$ kips	$M_T = 0$

The soil pressure is calculated from the relationship

$$p = \frac{P}{A} \pm \frac{M_L}{S_L} \pm \frac{M_T}{S_T}$$

Table 7–1 Vertical Loads, Lateral Forces, and Moments about Toe of Footing, Design Example of Figure 7–26

Type of Force	Magnitude	(k)	Arm (ft)	Moment (ft-k)
H_1 : back soil pressure	$\frac{0.294}{2}(36.67)(8.4)$	45.3	17.8	+ 806
H_2 : back soil pressure	$0.294(3 \times 3)(12)$	31.8	9.0	+ 286
H_3 : back soil pressure	$(0.714 - 0.294)\frac{9}{2}(12)$	22.7	7.0	+ 159
H_4 : back soil pressure	$0.714(3)(3 \times 9)$	57.8	1.5	+ 87
H_5 : back soil pressure	$(0.819 - 0.714)\frac{3}{2}(27)$	4.3	1.0	+ 4
H_6 : front soil pressure	$0.1225\left(\frac{3.5}{2}\right)(36.67)$	- 7.9	16.33	- 128
H_7 : front soil pressure	$0.1225(3 \times 3)(12)$	- 13.2	9.0	- 119
H_8 : front soil pressure	$(0.5425 - 0.1225)\frac{9}{2}(12)$	- 22.7	7.0	- 159
H_9 : front soil pressure	$0.5425(3)(3 \times 9)$	- 43.9	1.5	- 66
H_{10} : front soil pressure	$(0.6475 - 0.5425)\frac{3}{2}(27)$	- 4.2	1.0	- 4
Longitudinal force		+ <u>14.9</u>	19.0	+ <u>283</u>
Total longitudinal force		84.8		
Total overturning moment				1149
V_1 : weight of wing-walls	$2(10.2)$	- 20.4	7.6	- 155
V_2 : weight of back wall	$0.82(35.17)$	- 28.8	6.4	- 184
V_3 : weight of beam seat	$2.4(35.17)$	- 84.4	5.0	- 422
V_4 : weight of columns	21.6×3	- 64.8	5.0	- 324
V_5 : weight of footings	40.5×3	- 121.5	5.0	- 607
R : dead-load reaction	$3 \times 46.8 + 2 \times 50.2$	- 240.8	4.5	<u>-1084</u>
Total vertical force		-560.7		
Total righting moment				-2776

where the subscripts denote longitudinal and transverse directions. The section properties are calculated as follows

$$A = 9 \times 10 = 90 \text{ ft}^2, \quad S_L = 9 \times 10^2/6 = 150 \text{ ft}^3, \quad S_T = 10 \times 9^2/6 = 135 \text{ ft}^3$$

For outside columns

$$p = \frac{200.3}{90} \pm \frac{392}{150} \pm \frac{40}{135} = 2.22 \pm 2.61 \pm 0.30 = 5.13 \text{ or } -0.69 \text{ kips}/\text{ft}^2$$

For inside columns

$$p = \frac{290}{90} \pm \frac{392}{150} = 3.22 \pm 2.61 = 5.83 \text{ or } 0.61 \text{ kips}/\text{ft}^2$$

Since there can be no uplift pressure underneath the footing, the outside footings may be reanalyzed ignoring tension, or some soil weight above the footing may be included in the calculations. The maximum soil pressure 5.83 kips/ ft^2 is within the allowable.

Whether the longitudinal moment should be resisted equally by three columns and their footings depends mainly on the stiffness of the superstructure and the rigidity of the abutment. For this example, this assumption is valid. Other possible load conditions to be investigated include live load in one lane only. This would increase the lateral bending moment at the bottom of the outside column by about 50 percent, and would induce a lateral moment at the bottom of the inside column close to 20 ft-kips. The total

vertical load on the outside column would be somewhat increased, but the load on the inside column would be slightly decreased. The new soil pressure would change but not enough to warrant a larger footing.

Other Members

The design of the abutment is completed by calculating shears and moments in the beam seat, back wall, columns, and footings, and then estimating the amount of reinforcement to resist moments and shears in each member.

7.13 DESIGN EXAMPLE 7-4, ABUTMENT FOR A SIMPLE SPAN DECK TRUSS BRIDGE

A simple span highway deck truss bridge is 160 feet long and carries a two-lane deck. The design of the superstructure and the two abutments is based on the 1961 AASHTO Specifications and California Bridge Standards.

A typical end and front view of the abutment is shown in Figure 7-30(a) and (b), respectively. Special abutment features are a high back wall resulting from the superstructure depth, a long wing wall separated from the main abutment by means of an open joint and stepped up as shown, and a low beam seat.

Loads and forces. These are (1) dead load from the superstructure and the weight of abutment; (2) live load; (3) wind on structure and live load, (4) braking (longitudinal) forces; (5) seismic forces; and (6) special loads that may be specified by the supervising authority.

Design considerations. Apparently, the 160-foot long span designed as a truss is in reality too short to be economically desirable. It is used, however, to demonstrate the design principles and effects on the selection and design of the superstructures. A Warren-type truss is selected with eight 20-foot panels, and the trusses are spaced at 19-foot centers. The stringers in the deck are designed to span the 20-foot floor beams, which are placed at each upper panel point. The allowable foundation pressure is 8 kips/ft².

Horizontal forces acting normal to the structure do not ordinarily act in the same horizontal plane as the main truss supports, and thus produce a torsion or overturning effect. These forces will be transferred from the point of application to the supports through members that are the most stiff rather than members arbitrarily added or designated for this purpose. Therefore, judgment is needed to determine the method of analysis to be used for each particular case.

One method of dealing with the overturning effect is to make the deck continuous and stiff to carry the transverse forces to the ends, where they are transmitted to the main truss supports by means of end sway bracing. Another method is to make the deck discontinuous (expansion joints at each panel). In this way, the horizontal forces acting on the upper portion of the bridge are transferred to the lower chords by means of the bracing at each panel. In the latter case, relative mass and stiffness of members should be considered in conjunction with the character of forces involved.

Design of abutment wall. Referring to Figure 7-30, the critical section for bending is 21 feet below the top of the wall.

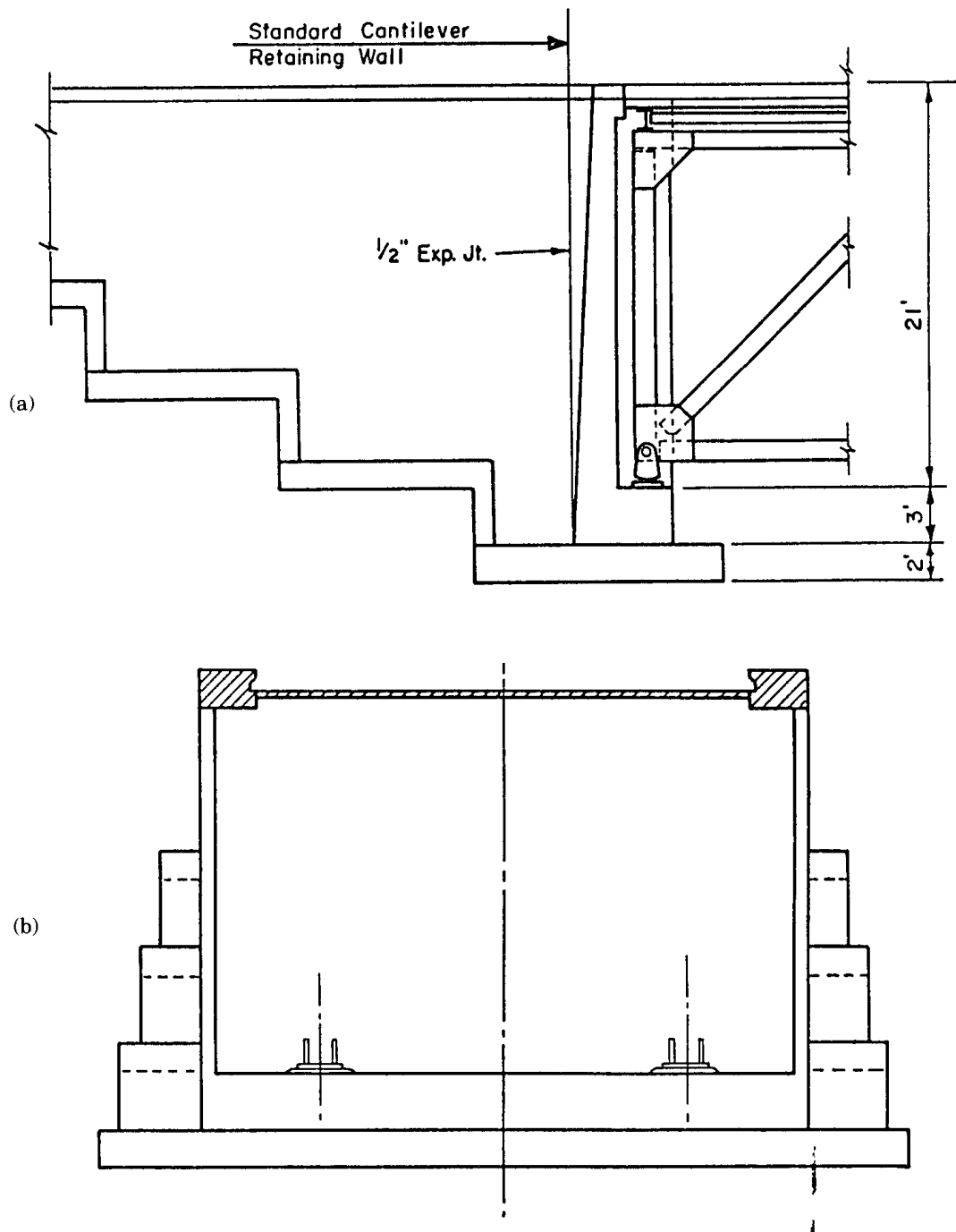


Figure 7-30 End and front view of abutment for truss bridge; Design Example 7-4.

Design stresses are: $f_s = 20,000 \text{ lb/in}^2$; $f_c = 1200 \text{ lb/in}^2$; and design lateral earth pressure = 36 lb equivalent fluid, plus 2 foot surcharge. Using a wall width at the top 12-inch minimum and a batter 5/8 in/ft, the wall thickness at the bottom is about 25 1/8 inches, giving $d = 22.5$ inches.

The moment at the base is computed as 71.4 ft-kips, hence

$$A_s = \frac{71.4}{1.46 \times 22.5} = 2.17 \text{ in}^2/\text{ft}, \text{ Use } \#11 @ 8\frac{1}{2} \text{ in} = 2.20 \text{ in}^2/\text{ft}$$

However, for a complete analysis the moments are calculated at various wall heights and A_s is computed accordingly. The results are shown in Figure 7-31 in graphical form. It can be seen that at about $H = 15.5$ feet the bar spacing can be doubled, that is, alternate #11 bars are omitted.

Stability analysis and bearing pressure. Because the abutment configuration is not uniform, the analysis will consider loads and forces acting on the entire structure, rather than on a foot length of the abutment. Referring to Figure 7-32, loads are computed in this manner, and moments are calculated about point 0, the back of the footing. The results are tabulated as follows.

Item		Weight	Arm x	M_o
Surcharge	$2 \times 6.25 \times 0.12 \times 32$	=	48	3.12
Backfill A	$5 \times 24 \times 0.12 \times 32$	=	460	2.50
Backfill B	$1/2 \times 1.25 \times 24 \times 0.12 \times 32$	=	58	5.42
Stem C	$1/2 \times 1.25 \times 24 \times 0.15 \times 32$	=	72	5.84
Stem D	$1 \times 24 \times 0.15 \times 32$	=	115	6.75
Truss Seat	$3 \times 3 \times 0.15 \times 32$	=	43	8.75
Curtain Walls	$2 \times 21 \times 3 \times 0.15 \times 1$	=	19	8.75
Footing	$13 \times 2 \times 0.15 \times 42$	=	164	6.50
Fill on toe	$3 \times 2.75 \times 0.12 \times 32$	=	32	11.62
Fill on ends of Footing	$3 \times 13 \times 0.12 \times 10$ + $1/2 \times 8.67 \times 13 \times 0.12 \times 10$	=	47	6.50
			68	4.33
Total				1,126 kips
				5,380 ft-kips

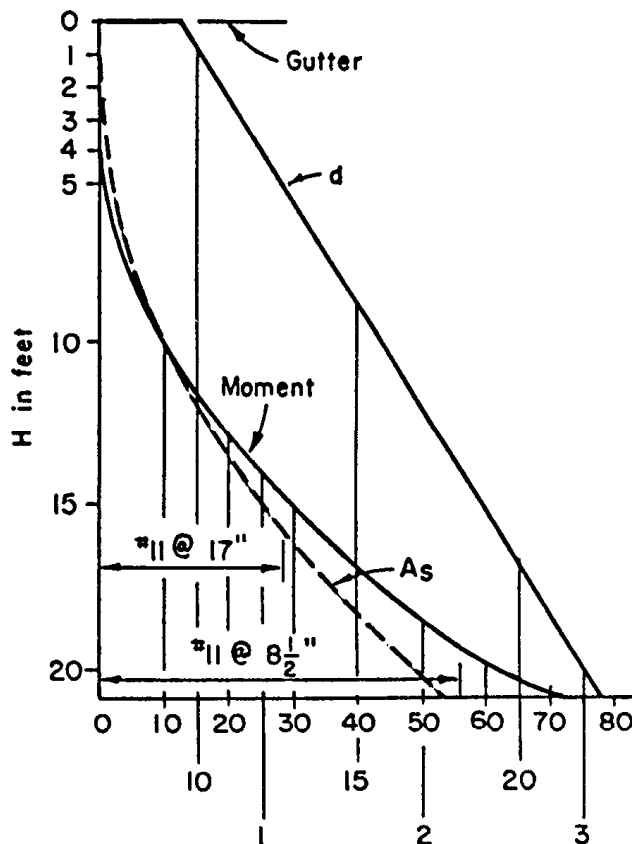


Figure 7-31 Moment and A_s diagram as a function of wall height; abutment of Figure 7-30.

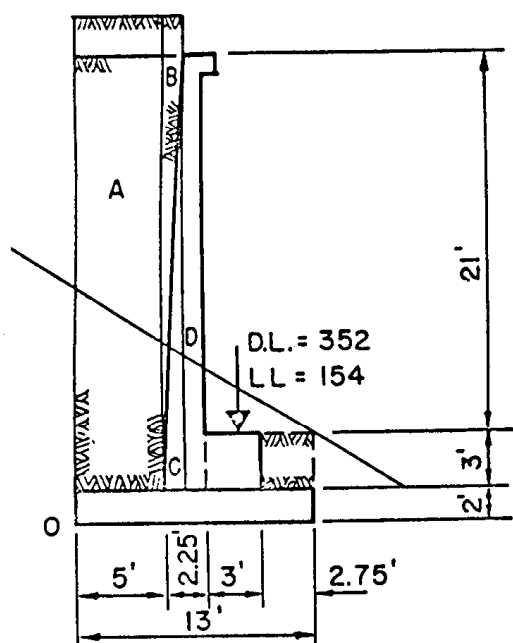


Figure 7-32 Abutment cross section showing dimensions and loads; Design Example of Figure 7-30.

Earth pressure with 2-foot surcharge (36 lb equivalent fluid) = 129.8 ft-kips per foot of abutment wall, or the entire abutment

$$\begin{aligned}
 M_{eo} &= 129.8 \times 26.75 & = 3,470 \text{ ft-kips} \\
 \text{DL Superstructure} &= 352 \times 8.75 & = 3,080 \text{ ft-kips} \\
 \text{LL Superstructure} &= 154 \times 8.75 & = 1,350 \text{ ft-kips} \\
 \text{Total} = \text{Vertical load} & \quad V = 1632 \text{ kips} & M_o = 13,280 \text{ ft-kips}
 \end{aligned}$$

Distance x of resultant from point 0 = $13280/1632 = 8.13$ feet

For a footing 13 feet wide \times 42 feet long, the section properties are

$$A = 13 \times 42 = 546 \text{ ft}, \quad I = 42 \times 13^3/12 = 7,700 \text{ ft}^4$$

Also, eccentricity $e = 8.13 - 6.50 = 1.63$ feet.

The footing pressure is obtained as

$$p = \frac{1632}{546} \pm \frac{1632 \times 1.63 \times 6.5}{7700} = 3.00 \pm 2.25$$

or

$$p_{max} = 5.25 \text{ kips/ft}^2, p_{min} = 0.75 \text{ kips/ft}^2$$

For stability against overturning we consider dead loads and earth pressures.

$$DL\text{ moment about point }0 = 5380 + 3080 = 8460 \text{ ft-kips}$$

DL reaction $\equiv 1126 + 352 \equiv 1478$ kips

Distance of resultant from point 0 = $8460/1478 = 5.72$ ft. or

$$\text{distance from toe} = 13.00 - 5.72 = 7.28 \text{ ft}$$

Balancing moment = $1478 \times 7.28 = 10759$ ft-kips

Balancing moment = $1478 \times 7.28 = 10759$ ft-kips,
and stability against overturning = $10759/3470 = 3.10$ OK

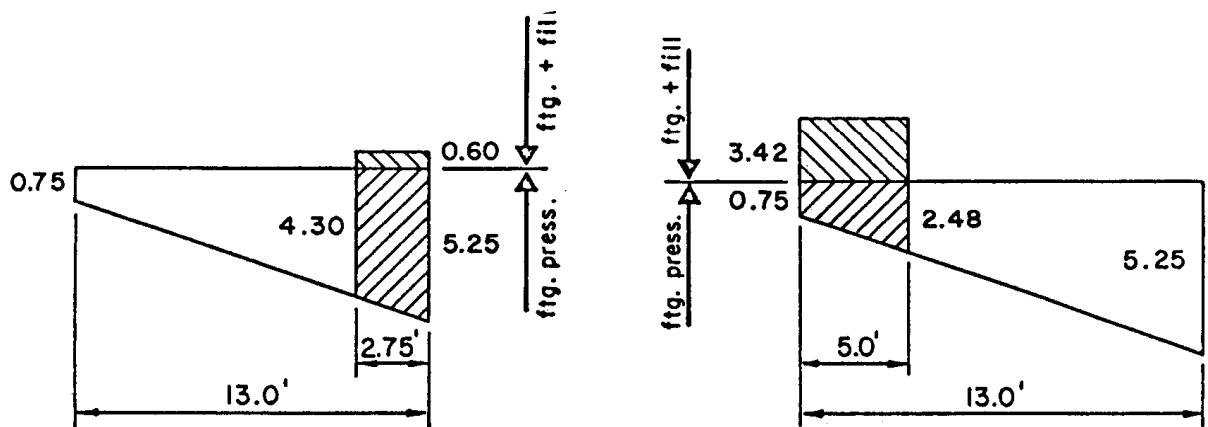


Figure 7-33 Pressure diagram, footing of Design Example 7-4.

For stability against sliding, the total lateral earth pressure is

$$10.66 \times 26.75 = 285 \text{ kips}$$

Using a coefficient of friction $\tan \delta = 0.35$, the force resisting sliding is $1478 \times 0.35 = 517$ kips, giving a factor of safety against sliding = $517/285 = 1.8$, OK.

Design of footing. For a 2-foot thick footing, $d = 20\frac{1}{2} \times \text{inches}$

Toe design. Footing weight = 0.30 kips/ft

Toe fill = 0.36 kips/ft

Total = 0.66 kips/ft

Moment at the face of the seat

$$M = (4.30 - 0.66)(2.75^2)/2 + (5.25 - 4.30)(2.75^2)/3 = 13.7 + 2.4 = 16.1 \text{ ft-kips}$$

$$A_s = \frac{16.1}{1.46 \times 20.5} = 0.54 \text{ in}^2$$

Extending alternate bars from the stem will be OK.

Heel design. Available $d = 21.5$ inches

Footing weight = $2 \times 0.15 = 0.30$

Fill on heel = $26 \times 0.12 = 3.12$

Total = 3.42 kips/ft

Moment at the face of the wall

$$M = (3.42 - 0.75)(5^2)2 - (2.48 - 0.75)(5^2)6 = 33.3 - 7.2 = 26.1 \text{ ft-kips}$$

$$A_s = \frac{26.1}{1.46 \times 21.5} 0.83 \text{ in}^2/\text{ft}, \text{ Use } \#7 @ 8\frac{1}{2} = 0.85 \text{ in}^2/\text{ft}$$

7.14 ABUTMENTS FOR ARCH BRIDGES

Arch bridges are structures shaped and supported in such a manner that intermediate transverse loads are transmitted to the supports primarily by axial compressive thrusts. Thus, the end supports (abutments) must be capable of developing lateral as well as normal reaction components.

An important decision in the design stage is the choice between abutments that are capable of providing the necessary horizontal reaction components and the use of a tied arch where the horizontal thrust is resisted by a tension bowstring (see also section 5.1).

Factors favoring the use of an elastic arch with spandrel columns and strong abutments are, in the sequence of importance: (1) strong foundation materials (such as competent rock) to withstand compression at or near the surface; (2) a high roadway alignment; and (3) site conditions allowing encroachment of the arch rib on the space between abutments. If the site is favorable, this choice is more economical because the ground strength is utilized to replace structural materials.

Typical arch forms. Early arches were of the voussoir or arch block, types. The early voussoir arch bridges consisted of a series of block usually with mortar joints. The individual arch blocks were held in equilibrium under the action of the lateral crown thrust T as shown in Figure 7-34. Once this crown thrust was determined, it could be combined with the various active external forces (dead or live) to form a line of axial pressure as shown. In these cases the abutment or end support was merely the end block of the system, and its function was to transmit the axial thrust and vertical load to the underlying foundation materials.

Modern arch bridges are monolithic or elastic structures. The term "elastic" refers to relevant elastic theories whereby the analysis takes into account the deflection or elastic distortion of the truss members under load. An example of an arch proper for concrete bridges is shown in Figure 7-35. Usually, this consists of a series of independent solid ribs or a single solid barrel. The stress distribution articulates two distinct structural forms: fixed arches and hinged arches, as shown in Figure 7-36. The latter

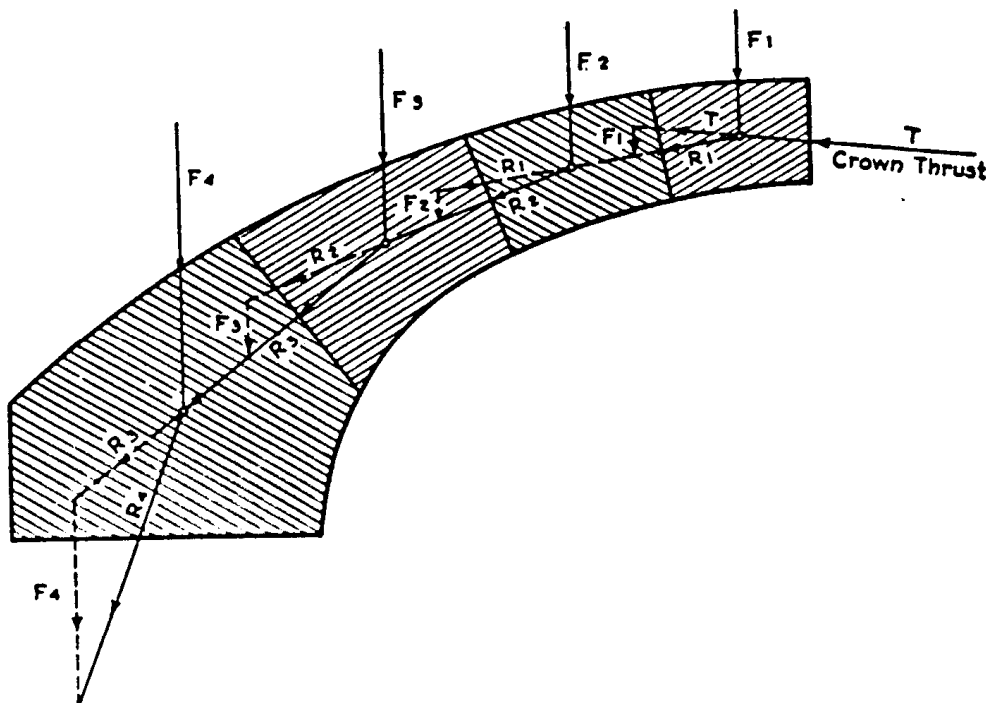


Figure 7-34 Early Arch (Voussoir type).

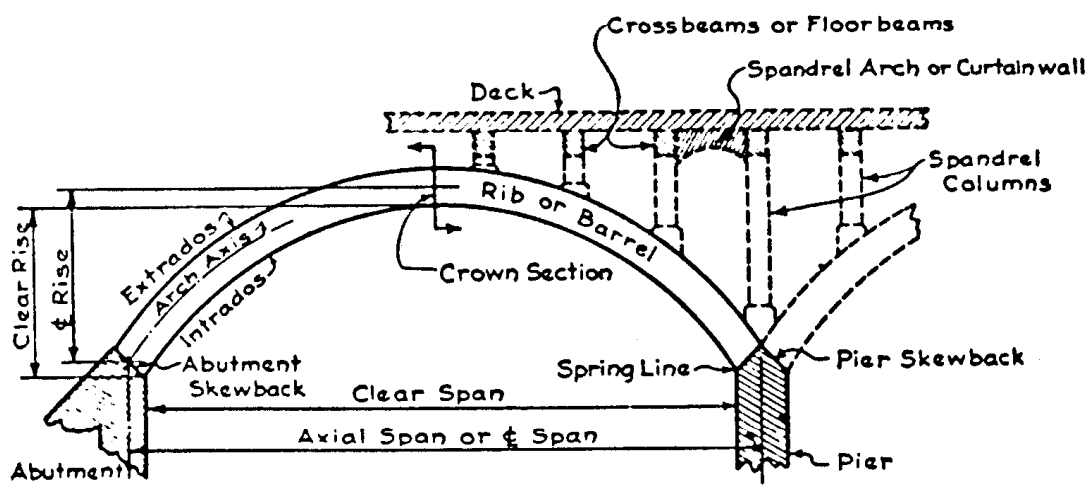


Figure 7-35 Structural arrangement of arch proper.

may be arranged as a single-hinge, two-hinge, or three-hinge type. The hingeless or fixed arch is by far the most common type in concrete bridges, although the other types are also utilized to some extent. For steel construction both fixed and hinged types are common.

The fixed arch, the two-hinged arch, and the single-hinged arch are subjected to stresses because of changes in temperature, differential settlement, or displacement of supports, or because of any compression, shrinkage and long-term creep in the material. The three-hinged arch is a statically determinate structure, hence free from these stresses.

Various configurations of abutments are shown in Figures 7-35 and 7-36. Essentially, these are massive structures shaped to receive the load primarily in com-

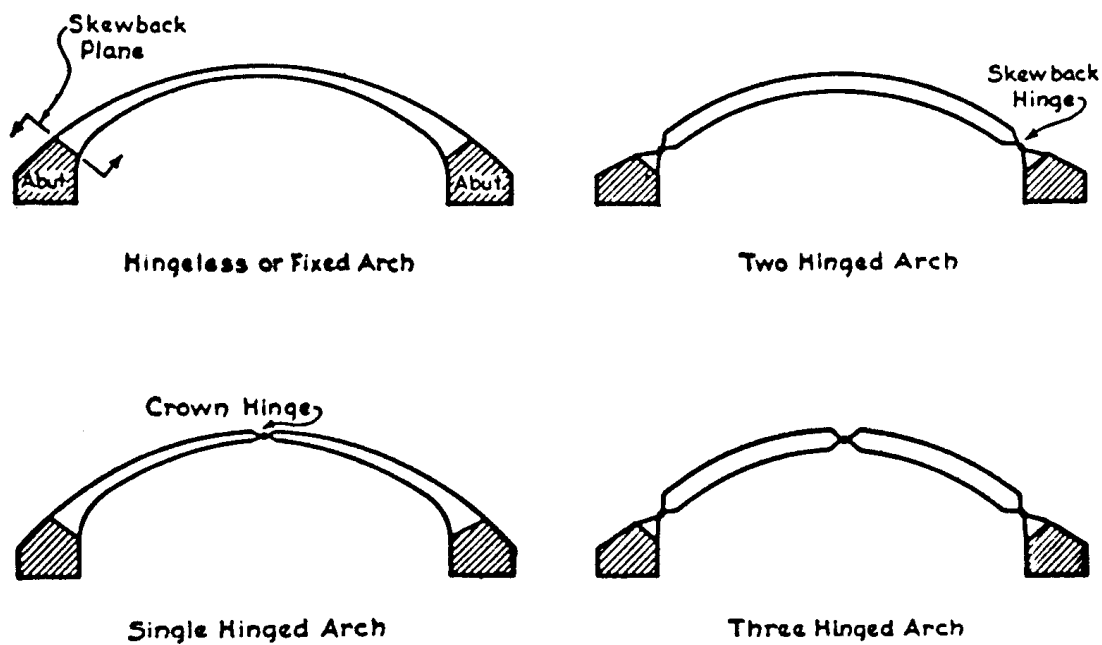


Figure 7-36 Stress distribution in arch proper, fixed and hinged arches.

pression and transfer this load (axial or lateral) to underlying rock or other firm material. Where solid rock is not available, the abutment may be designed and detailed to transfer the loads to piles or other suitable foundation elements. Hence, abutment configurations for arch bridges are not standardized, but are shaped according to the arch form, applied loads, and foundation materials.

Effect of support displacement. If the end supports can be assumed as fixed and unyielding, the end reactions perform zero work, and the first order analysis need not be modified. Where the abutments are expected to yield under load, a portion of the external energy will be used up in displacing them, so that the amount of energy absorbed by the frame will be reduced by the same amount. The effect of support displacement may be evaluated by introducing between the true structure and its supports an "ideal" section whose unit distortion is such as to completely reproduce the effect of the support. This ideal section is assumed in turn to rest on a rigid support, so that the original method of analysis can be carried out. Support movements are thus handled in the context of the analysis, either if they are known in absolute terms or if they are functions of the reactive forces.

For the example shown in Figure 7-37(a), the left abutment is not truly fixed at the skewback section *a-a*, but distorts under load to some position such as section *b-b*.

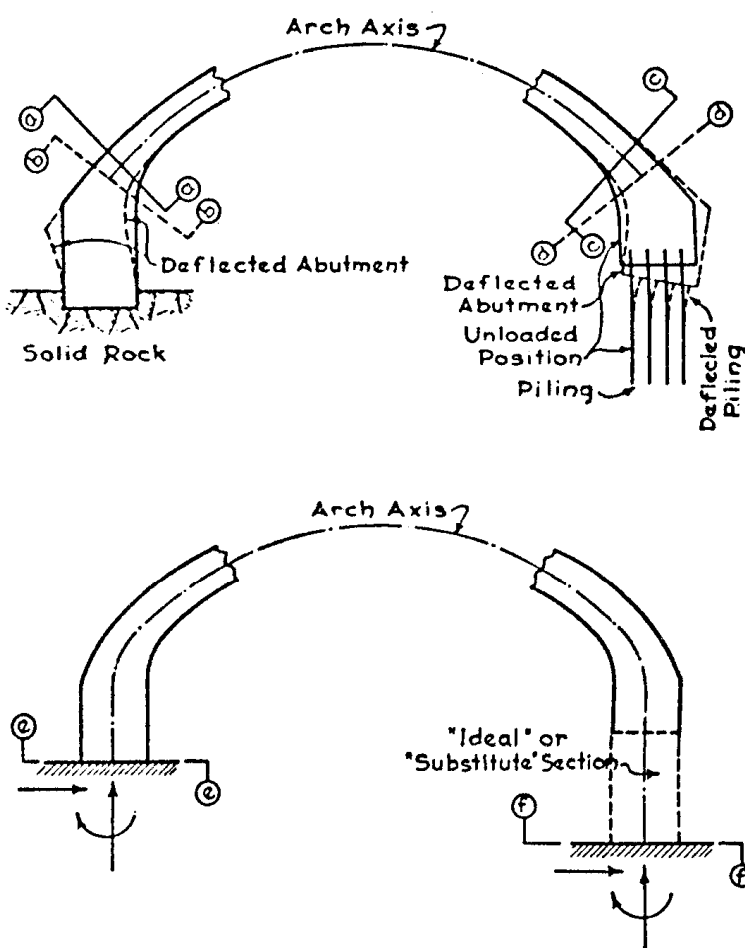


Figure 7-37 Example of yielding supports.

The base of the abutment rests, however, on solid rock so that the analysis can be completed without significant error if we assume the rock extends clear around to the rock base. This means that we consider section *e-e* in Figure 7-37(b) as the skewback section.

For the condition shown at the right support, the solution is not simple. However, if we can estimate the displacement that the pile footing will undergo under load, we may replace this footing by an "ideal" or "substitute" section of the same basic material as the arch rib proper, having dimensions that will make it deflect or distort under load exactly the same amount as the original footing. Figure 7-37(b) shows a condition where this substitution has been made. Thus, the "equivalent" frame has the skewback sections at *e-e* on the left support and *f-f* on the right. This structure may be analyzed as a fixed arch (Xanthakos, 1994).

7.15 ABUTMENTS FOR SUSPENSION BRIDGES

The cables of suspension bridges have a profile that is the reversed shape of an arch, and must resist tension forces. The abutments must therefore carry these forces and transfer them to the ground.

In rare cases it is possible to anchor the cables in natural rock. The shaft or tunnel that is to contain the anchor chain must then be driven to such depth and to reach and penetrate rock that is perfectly sound, proof against weathering, and of sufficient thickness to accommodate the anchorage.

Masonry anchorages and concrete blocks may be embedded below ground level, with backstays connecting them to the nearest towers, or they may constitute the end abutments of the side spans. The latter arrangement generally requires bending or curving the line of the cable or chain from its initial inclination to a more vertical direction in order to secure the necessary depth of anchor plate without excessive length of anchorage. In either scheme, the tensile forces transmitted to the masonry construction or end abutments must be resisted by friction at the base and by resisting pressure of the abutting earth. In addition to stability against sliding, these structures must also be designed for stability against tilting or overturning. The extreme pressures on the base should also be checked to ensure that they do not exceed the allowable stresses on the foundation materials.

Foundations on piles should be avoided where possible because they may give insufficient security against displacement of the anchorage. If such foundations are unavoidable, an ample proportion of bottom piles should be provided.

Special example. An unusual abutment is the foundation anchorage for the Humber suspension bridge in England, currently the longest suspension span in the world. The 36,000 ton (metric) pull from the suspension cables is eventually transferred into a clay formation at the Barton site by an anchorage scheme of composite construction. The initial high stress concentration is dissipated by terminating the steel cables in the upper half of the anchorage block. The lower part of the structure consists of five sections 24.5 meters (80 ft) deep excavated between diaphragm walls, as shown in Figure 7-38. The composite construction is over 70 meters (240 ft) long and has an average width of 40 meters (131 ft).

The main purpose of the composite construction was to penetrate the underlying clay in a controlled manner in order to prevent flooding of the excavation that might soften the clay formation and cause anchorage problems. The possibility of long-term effects was also considered, and the decision was to accelerate the construction program

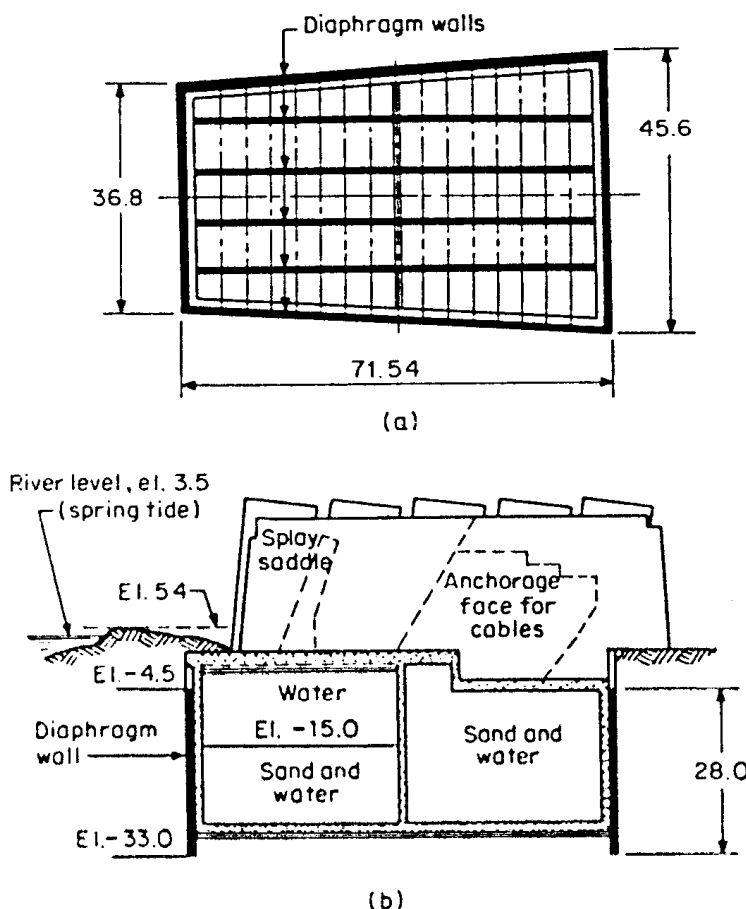


Figure 7-38 Foundation anchorage for the Humber suspension bridge at the Barton site: (a) plan showing diaphragm wall block and anchorage; (b) longitudinal section. All dimensions and elevations in meters.

to avoid these effects. However, simultaneous excavation of two adjoining cells between diaphragm walls was avoided. The bottom concrete in the cells was placed immediately following the removal of the overburden. By reducing the time the excavation was open, it was possible to control swelling and bottom softening that might result in a loss of strength.

The dead weight of the cell structure of the anchorage was increased considerably by pumping sand and water inside. The load from this operation was introduced progressively in order to control and check the response of the foundation.

The horizontal bracing of diaphragm walls across the five sections was provided by precast concrete struts placed in sets of two. This type of bracing on a project of this magnitude may well be regarded as the progenitor of the adaptation of precast members in large underground works.

A partial view of the two massive blocks is shown in Figure 7-39. The prefabricated struts have been left as permanent bracing. Although the entire construction is hardly a derivative of the classical abutment type, it is consistent with general definition of the end supports of the bridge, that is, the massive blocks receive the enormous tensile forces from the superstructure and transmit these forces to the foundation strata.

Vehicle loading. Section 2.3 provided a brief commentary on the rational design of long-span bridges and the associated vehicle loading. In general, the lack of an explicit design code inhibits the design approach, and very often the live load is established by the design consultant. Certain types of long-span bridges may become sensitive to er-

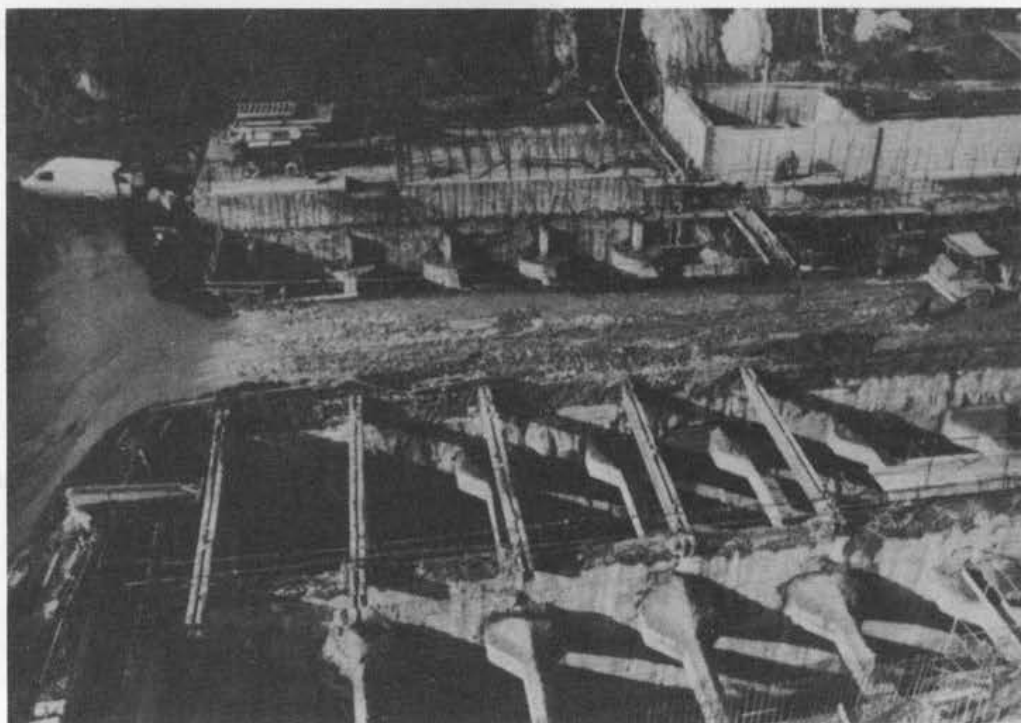


Figure 7-39 Part of the Humber bridge-foundation anchorage showing one of the five cells during excavation. Note the sets of precast-concrete struts (ICOS).

rors or to changes in the live load model and distribution. Cable-stayed and suspension bridges may be considered typical cases that usually would fall outside the range of most codes normally appropriate for a shorter bridge under the same conditions.

Whereas the credible load occurring on a short-span bridge is the heaviest truck or trucks that can travel on the bridge deck, this is not necessarily the case for a long-span bridge, because the structure will not be entirely covered by the heaviest possible vehicles. For example, maximum loading on suspension bridges is known to occur when the traffic is stationary and bumper-to-bumper. When traffic begins to move, vehicle distance increases and load intensity decreases. For the maximum loading, therefore, the traffic is stationary and allowance should not be made for full impact.

Based on the foregoing criteria the ASCE Committee on Loads and Forces for Bridges (1981) provided recommendations for a basic lane load consisting of a uniformly distributed load U , and a single concentrated load P (Xanthakos, 1994). If more than one span is loaded, only one concentrated load P will be used per lane. No allowance is made for impact. As an example, for a loaded length of 6400 feet (1950 m), the concentrated load is 168 kips and the lane load is 400 lb/ft of lane.

The rate of dead to live load becomes quite relevant to the method of analysis. With the working stress method, the ultimate strength state is automatically exceeded when the allowable stress (usually 40 to 50 percent the ultimate strength) is exceeded, and this applies to both the structure and the soil. With strength design (load factor), the required strength is merely the sum of the factored loads. If the dead load D is the predominant load, the resulting required strength is merely $1.3D$. Considering the variability of resistance, engineers may be tempted to use strength design indiscriminately because it will give a more "economical" design, although the level of safety may not correspond to allowable stress design.

7.16 INTEGRAL ABUTMENTS

Fully integrated continuous construction was briefly discussed in section 1.3, and abutment details for integral bridges are shown in Figure 1–11(a) through (c) for three states, namely Illinois, Tennessee, and Ohio.

The routine use of continuous construction in the United States and Canada and the increase in the number of transportation departments that have adopted this design is shown in Figure 7–40. As of 1990, about 87 percent of responding departments used continuous construction with integral abutments for short- and medium-span bridges.

Many bridges built with deck joints at the abutments have been severely damaged because of the growth and pressure generated by jointed rigid pavements. After the deck joints are closed, the bridge deck is squeezed by the generation of pavement pressures that can easily exceed 1000 lb/in². Cumulatively, the total force generated by these pressures can reach 650 tons per lane of approach pavement (Burke, 1987). When the design of abutments for nonintegral bridges is finalized, these forces are not accounted for. In longer bridges with intermediate deck joints, piers have been cracked and in some instances fractured.

Stress considerations in integral bridges. The usual response to integral bridges is concern for potentially higher stresses that may develop in longer bridges, since integral construction is essentially equivalent to bridges with deck joints that closed. Although the majority of bridges with integral abutments have performed satisfactorily, many of them have demonstrated high stress levels. For example, an abutment supported on a single row of piles (see also section 1.3) may be considered flexible enough to accommodate longitudinal thermal cycling of the superstructure and dynamic end rotations induced by moving vehicles. However, the piles are routinely subjected to axial and flexural stresses that may approach, equal, or exceed the yield stress (Wolde-Tinsae, Greimann, and Yang, 1982; Jorgenson, 1983). Gamble (1984) has emphasized the effect of restraint stresses and the cracking that has occurred in continuous concrete frame bridges. In some instances, concrete strength below the specified and absence of shear reinforcement contributed to the overstress problem, although the failure of the structure was caused mainly by its stiffness and resistance to shrinkage and contraction of

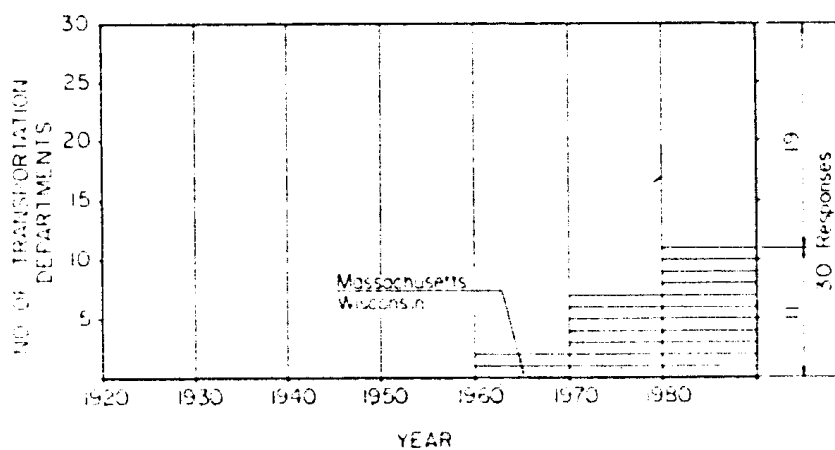


Figure 7–40 Design trends for continuous bridges: early conversion of simple spans to continuous spans.

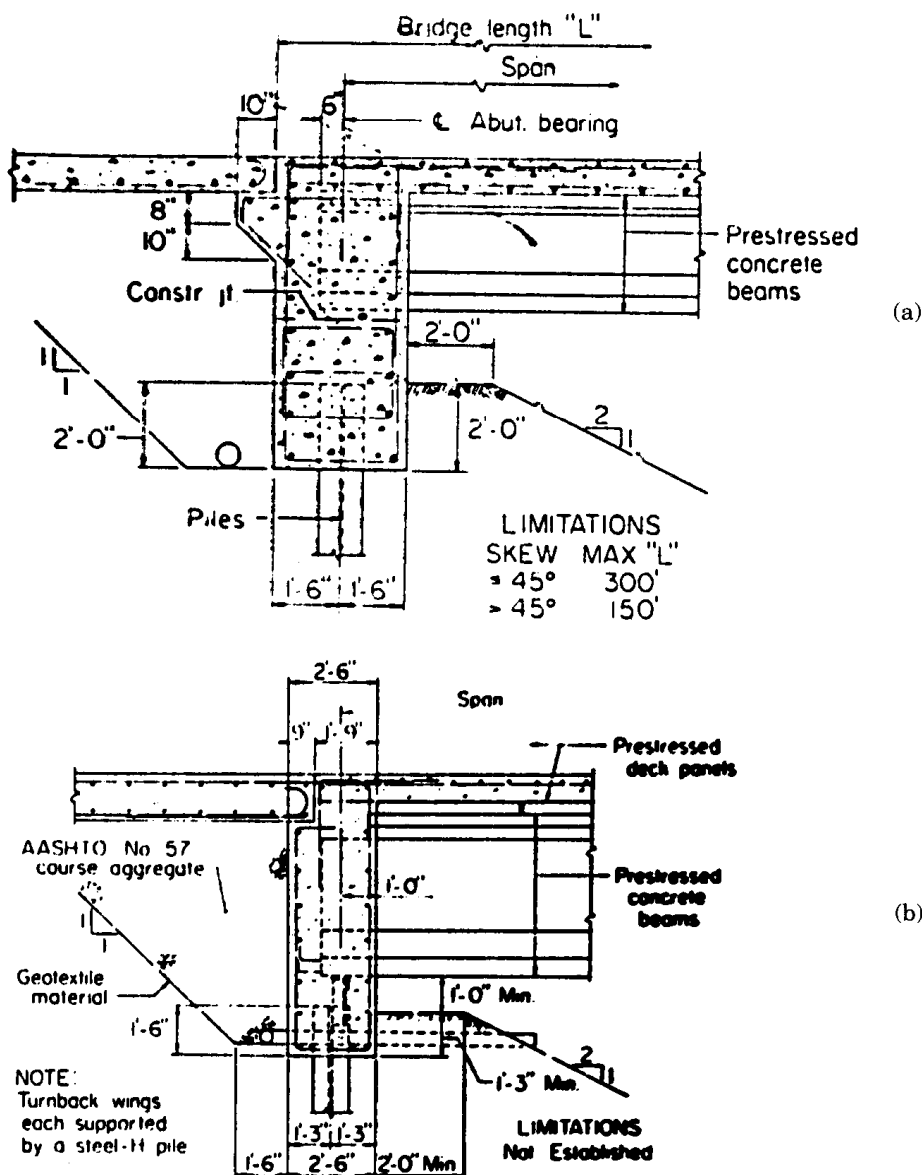


Figure 4-41 Integral abutment details; (a) Iowa; (b) Pennsylvania; (c) North Dakota; (d) semi-integral abutment, Ohio.

the bridge deck. These modes of failure demonstrate the need to provide flexibility in substructure design with appropriate reinforcement to withstand secondary stresses induced by foundation restraint and superstructure shortening.

Design of integral abutments. Figure 7-41(a) through (d) shows details of integral and semi-integral abutments. These supplement the abutment configurations shown in Figure 1-11(a) through (c). The obvious similarity between these abutments reflects the experience gained from early successful designs. Interestingly, the attributes of integral bridges are not always achieved without cost. Certain sections may operate at very high stresses that cannot be easily quantified and often are above the permitted levels. It may appear that the choice to build integral bridges and tolerate the higher

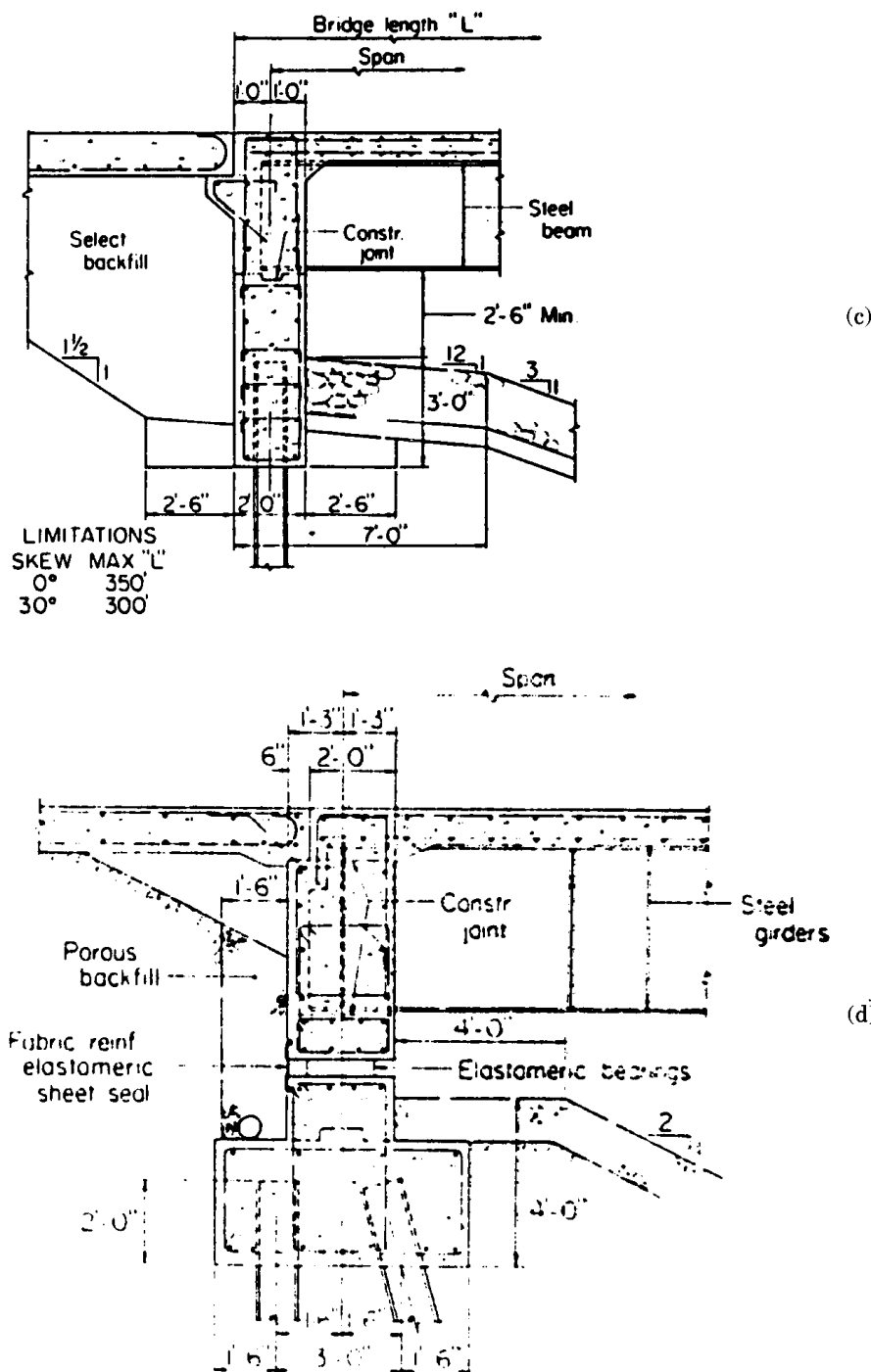


Figure 7-41 (continued)

stresses must be judged in terms of the more expensive jointed bridges with the associated vulnerability to destructive pavement pressures.

These details do not reflect other important design aspects such as skew and construction procedures that should be considered for specific bridges. For abutment design, the main factors that have a marked effect on performance, integrity, and durability are the passive pressure behind the abutment wall, and pile distress caused by lateral abutment movement.

Solutions that have been used to minimize or inhibit the development of passive pressure in abutment backfills as the bridge expands were mentioned in section 1.3, and include the use of selected backfill placed in a loose state, approach slabs supported on the abutment backwall thereby preventing live load surcharge loads, and semi-integral abutments as shown in Figure 7-41(d).

Pile distress under axial load and lateral movement may be controlled by the use of a single row of slender piles and by the use of an abutment hinge (see also section 1.3).

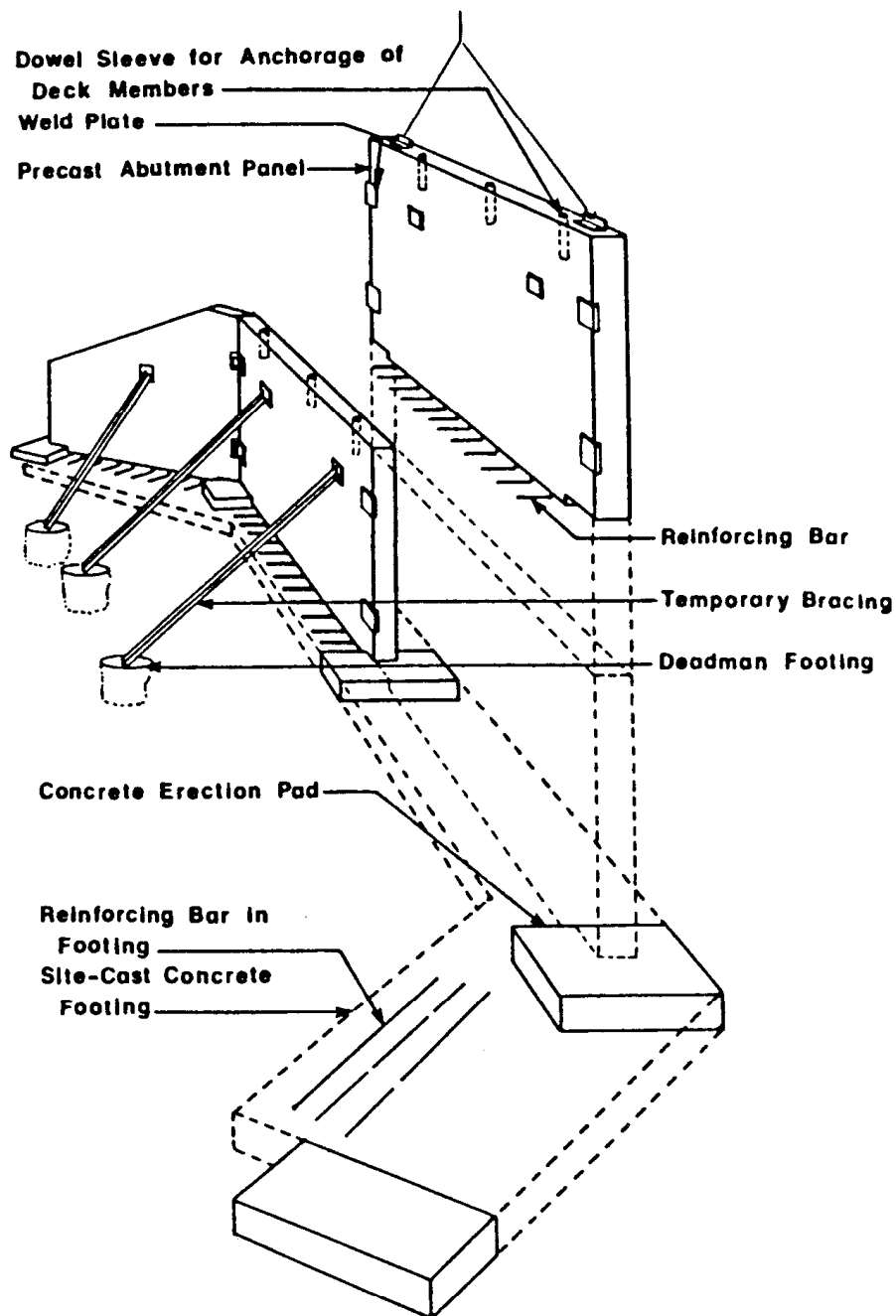


Figure 7-42 Precast abutment and wing walls.

AASHTO requirements. AASHTO recommends to design integral abutments to resist the forces generated by the thermal movement of the superstructure. Integral abutments should not be founded or keyed into rock. The movement should include the combined effect of temperature, creep, and long-term prestress shortening.

Maximum span lengths and design considerations should comply with recommendations outlined in FHWA Technical Advisory T5140.13 (1980) except where regional experience indicates otherwise. Appropriate drainage provisions should be made for any entrapped water behind the abutment.

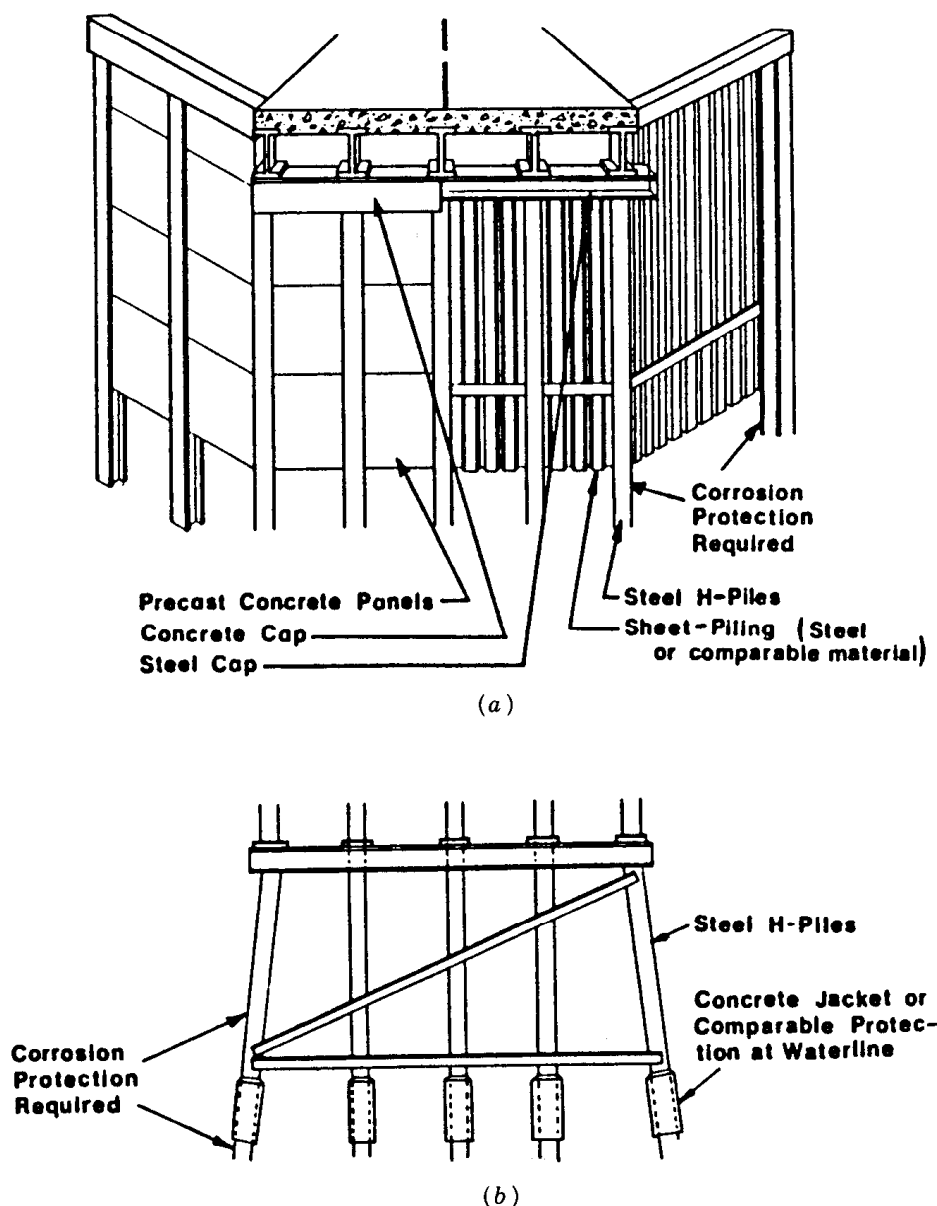


Figure 7-43 (a) Pile substructure and abutment details; (b) pile substructure and pier details.

7.17 PREFABRICATED CONCRETE SECTIONS

The substructure (piers and abutments) often requires 60 to 70 percent of the time required to construct a bridge (Sprinkel, 1978). Significant time savings can thus be realized if the time for substructure construction can be reduced through the use of prefabricated elements and innovative techniques. In many instances construction schedules can be telescoped by prefabricating and stockpiling the substructure members.

Figures 7-42 and 7-43 illustrate the use of precast concrete abutments and wing walls, and prefabricated piling, piers, and caps. Prominent features of the precast abutment shown in Figure 7-42 are the modular panels, conveniently prefabricated in various shapes and sizes to accommodate the abutment configuration and roadway width. The panels are set on cast-in-place concrete pads, temporarily supported, and then connected with weld plates and cast-in-place concrete footing (see also section 7.6). Other systems and configurations based on modular precast units may be combined to obtain a comparable abutment.

The pile substructure schemes shown in Figure 7-43 consist of prestressed concrete or steel H-piles with a concrete or steel cap. The piles are driven to the required depth and cut to the required height. Then they are capped with cast-in-place or precast concrete. For abutments, the piling may be backed with a precast concrete plank, a steel bridge plank, or a suitable cribbing to retain the soil.

Practical considerations for the use of prefabricated substructure elements are summarized by GangaRao (1978), but with a limited applicability because of the many physical differences between bridge sites. The use of standardized elements is further inhibited by variable soil characteristics, bedrock location, and depth at which ample bearing is available. Almost all concepts for substructure applications require the use of either portland cement grout, mortar, concrete, or posttensioning to tie the elements together.

REFERENCES

- AASHTO, 1994: AASHTO LRFD Bridge Design Specifications.
- BROWN, W. G., 1964: "Difficulties Associated with Predicting Depth of Freeze or Thaw," *Canadian Geotech. Journ.*, vol. 1, No. 4, pp. 215-226.
- BURKE, M. P., Jr., 1987: *Bridge Approach Pavements, Integral Bridges and Cycle Control Joints*. In Transportation Research Record 1113, TRB, National Research Council, Washington, D.C.
- California Division of Highways, 1976: "Damage in the San Fernando Earthquake," *Prelim. Report, State of California Business and Transportation Agency, Dept. of Public Works, Div. of Highways, Bridge Dept.*
- CLOUGH, G. W., and R. F. FRAGASZY, 1977: "A Study of Earth Loadings on Floodway Retaining Structures in the 1971 San Fernando Valley Earthquake," *Proc. 6th World Conf. on Earthquake Engineering*, New Delhi, pp. 7-37 to 7-42.
- D'APPOLONIA, D. J., E. D'APPOLONIA and R. F. BRISSETTE, 1970: "Settlement of Spread Footings on Sand," (closure), *Proc. Journ. of Soil Mech. and Found. Div.*, ASCE, vol. 96, No. SM2, pp. 754-761.
- ELLISON, B., 1971: "Earthquake Damage to Roads and Bridges, Madang, R.P.N.G., Nove. 1970," *Bull. New Zealand Society of Earthquake Engineering*, vol. 4, pp. 243-257.
- ELMS, D. A. and G. R. MARTIN, 1979: "Factors Involved in the Seismic Design of Bridge

- Abutments, "Proc. Workshops on Seismic Problems Related to Bridges," Applied Technology Council, Berkeley.
- EVANS, G. L., 1971: "The Behavior of Bridges Under Earthquakes," *Proc. New Zealand Roading Symp.*, Victoria University, vol. 2, pp. 664-684.
- FRANKLIN, A. G. and F. K. CHANG, 1977: "Earthquake Resistance of Earth and Rockfill Dams: Report 5: Permanent Displacements of Earth Embankments by Newmark Sliding Block Analysis," *Misc. Paper S-71-17, Soils and Pavements Lab., U.S. Army Engineer Waterways Experiment Station*, Vicksburg, Miss.
- FUNG, G. G., R. F. LEBEAU, E. D. KLEIN, J. BELVEDERE, and A. G. GOLDSCHMIDT, 1971: "Field Investigation of Bridge Damage in the San Fernando Earthquake," *Prelim. Report, State of California Business and Transportation Agency, Dept. of Public Works*.
- GAMBLE, W. L., 1984: *Bridge Evaluation Yields Valuable Lesson*. Concrete International, June, pp. 68-74.
- GANGARAO, H. V. S., 1978: "Conceptual Substructure Systems for Short-Span Bridges," *Transportation Engineering Journ.*, ASCE, New York, Jan.
- JORGENSEN, J. L., 1983: *Behavior of Abutment Piles in an Integral Abutment Bridge*. In *Transportation Research Record 903*, TRB, National Research Council, Washington, D.C.
- MONONOBE, N., 1929: "Earthquake-Proof Construction of Masonry Dams," *Proc. World Eng. Conf.*, vol. 9, p. 275.
- NEWMARK, N. M., 1965: "Effects of Earthquakes on Dams and Embankments," *Geotechnique*, vol. 14, No. 2, pp. 139-160.
- OKABE, S., 1926: "General Theory of Earth Pressure," *Journ. Japanese Soc. of Civ. Engineers*, vol. 12, No. 1.
- PODOLNY, W., JR., and J. M. MULLER, 1982: *Construction and Design of Prestressed Concrete Segmental Bridges*, Wiley, New York, pp. 561.
- PRAKASH, S., and H. D. SHARMA, 1990: *Pile Foundations in Engineering Practice*, Wiley, New York, p. 735.
- RICHARDS, R. and D. G. ELMS, 1979: "Seismic Behavior of Gravity Retaining Walls," *Journ. of the Geotech. Engineering Div.*, ASCE, vol. 105, No. GT4.
- SEED, H. B. and R. V. WHITMAN, 1970: "Design of Earth Retaining Structures for Dynamic Loads," *ASCE Specialty Conference-Lateral Stresses in the Ground and Design of Earth Retaining Structures*, ASCE.
- SPRINKEL, M. M., 1978: "Systems Construction Techniques for Short Span Concrete Bridges," *Transportation Research Record 665: Bridge Engineering*, vol. 2, Transportation Research Board, National Research Council, Washington, pp. 226-227.
- TERZAGHI, K., and R. B. PECK, 1967: *Soil Mechanics in Engineering Practice*, 2nd ed., Wiley, New York, pp. 729.
- U. S. Army Corps of Engineers, 1949: "Report of Frost Penetration," Addendum No. 1, 1945-47, *Corps of Engineers, U.S. Army*, New England Division, Boston.
- Virginia Prestressed Concrete Association, 1973: "New Approaches in Prestressed, Precast Concrete for Bridge Superstructure Construction in Virginia," Aug., pp. 4, 6, 10, 14, 17, 19, 25.
- WOLDE-TINSAE, A. M., L. F. GREIMANN, and P. S. YANG, 1982: *Nonlinear Pile Behavior in Integral Abutment Bridges*, Iowa State Univ., Ames.
- WOOD, J. H., 1973: "Earthquake-Induced Soil Pressures on Structures," Report No. EERL 73-05, *Earthquake Engineering Research Lab.*, Calif. Inst. of Technology, Pasadena.
- XANTHAKOS, P. P., 1994: *Theory and Design of Bridges*, Wiley, New York, p. 1445.

CHAPTER

8

Footings

8.1 FACTORS AFFECTING SELECTION OF FOUNDATION TYPE

As mentioned in section 1.5, the main factors to be considered in selecting spread footings relate to suitable depth, groundwater effects, potential uplift, and influence of adjacent structures. In general, the selection process should consider the magnitude, type, and application of loads, proximity to suitable bearing layers, previous groundwater history, potential for liquefaction, undermining or scour, swelling potential, frost depth penetration, and cost considerations.

Probable Depth of Scour

Scour is the process of displacing stream bed materials as a result of the erosive action of flowing water. This action undercuts the soil, and may occur naturally or following channel restrictions and changes in flow pattern. For the usual conditions, the greatest scour should be expected to occur during the largest flood.

Scour rates vary according to the type of material. Loose granular soils are very susceptible to scour, whereas soils with cohesion or with some cementation are less prone to this process. AASHTO (1970) articulates typical scour rates for stream bed materials, expressed in terms of the time necessary to reach the maximum scour depth (Table 8–1).

For bridges located at stream crossings, the potential for scour should be investigated considering the worst conditions resulting from the 100-year flood. This usually involves designing the foundation for conditions after scour (see also chapter 3). This analysis is based on the assumption that all the stream bed materials within the scour

Table 8-1 Typical Scour Data.

Material	Time for Maximum Scour
Sands & gravels	hours
Cohesive soils	days
Glacial tills, sandstones & shale	months
Limestones	years
Dense granites	centuries

prism have been wasted away, and thus a reduced area is available for bearing or lateral support.

The scour depth will depend on the geological history of the site (depth of prior erosion to bedrock and subsequent redeposition of sediments, stream velocity, and area runoff), the hydraulics of flow, and the properties of the stream bed materials. Where the redeposition of sediments in the stream bed is of the order of 100 to 150 feet, careful analysis of borings is necessary to predict the depth of maximum scour. A detailed discussion on these topics is given by FHWA (1988), AASHTO (1970), and Copp and Johnson (1987).

Predictions on scour interact with several engineering principles such as hydraulics and hydrology, boring records, past experience with the performance of a given stream, and judgment. If careful records of driving resistance are available, the scour depth may be predicted as being where the penetration (SPT or CPT) resistance increases substantially (Kuhn and Williams, 1961). The AASHTO (1970) report lists several procedures for predicting scour, but concludes that engineering judgment is used more than any other method to estimate scour depth. Scour is accelerated if the foundation creates channel obstructions. These effects are the principal cause of differences resulting from theoretical predictions.

A normal approach to the scour problem should involve the following steps:

1. Select a suitable foundation type;
2. estimate the scour potential and effects such as depth, etc.;
3. estimate the cost of foundation for normal conditions and various scour scenarios; and
4. analyze cost versus risk, and assess the initial design accordingly.

In the absence of a detailed investigation, Terzaghi and Peck (1967) recommend placing the foundation at a depth not less than the elevation of the bottom of low-water channel plus four times the greatest rise of the river level (see also section 3.15).

Frost Effects

Frost effects were discussed briefly in section 7.8 (see also Figure 7-11). In general, footings should be placed below the frost line, because alternate freezing and thawing of the soil tends to maintain it in an unconsolidated (loose) state. Figure 8-1 shows approximately maximum frost depths for regions of the United States (Bowles, 1988); however, local codes should be consulted since they may provide data based on local experience. Recent weather extremes may also be consulted from weather records to confirm the possible effect of cold-weather cycles on frost depth.

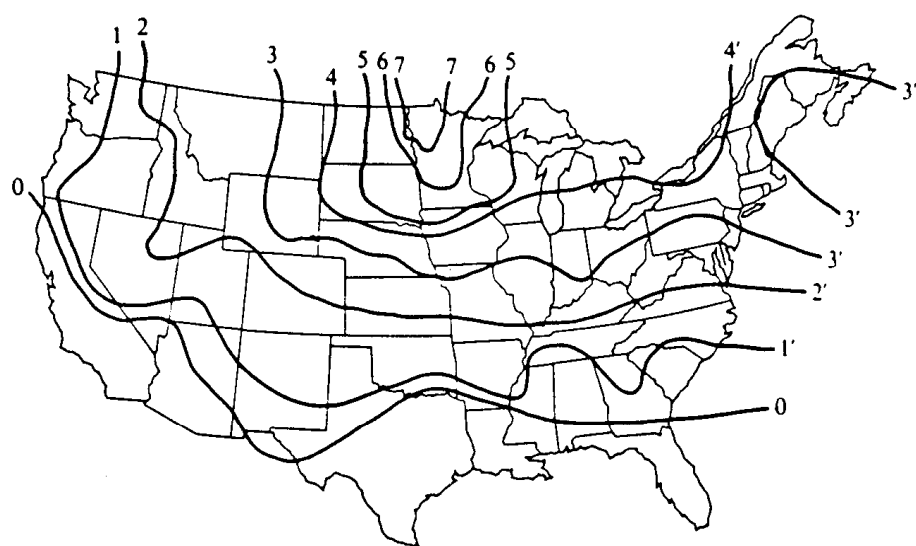


Figure 8-1 Approximate frost-depth contours for the United States, based on a survey of a selected group of cities.

Where frost protection is marginal or deficient, the design may consider the use of insulation to improve frost conditions.

Groundwater and Moisture Fluctuations

Groundwater. Seepage forces and hydraulic gradients should be evaluated where foundation excavations are to be extended below the groundwater table. Upward seepage forces in the bottom of an excavation can lead to piping in dense granular soil or heaving in loose granular soil with subsequent bottom instability. These problems can be controlled by adequate dewatering, usually using wells or well points.

The influence of groundwater table on bearing capacity of soils and rocks has been demonstrated in practical applications. Associated settlements should be considered, and where seepage forces are present they should be included in the analysis. An example of the effect of lowering the groundwater table on the bearing capacity of soils is given in section 3.13.

Moisture fluctuations. Clayey soils tend to shrink on drying and expand when wet. The lower the shrinkage limit and the wider the range of plasticity index, the more likely volume change is to occur and the greater its extent. These volumetric changes can follow the drying of the soil after it is depleted of natural moisture.

On a regional basis, volume changes are particularly troublesome in areas of the southwestern United States subjected to long dry periods and occasional heavy rains of short duration. The dry periods tend to desiccate the soil, while the rain causes swelling. Because the rainfall is not enough to leach and weather the clay minerals, they remain unchanged near the ground surface and are rapidly wetted during the rainy periods. Soils in these areas are difficult to use as foundation soils, since water vapor migrating from the water table condenses on the bottom sides of mat foundations and footings.

Nearby Structures

Occasionally foundations must be placed close or adjacent to existing structures. In this case the mutual influence on the behavior of the new and existing foundations should be investigated.

Figure 8-2 demonstrates potential problems that may arise when placing new footings adjacent to existing. The line from the base of the new footing to the edge of the existing footing should be at 45° or less with the horizontal. From this it follows that the distance m should be greater than the difference in elevation z_f . This criterion should produce conservative pressures in the common zone with contributions from more than one footing.

In Figure 8-2(b) a different situation prevails. If the new footing is lower than the existing, the possibility will exist that soil may flow laterally from beneath the existing footing. This may result in a corresponding settlement. As a first approximation, the problem may be analyzed by referring to Mohr's failure stress circle for triaxial compression.

Figure 8-3 shows the effects of excavation too close to an existing footing. In this case the qN_q term (see also subsequent sections) of the bearing capacity equation is lost. Problems of this nature may be avoided if a ground support system is placed to retain the soil in the K_0 state, or if some form of ground improvement precedes the excavation.

Expansive and Collapsible Soils

The soils discussed at the beginning of this section (undergoing volume changes upon wetting and drying) are termed expansive soils. When such soils are encountered, the following solutions may be tried: (1) alter the soil by adding lime, cement or other admixtures, and institute compaction to low densities of water contents on the wet side of optimum; (2) control the direction of expansion, by allowing the soil to expand into cavities built in the foundation; (3) provide water control, so that the soil may be excavated to a depth where the weight of soil will control heave; (4) place the footing at a sufficient depth and/or leave an expansion zone between the ground surface and the foundation so that swell can take place without causing detrimental movement; and (5) load the soil to sufficient pressure (artificial) to balance swell pressure.

Collapsible or metastable soils are by definition unsaturated soils undergoing a

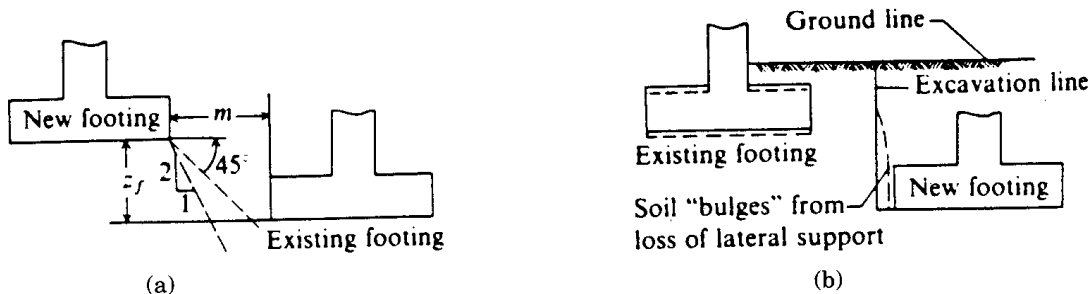


Figure 8-2 Location considerations for spread footings. (a) An approximation for spacing footings to avoid interference between old and new footings. If "new" footing is in relative position of "existing" footing, interchange words "existing" and "new". Make $m > z_f$; (b) Possible settlement of "existing" footing because of loss of lateral support of soil wedge beneath existing footing.

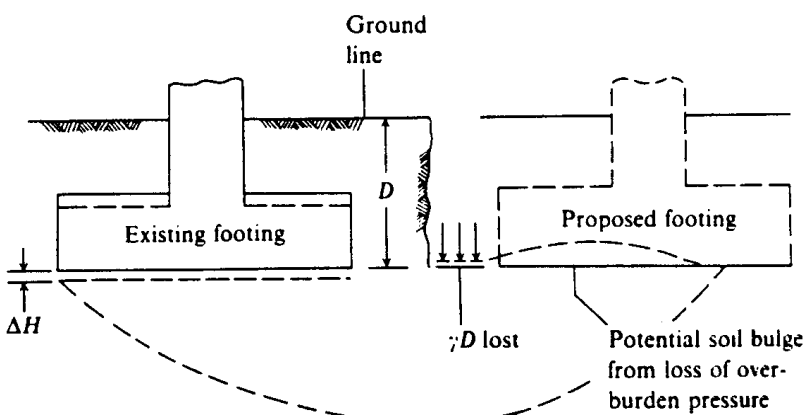


Figure 8-3 Potential settlement from loss of overburden pressure.

radical particle rearrangement and considerable volume loss upon wetting with or without additional loading (Clemence and Finbarr, 1981). Difficulties associated with the use of these soils as foundation support have long been recognized, but until recently concern was limited because such soils are located in arid regions with modest economic development potential. With recent advances in irrigation these regions have become available for development and associated construction, and collapsible soils are becoming relevant to the analysis and design of foundations.

Comprehensive reviews on the subject are given by Clemence and Finbarr (1981), Northen (1969), Sultan (1969), and Dudley (1970). Since 1970, major effort has focused on determining the mechanics of collapse, on predictive techniques and treatment methods, and on evaluating case histories.

8.2 FOOTING TYPES

Several footing types common in bridge foundations are shown in Figure 8-4. Footings generally can be divided into column and wall footings. A wall footing shown in Figure 8-4(e) is simply a strip of reinforced concrete, wider than the wall, used to distribute the load to the foundation soil. Strip footings are typically used with solid pier walls. Single column footings, shown in Figure 8-4(a) and (b), are usually square and some-

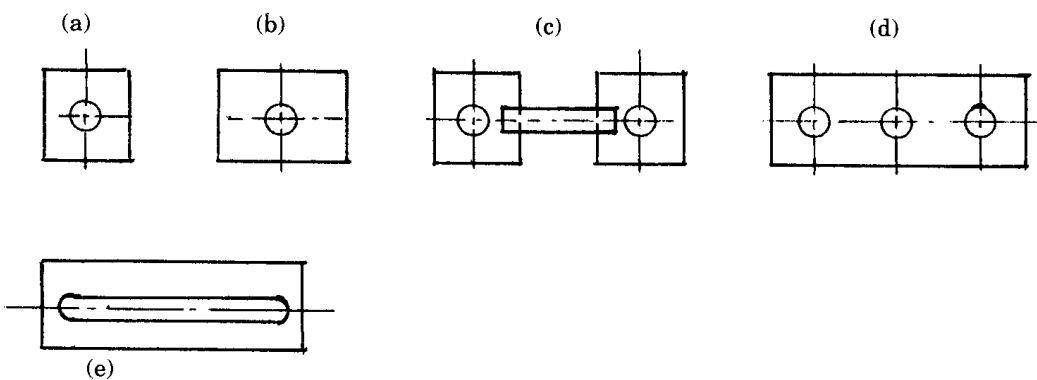


Figure 8-4 Footing types common in bridge foundations.

times rectangular. The choice depends on the variation of the transverse moments in the two principal directions. Unlike strip footings that display essentially one-dimensional action, single column footings (also referred to as spread footings) distribute the loads in two directions.

The combined footings under two or more columns shown in Figure 8-4(d) may be used under closely spaced or heavily loaded columns where single footings might completely or nearly merge. The footing shown in Figure 8-4(c) merely has a connecting beam that increases the stability of the foundation against overturning and against lateral forces.

Wall or column individual and combined footings are the most frequent types of spread foundations on soils of reasonable bearing capacity. If the soil at relatively shallow depth is weak, or if the column loads are great, the required footing area may become so large as to be uneconomical. In this case a deep foundation may be considered.

Occasionally spread footings may have pedestals, or they may be stepped or tapered to save materials. Strip, spread, and combined footings are considered in this chapter since they are the most basic and common types in bridge foundations.

8.3 BEARING CAPACITY THEORIES

General Principles

Currently there is no method for obtaining the ultimate bearing capacity of a foundation other than as an estimate. At least ten and probably fifteen theoretical solutions have been formulated since 1940. Little experimental verification has been provided except by using model footings. Using models with $B = 25$ to 75 mm and $L = 25$ to 200 mm (widths and lengths, respectively) appear to be popular because the ultimate bearing can be induced in the laboratory on a small prepared box of soil. Full size footings with dimensions $1\text{ m} \times 1\text{ m}$ (3.3×3.3 ft) can develop ultimate loads 600 to 1000 kips, but require a rather expensive preparation and equipment to induce and measure loads of this magnitude.

Models, especially in sand, do not always give reliable test results compared to full-scale prototypes. This is because of scale effects where the model reaction engages only a small quantity of soil grains. Sand also requires confinement to develop resistance, and this is more feasible with very small models. In spite of these shortcomings, the use of models has gained popularity.

Bearing Capacity Equations

The Terzaghi Bearing Capacity Equation. This is one of the early theories proposed by Terzaghi (1943). The equation has the following form (general shear failure)

$$q_{ult} = cN_c s_c + 0.5 \gamma BN_\gamma s_\gamma + qN_q \quad (8-1)$$

where q_{ult} = ultimate bearing capacity for uniform bearing pressure (ksf); c = soil cohesion (ksf); s_u = undrained shear strength; γ = total unit weight of soil (kcf); q = effective overburden pressure at base of footing (ksf); N_c , N_γ , N_q = bearing capacity factors based on the value of internal friction of the foundation soil.

The coefficients s_c and s_γ are as follows

$$s_c = 1.0 \text{ (strip), } 1.3 \text{ (round), } 1.3 \text{ (square)}$$

$$s_\gamma = 1.0 \text{ (strip), } 0.6 \text{ (round), } 0.8 \text{ (square)}$$

For a continuous footing ($L > 5B$), $s_c = s_\gamma = 1.0$, hence

$$q_{ult} = cN_c + 0.5\gamma BN_\gamma + qNq \quad (8-2)$$

which is AASHTO Eq. (4.4.7.1-1). All notations refer to Figure 8-5.

The values of N_c , N_γ and N_q may be obtained directly from AASHTO Table 4.4.7.1A.

Equation (8-1) introduces shape factors to extend the applicability of the bearing capacity theory. Terzaghi's criterion was produced from a slightly modified bearing-capacity theory developed by Prandl (1920), who used the theory of plasticity to analyze the punching of a rigid base into a softer (soil) material. This bearing-capacity equation is intended for shallow foundations where

$$D_f \leq B \quad (8-3)$$

so that the shear resistance along the edge of the soil mass engaged in the interaction can be neglected. The dimensionless factor N_γ is a function of the coefficient $K_{p\gamma}$. Since

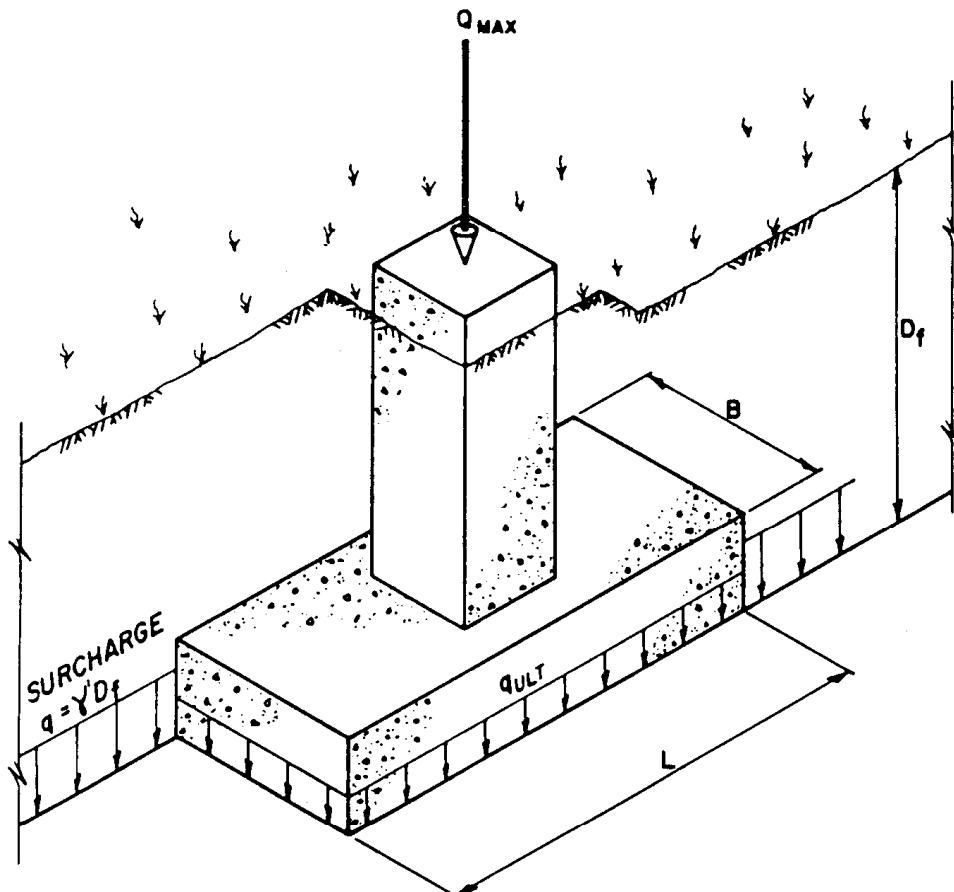


Figure 8-5 Design terminology for spread footing foundations.

Terzaghi did not explain how values of $K_{p\gamma}$ were obtained to compute N_γ (other than a $\phi - N_\gamma$ curve with three specific values), several investigations have arrived at approximate values of N_γ from back analysis and other theoretical considerations (Meyerhof, 1951, 1963; Vesic, 1973).

Meyerhof's bearing capacity equation. Meyerhof (1951, 1963) introduced a bearing capacity equation essentially similar to Equation (8–1), but including a shape factor s_q for the depth term Nq . He also included depth factors d_i and inclination factors i_i to deal with cases where the footing load is inclined from the vertical. Meyerhof (1963) modified somewhat his 1951 values for the shape, depth, and inclination factors. This theory has been used as a basis to produce a modified form of the general bearing capacity equation to account for these effects, and has produced AASHTO Eq. (4.4.7.1.1–1).

Hansen's bearing capacity method. Hansen (1970) proposed a general bearing capacity equation, which is essentially a further extension of Meyerhof's work. Hansen's shape, depth, and other factors contributing to the general equation are given in Table 8–2, and they represent revisions and extensions from earlier proposals. These extensions include a factor for a footing tilted from the horizontal b_i and for the possibility of the footing being on a slope g_i .

Referring to the notation of Table 8–2, the Hansen theory is valid for any D/B ratio and thus can be used for shallow (footings) and deep (piles, drilled shafts) foundations.

Commentary. Among the many bearing capacity theories, some of which were briefly mentioned, the Terzaghi equations were the first proposed and have been widely used. They are still popular, especially where it is not necessary to compute shape, depth, and other factors. They are, however, suitable for a concentrically loaded horizontal footing, which is most often the case with bridge foundations.

Some opinion has been expressed that the Terzaghi equations sometimes are unduly conservative, and probably should be applied to soils with little cohesion and with D_f probably in the range $B/2$ to $2B$ (Figure 8–5). Both the Meyerhof and Hansen methods are substantially used, especially where depth, shape, and inclination factors must be considered.

In developing the bearing capacity equation, Terzaghi considered a general shear failure in dense soil and a local shear failure for a loose soil. Thus, if local or punching shear is possible, the value of q_{ult} in Equation (8–2) should be computed using reduced shear strength parameters c^* and ϕ^* as follows:

$$\left. \begin{aligned} c^* &= 0.67c \\ \phi^* &= \tan^{-1}(0.67 \tan \phi) \end{aligned} \right\} \quad (8-4)$$

which are AASHTO Eqs. (4.4.7.1–3 and 4).

The following comments about the bearing capacity equations can be made:

1. The cohesion term predominates in cohesive soils.
2. The depth term qN_q is the main contributing factors in granular soils without cohesion. A small increase in D_f can increase q_{ult} considerably.
3. The footing-width term $0.5\gamma BN_\gamma$ increases the bearing capacity in both cohesive and cohesionless soils. However, this effect becomes less important as the footing width B decreases.

Table 8-2 Shape, Depth, Inclination, Ground and Base Factors for Use in either the Hansen (1970) or Vesic (1973) Bearing-Capacity Equations, (Factors apply to either method unless subscripted with (H) or (V) . Use primed factors when $\phi = 0$)

Shape Factors	Depth Factors	Inclination Factors	Ground Factors (base on slope)
$s'_c = 0.2 \cdot \frac{B}{L}$	$d'_c = 0.4k$	$i'_c(H) = 0.5 - 0.5 \sqrt{1 - \frac{H}{A_f c_a}}$	$g'_c = \frac{\beta^\circ}{147^\circ}$ for Vesic use $N_\gamma = -2 \sin \beta$ for $\phi = 0$
$s_c = 1 + \frac{N_q}{N_c} \cdot \frac{B}{L}$	$d_c = 1 + 0.4k$	$i'_c(V) = 1 - \frac{mH}{A_f c_a N_c}$	$g_c = 1 - \frac{\beta^\circ}{147^\circ}$
$s_c = 1$ for strip		$i_c = i_q - \frac{1-i_q}{N_q-1}$ (Hansen and Vesic)	
$s_q = 1 + \frac{B}{L} \tan \phi$	$d_q = 1 + 2 \tan \phi (1 - \sin \phi) k$		$g_{q(H)} = g_{\gamma(H)} = (1 - 0.5 \tan \beta)^5$
	$d_\gamma = 1.00$ for all ϕ	$i_q(H) = \left(1 - \frac{0.5H}{V + A_f c_a \cot \phi}\right)^5$	$g_{q(V)} = g_{\gamma(V)} = (1 - \tan \beta)^2$
$s_\gamma = 1 - 0.4 \cdot \frac{B}{L}$	$k = \frac{D}{B}$ for $\frac{D}{B} \leq 1$ $k = \tan^{-1} \frac{D}{B}$ for $\frac{D}{B} > 1$ (rad)	$i_q(V) = \left(1 - \frac{H}{V + A_f c_a \cot \phi}\right)^m$	Base factors (tilted base)
			$b'_c = \frac{\eta^\circ}{147^\circ}$ $b_c = 1 - \frac{\eta^\circ}{147^\circ}$
where A_f = effective footing area $B' \times L'$ (see Fig. 8-6)		$i_\gamma(H) = \left(1 - \frac{0.7H}{V + A_f c_a \cot \phi}\right)^5$ ($\eta = 0$)	$b_{q(H)} = \exp(-2\eta \tan \phi)$ $b_{\gamma(H)} = \exp(-2.7\eta \tan \phi)$
c_a = adhesion to base = cohesion or a reduced value		$i_\gamma(H) = \left(1 - \frac{(0.7 - \eta^\circ/450)H}{V + A_f c_a \cot \phi}\right)^5$ ($\eta > 0$)	$b_{q(V)} = b_{\gamma(V)} = (1 - \eta \tan \phi)^2$
D = depth of footing in ground (used with B and not B')		$i_\gamma(V) = \left(1 - \frac{H}{V + A_f c_a \cot \phi}\right)^{m+1}$	Notes: $\beta + \eta \leq 90^\circ$ $\beta \leq \phi$
e_B, e_L = eccentricity of load with respect to center of footing area		$m = m_B = \frac{2+B/L}{1+B/L} H$ parallel to B	
H = horizontal component of footing load with $H \leq V \tan \delta + c_a A_f$		$m = m_L = \frac{2+L/B}{1+L/B} H$ parallel to L	
V = total vertical load on footing			
β = slope of ground away from base with downward = (+)			
δ = friction angle between base and soil—usually $\delta = \phi$ for concrete on soil			
η = tilt angle of base from horizontal with (+) upward as usual case			
<i>General:</i> 1. Do not use s_i in combination with i_i .			
2. Can use s_i in combination with d_i , g_i , and b_i .			
3. For $L/B \leq 2$ use ϕ_{tr} For $L/B > 2$ use $\phi_{ps} = 1.5\phi_{tr} - 17$ For $\phi \leq 34$ use $\phi_{ps} = \phi_{tr}$		Note: $i_q, i_\gamma > 0$	

(From Hansen, 1970)

4. When the soil beneath a footing is nonhomogeneous or stratified, some judgment is necessary in determining the bearing capacity, since there can be a number of interpretations.
5. The Terzaghi equation is simpler and easier to use. For example, it can be applied to a particular footing load without an iterative procedure.

Effect of eccentric loading. Eccentricity in pier footings is introduced with an axial load and moments about one or both principal directions of the footing. Referring to Figure 8-6, the effective (reduced) footing dimensions can be obtained as (Meyerhof, 1953; Hanson, 1970)

$$L' = L - 2e_x, \quad B' = B - 2e_y \quad (8-5)$$

so that the effective footing area is now

$$A' = B'L' \quad (8-6)$$

Note that the last two equations are AASHTO Eqs. (4.4.7.1.1-1 and 2) and (4.4.7.1.1-3).

The value of q_{ult} obtained using the reduced footing dimensions B' and L' represents an equivalent uniform bearing pressure and *not* the actual contact pressure distribution beneath the footing. This equivalent pressure may be multiplied by the reduced area A' to calculate the ultimate load Q_{ult} from the standpoint of bearing capacity, or

$$Q_{ult} = q_{ult}(B'L') \quad (8-7)$$

where q_{ult} is computed from Equation (8-2) using B' in the γBN_y term. The actual contact pressure distribution (usually trapezoidal) should be used in computing the reinforcement requirements (moments, shears, etc.).

The actual distribution of contact pressure for a rigid footing with eccentric loads

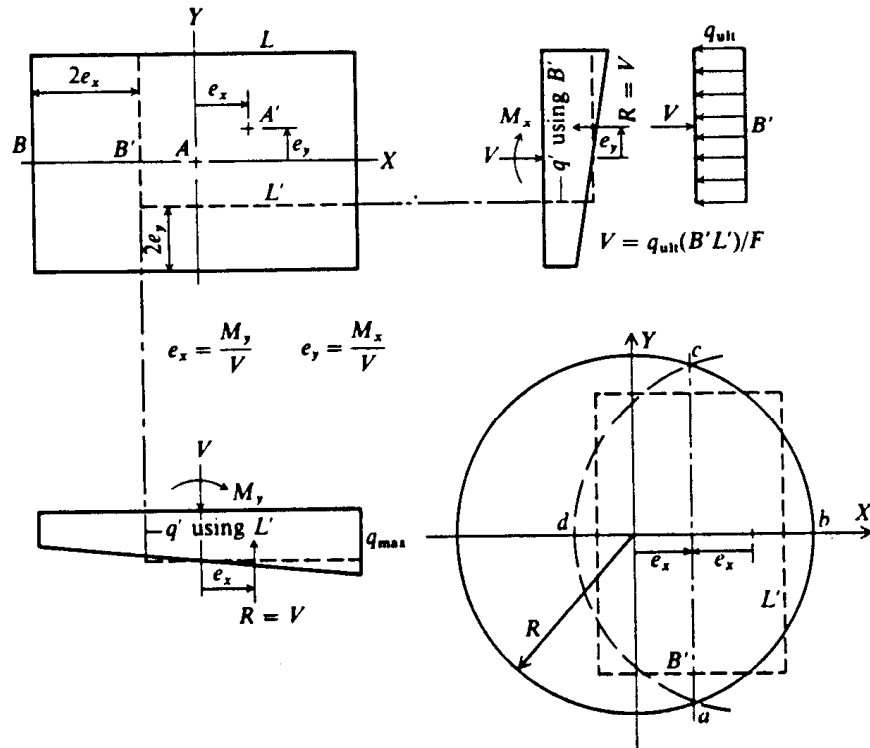


Figure 8-6 Method of computing effective footing dimensions when footing is eccentrically loaded for both rectangular and round bases.

may be computed from statics and flexural theory. Referring to Figure 8-7, if the resultant Q lies in the middle third ($e_L < L/6$)

$$\left. \begin{aligned} q_{\max} &= Q[1 + (6e_L / L)] / BL \\ q_{\min} &= Q[1 - (6e_L / L)] / BL \end{aligned} \right\} \quad (8-8)$$

For $L/6 < e_L < L/2$

$$\left. \begin{aligned} q_{\max} &= 2Q / (3B[(L/2) - e_L]) \\ q_{\min} &= 0 \end{aligned} \right\} \quad (8-9)$$

For an eccentricity in both directions, reference is made to AASHTO (1992).

Effect of groundwater table. In the foregoing equations q is based on the effective weight of the soil (see also Figure 8-5). The water table, however, is seldom above the base of the footing, since this would cause construction problems.

Ultimate bearing capacity should be computed on the basis of the highest anticipated groundwater level at the footing location. Where this effect must be considered, the q term may require adjustment. If the water table is at ground surface, the effective soil weight is approximately one-half, giving a q term about one-half the value with the water table below the footing level.

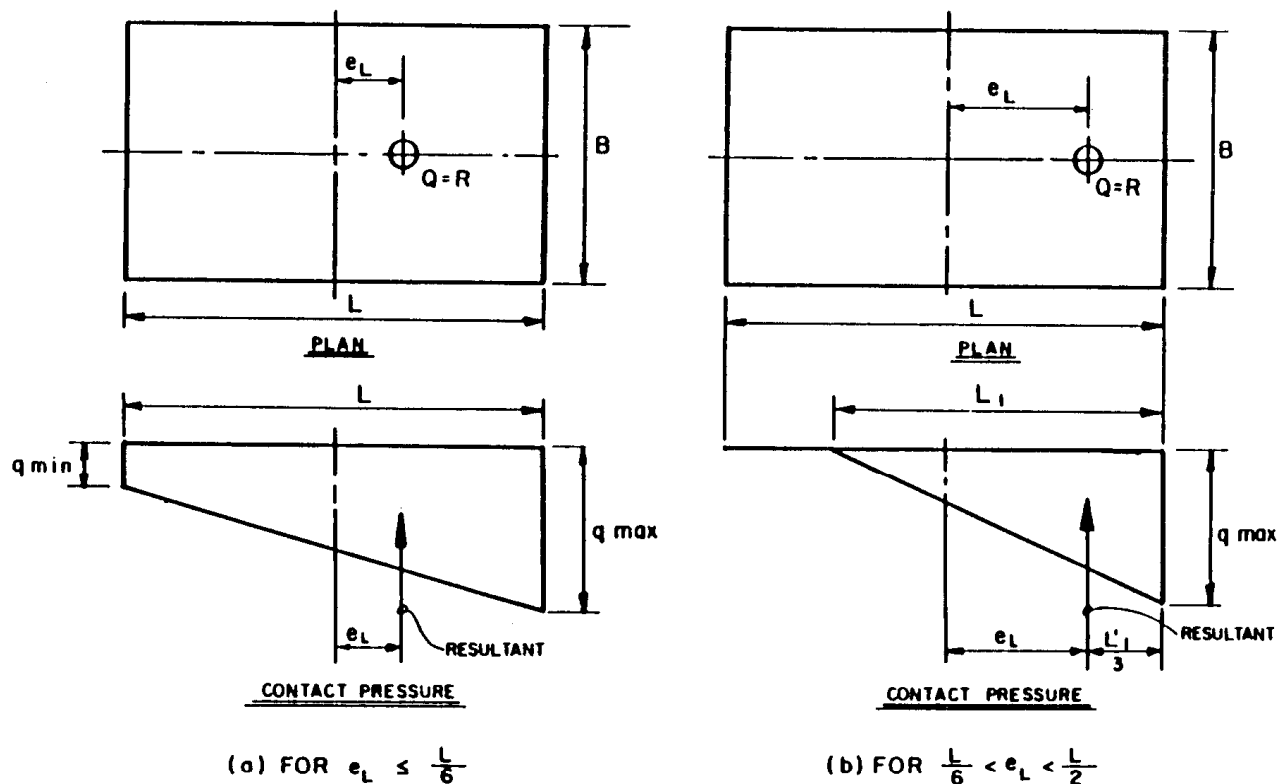


Figure 8-7 Contact pressure for footing loaded eccentrically about one axis.

When the groundwater level is below the wedge zone approximated depth of $0.5B\tan(45 + \phi/2)$, the groundwater effects can be ignored for bearing capacity. When the water table lies within the wedge zone, the effects should be considered.

Referring to Figure 8-8, the effect of groundwater table on the ultimate bearing capacity may be considered by using the weighted average soil unit weight in Equation (8-2). If $\phi < 37^\circ$, the weighted average unit weight may be computed from

$$\begin{aligned} \text{For } z_w \geq B & \quad \gamma = \gamma_m \quad (\text{no effect}) \\ \text{For } z_w < B & \quad \gamma = \gamma' + (z_w / B)(\gamma_m - \gamma') \\ \text{For } z_w < 0 & \quad \gamma = \gamma' \end{aligned} \quad (8-10)$$

where γ = total unit weight; γ' = submerged (effective) unit weight; and γ_m = moist unit weight of soil.

Layered soils. In general, if the soil profile shows stratified deposits, the bearing-capacity equations should be modified to account for differences in failure mode between the homogeneous and the layered soil. Three general cases may be identified as follows:

1. The footing is on layered clays ($\phi = 0$) with two possible conditions: (A) the top layer is weaker than the lower layer; and (B) the top layer is stronger than the lower layer.
2. The footing is on layered soil with friction and cohesion, and with two conditions as in case 1.

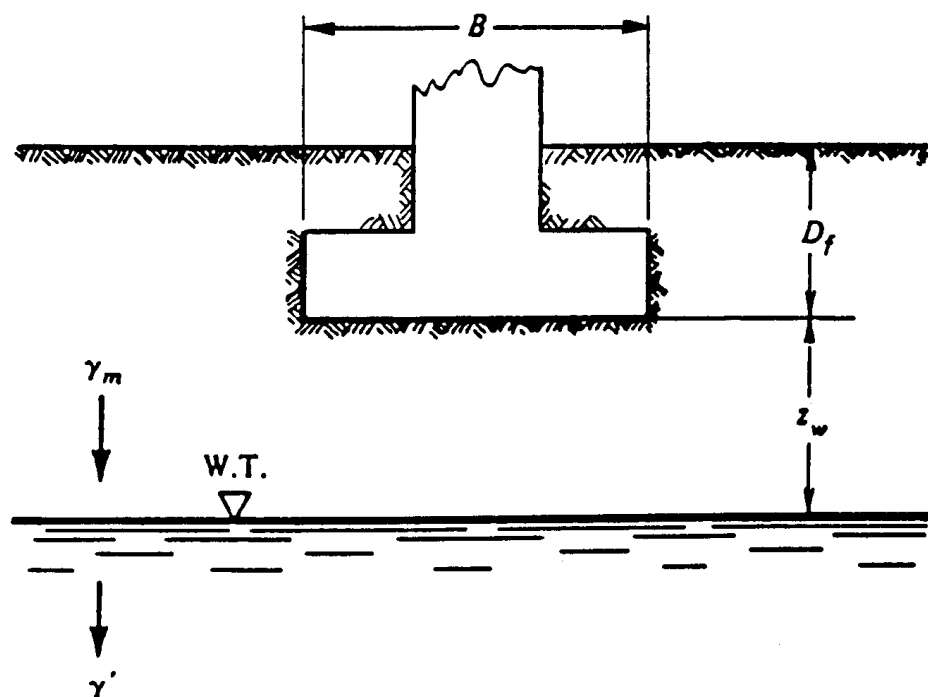


Figure 8-8 Definition sketch for influence of ground water table on bearing capacity.

3. The footing is on layered sand and clay soils with two possible conditions: (A) sand overlying clay; and (B) clay overlying sand.

Most of the experimental work carried out to provide criteria for q_{ult} has been confined to small models. Several analytical procedures have been introduced, and among those is the work by Button (1953), who used a circular arc as failure criterion, and established an approximate minimum $N_c = 5.5 < 2\pi$. Other work on this subject has been carried out by Meyerhof and Brown (1967), and Purushothamaraj et al. (1974).

Other conditions. Theories have been formulated to calculate the bearing capacities for foundations on slopes or adjacent to slopes (Meyerhof, 1953), and for foundations with inclined base (Kulhawy, Trautmann, Beech, O'Rourke, and McGuire, 1983).

Table 8-3 Presumptive Allowable Bearing Pressures for Spread Footing Foundations under Service Loads

Type of Bearing Material	Consistency in Place	Bearing Pressure (TSF)	
		Ordinary Range	Recommended Value of Use
Massive crystalline igneous and metamorphic rock: graphite, diorite, basalt, gneiss, thoroughly cemented conglomerate (sound condition allows minor cracks)	Very hard, sound rock	60 to 100	80
Foliated metamorphic rock: slate, schist (sound condition allows minor cracks)	Hard sound rock	30 to 40	35
Sedimentary rock: hard cemented shales, siltstone, sandstone, limestone without cavities	Hard sound rock	15 to 25	20
Weathered or broken bedrock of any kind, except highly argillaceous rock (shale)	Medium hard rock	8 to 12	10
Compaction shale or other highly argillaceous rock in sound condition	Medium hard rock	8 to 12	10
Well-graded mixture of fine- and coarse-grained soil: glacial till, hardpan, boulder clay (GW-GC, GC, SC)	Very dense	8 to 12	10
Gravel, gravel-sand mixture, boulder-gravel mixtures (GW, GP, SW, SP)	Very dense Medium dense to dense Loose	6 to 10 4 to 7 2 to 6	7 5 3
Coarse to medium sand, and with little gravel (SW, SP)	Very dense Medium dense to dense Loose	4 to 6 2 to 4 1 to 3	4 3 1.5
Fine to medium sand, silty or clayey medium to coarse sand (SW, SM, SC)	Very dense Medium dense to dense Loose	3 to 5 2 to 4 1 to 2	3 2.5 1.5
Fine sand, silty or clayey medium to fine sand (SP, SM, SC)	Very dense Medium dense to dense Loose	3 to 5 2 to 4 1 to 2	3 2.5 1.5
Homogeneous inorganic clay, sandy or silty clay (CL, CH)	Very stiff to hard Medium stiff to stiff Soft	3 to 6 1 to 3 0.5 to 1	4 2 0.5
Inorganic silt, sandy or clayey silt, varved silt-clay-fine sand (ML, MH)	Very stiff to hard Medium stiff to stiff Soft	2 to 4 1 to 3 0.5 to 1	3 1.5 0.5

(Modified after U.S. Department of the Navy, 1982)

8.4 PRESUMPTIVE BEARING PRESSURES

Where presumptive values must be used, they should be based on a reasonable knowledge of geological conditions at or near the site. Presumptive bearing pressures provide a quick (but least accurate) method of determining allowable bearing loads for foundations. This easy reference relates the allowable pressure to the soil type and to a qualitative description of its condition, termed consistency in place. Unless more accurate or appropriate regional data are available, the presumptive values given in Table 8-3 may be used. These are allowable bearing pressures and apply only at service limit states.

The procedure in this case is direct and simple. With the allowable bearing pressure determined by reference to data such as Table 8-3, the required footing size may be obtained merely by dividing the load by the bearing pressure. Although the procedure is quick and correlates footing size with actual load and an allowable pressure, in most cases it may essentially give inaccurate predictions. It is seldom expedient in engineering terms to make estimates of allowable bearing pressure based on the soil type and a qualitative description of its consistency. In this context, presumptive bearing values may sometimes yield overconservative designs or results that are unsafe. Reference to these values is convenient for preliminary estimates and rule-of-thumb designs.

8.5 BEARING PRESSURES FROM TESTS

The bearing resistance of foundation soils may be estimated from the results of in situ tests or by observing foundations on similar soils. If in situ tests are contemplated, interpretation of results should take local experience into consideration. There are two types of tests: standard penetration tests (SPT), and cone pressuremeter tests (CPT).

Standard Penetration Tests (SPT)

SPT blow counts are commonly used to estimate soil properties such as the undrained shear strength s_u of clays and the angle of friction ϕ of sands. These provide index parameters that may be introduced in the bearing-capacity equations to compute the ultimate bearing resistance. SPT blow counts may also be used to estimate bearing pressure directly. This involves the use of semi-empirical procedures. Meyerhof (1956) proposed the following equation

$$q_{ult} = \frac{\bar{N}B}{10} \left(C_{W1} + C_{W2} \frac{D_f}{B} \right) R_1 \quad (8-11)$$

where \bar{N} = average value of corrected SPT blow count within the range of depth from footing base to $1.5 B$ below the footing; C_{W1} , C_{W2} = dimensionless correction factors for ground water effect, as specified in Table 8-4; R_1 = dimensionless reduction factor accounting for the effect of load inclination, as shown in Table 8-5; and the rest of the symbols correspond to the notation of Figure 8-5.

The value of \bar{N} is determined in two steps. First, in saturated very fine sand the measured SPT blow count is corrected for submergence effects as follows:

$$N = 15 + 1/2 (N' - 15) \text{ for } N' > 15 \quad (8-12)$$

Table 8-4 Coefficients C_{W1} and C_{W2} for Various Ground Water Depths

D_W	C_{W1}	C_{W2}
$>1.5B + D_f$	1.0	1.0
D_f	0.5	1.5
0.0	0.5	0.5

where N' = measured SPT blow count.

The average value of N determined as explained is used in Equation (8-11) to obtain q_{ult} , and also in analyses of footing settlement.

Cone Penetration Tests (CPT)

This procedure has gained broad acceptance in the United States, probably because it provides a continuous record of resistance to penetration. A 10-cm² penetrometer is used and may be combined with conventional methods for drilling and sampling. Cone penetration resistance is the tip bearing pressure necessary to cause continuous penetration of the cone through the soil at a speed of 2 cm/sec. The tip resistance q_c is usually reported in kg/cm², which is the same value when converted to tons/ft².

Values of q_c are used to estimate soil properties such as s_u and ϕ to be subsequently entered into the bearing capacity equations. Alternatively, cone penetration resistance can be used directly to estimate ultimate bearing capacity through empirical correlations. A relationship between ultimate bearing capacity in sand and cone penetration resistance is given as (Meyerhof, 1956)

$$q_{ult} = \frac{q_c B}{40} \left(C_{W1} + C_{W2} \frac{D_f}{B} \right) R_1 \quad (8-13)$$

where q_c = average value of cone penetration resistance*; and the factors C_{W1} , C_{W2} , and R_1 are taken from Tables 8-4 and 8-5 to represent the effect of water table and inclination as before.

Awkati has correlated values of ultimate bearing capacity to cone penetration resistance in clays (Schmertmann, 1977). Recommended values are summarized in Table 8-6 for strip and square footing.

The data shown in Table 8-6 can be used for footings that are below the ground surface. For footings in clay, it is not necessary to make corrections for the position of the groundwater table.

Pressuremeter Tests (PMT)

This procedure is carried out by inflating a membrane within a drilled hole and then measuring the volume of expansion in terms of the applied pressure. This test is common and popular abroad, and appears to be gaining broader acceptance in the United States. It requires specialty contractors who also provide recommendations about the interpretation of the test results. Useful data on this subject are given by Briaud (1990).

*Measured within the range of depth from footing base to 1.5 B below the footing.

Table 8–5 Load Inclination Factor, R_1

(i) For Square Footings			(ii) For Rectangular Footings			(iii) For Rectangular Footings		
			Load Inclination Factor, R_1			Load Inclination Factor, R_1		
			Load Inclined in Width Direction			Load Inclined in Length Direction		
H/V	$D_f/B = 0$	$D_f/B = 1$	$D_f/B = 5$	H/V	$D_f/B = 0$	$D_f/B = 1$	$D_f/B = 5$	H/V
0.10	0.75	0.80	0.85	0.10	0.70	0.75	0.80	0.10
0.15	0.65	0.75	0.80	0.15	0.60	0.65	0.70	0.15
0.20	0.55	0.65	0.70	0.20	0.50	0.60	0.65	0.20
0.25	0.50	0.55	0.65	0.25	0.40	0.50	0.55	0.25
0.30	0.40	0.50	0.55	0.30	0.35	0.40	0.50	0.30
0.35	0.35	0.45	0.50	0.35	0.30	0.35	0.40	0.35
0.40	0.30	0.35	0.45	0.40	0.25	0.30	0.35	0.40
0.45	0.25	0.30	0.40	0.45	0.20	0.25	0.30	0.45
0.50	0.20	0.25	0.30	0.50	0.15	0.20	0.25	0.50
0.55	0.15	0.20	0.25	0.55	0.10	0.15	0.20	0.55
0.60	0.10	0.15	0.20	0.60	0.05	0.10	0.15	0.60

(From Meyerhof, 1956)

Table 8–6 Correlation between Cone Penetration Resistance and Ultimate Bearing Capacity in Clays

q_c (kg/cm^2 or t/ft^2)	Value of q_{ult} (t/ft^2)	
	Strip Footing	Square Footing
10	5	9
20	8	12
30	11	16
40	13	19
50	15	22

(From Awkati).

The bearing resistance of foundation soils may be determined from results of pressuremeter tests as

$$q_{ult} = r_o + \kappa(P_l - P_o) \quad (8-14)$$

where r_o = initial total vertical pressure at foundation level; κ = empirical bearing capacity coefficient, taken from Figure 8–9; P_l = limit pressure measured in the pressuremeter test; and P_o = total horizontal pressure at depth where the test is performed. Equation (8–14) is an empirical relationship suggested by Menard (1965), Baguelin, Jazequel, and Shields (1978), and Briaud (1990).

Any consistent pressure units can be used in the calculations. An average value of limit pressure is taken over the range of depth from $1.5B$ above to $1.5B$ below the foundation level. Where the values of P_l vary considerably within a depth B above or below the foundation level, special averaging procedures are recommended (Baguelin et al., 1978).

8.6 BEARING RESISTANCE OF ROCK

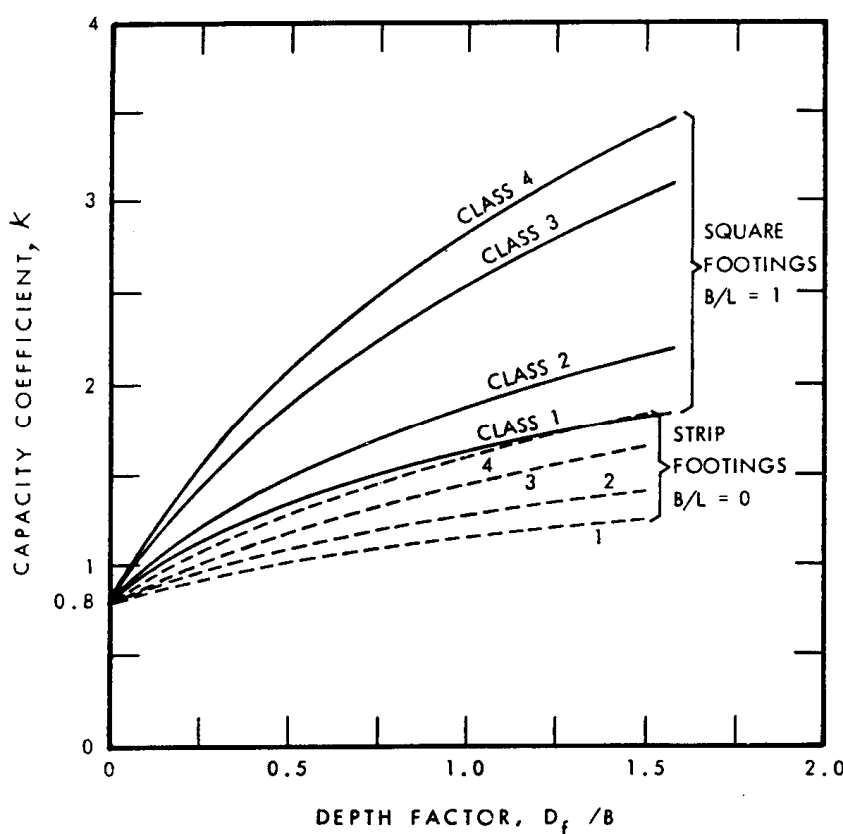
Geotechnical Considerations

The bearing capacity and settlement of footings on rock is influenced by the presence, orientation, and condition of discontinuities, weathering profiles and other similar profiles as they apply at a given site, and the degree to which they must be considered in the analysis.

For footings placed on competent rock, reliance may be based on simple and direct analyses that have their origin in the uniaxial compressive strength and rock quality designation (RQD). Competent rock may be defined as a rock mass with tight discontinuities or with openings not wider than $1/8$ in. For footings on less competent rock, more extensive investigations are necessary to assess the effects of weathering, and the presence and condition of discontinuities.

Bearing Capacity

Competent rock. The allowable bearing (contact) pressure for footings on level surfaces of competent rock may be determined as proposed by Peck, Hanson, and Thornburn (1974), shown in Figure 8–10. The RQD used in these data should be the av-



Soil Type	Consistency or Density	$(P_f - P_o)(t/ft^2)$	Class
Clay	Soft to Very Firm	< 12	1
	Stiff	8-40	2
Sand and Gravel	Loose	4-8	2
	Very Dense	30-60	4
Silt	Loose to Medium	< 7	1
	Dense	12-30	2
Rock	Very Low Strength	10-30	2
	Low Strength	30-60	3
	Medium to High Strength	60-100	4

Figure 8-9 Values of empirical capacity coefficient, K (from Canadian Foundation Engineering Manual, 1985).

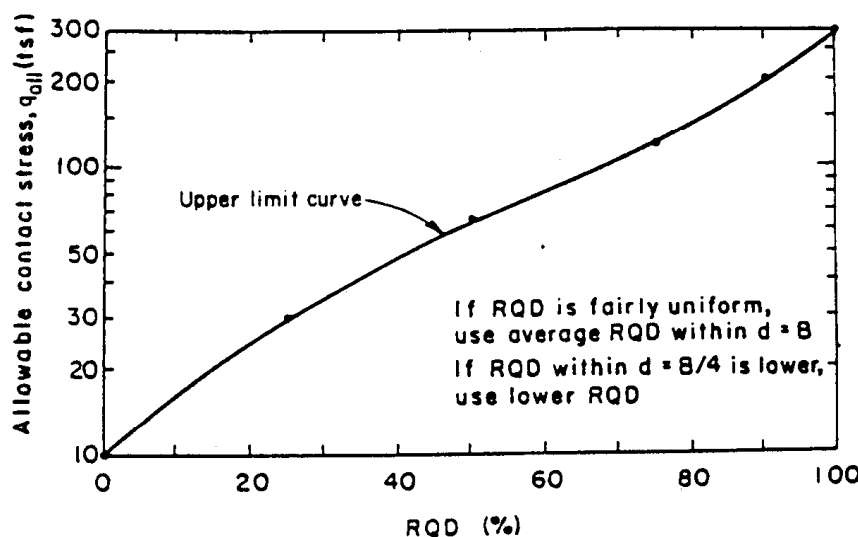


Figure 8-10 Allowable contact stress for footings on rock with tight discontinuities (from Peck *et al.*, 1974).

verage RQD for the rock within a depth of B below the footing level, if the RQD values are essentially uniform within that depth. If rock within a depth of $0.5B$ below the base of footing has a lower quality, the RQD of the less competent rock should be used in the analysis. The maximum allowable contact pressure should not exceed the allowable bearing stress in the concrete.

Broken or jointed rock. For footings on broken or jointed rock, the bearing resistance may be determined from empirical correlations with the Geomechanics Rock Mass Rating (RMR) proposed by the Norwegian Geotechnical Institute, Rock Mass Classification System (Barton, Lein, and Linde, 1974), and as developed by Carter and Kulhawy (1988) and modified by Hoek (1983). The procedure is based on the unconfined compressive strength of the intact rock core sample. Depending on rock mass quality, measured in terms of RMR or NGI systems, ultimate bearing capacity varies from a small fraction to six times the unconfined compressive strength of intact rock core samples.

Analytically, the ultimate bearing capacity of footing on broken or jointed rock may be estimated from the relationship

$$q_{ult} = N_{ms} C_o \quad (8-15)$$

where N_{ms} = a coefficient, and C_o = uniaxial compressive strength of intact rock. Values of N_{ms} are given in AASHTO Table 4.4.8.1.2A. Values of C_o should be determined from results of laboratory tests of rock core samples obtained within $2B$ of the base of footing. Where the rock strength within this depth zone varies, the rock with the lowest capacity should be used. Alternatively, AASHTO Table 4.4.8.1.2B may be used to determine C_o . If the rock is of poor quality, the value of q_{ult} should be determined as the value of q_{ult} of an equivalent soil mass.

8.7 FAILURE BY SLIDING

Failure of footings by sliding is essentially subject to the same considerations as the stability of walls against sliding discussed in section 6.6. For foundations in clay, the possible presence of a shrinkage gap between the soil and the foundation should be considered. If passive resistance is included as part of the solution to resist sliding, consideration should be given to possible future removal of the soil in front of the foundation. For footings on cohesionless soils, sliding resistance is influenced by the roughness of the interface between the foundation and the soil. Sliding will occur if the shear strength at any point of the assumed slip surface (commonly taken as the foundation-soil interface) is less than the shear stress applied on the same slip surface under service loads.

For footing on soils with $\phi-c$ characteristics, the sliding resistance is expressed in Equation (6-19) in section 6.6, and is rewritten here in a different form as

$$Q_R = Q \tan \delta + c_a B \quad (8-16)$$

where Q_R = resistance to sliding of the footing, and Q , δ , c_a , and B are as before. If the soil beneath the foundation is sand and the base of the footing is rough (this is the usual case for concrete placed directly on soil), the full shear resistance of the soil will be mobilized so that $\tan \delta = \tan \phi$. For precast concrete footings, the coefficient of friction may be taken as $\tan \delta = 0.8 \tan \phi$, since in this case the footing will be relatively smooth.

If the foundation soil is clay, consideration should be given to the possibility of sliding by shear within a zone of clay beneath the footing, if this is a weaker plane. The sliding resistance in this case may be taken as the lesser of (1) the cohesion of the clay, or (2) one-half the normal stress on the interface between footing and soil. If the concrete is wet, the cohesion of the clay may be reduced to $0.5 + 0.7$ times the undrained shear strength.

8.8 AASHTO AND LRFD REQUIREMENTS

AASHTO Requirements (Standard Specifications)

Footing excavations. In granular soils with relatively high permeability, footing excavations below the groundwater table should be made such that the hydraulic gradient in the excavation bottom is not increased to a level that could cause loosening or softening of the soil because of upward water flow. Furthermore, the excavations should be made such that hydraulic gradients and the removal of material has no adverse effect on adjacent structures.

Footing excavations in nonresistant, weathered moisture-sensitive rocks should be protected immediately after excavation with a lean concrete mix or other suitable materials.

Anchorage. Where footings are placed on inclined smooth rock surfaces that are not restrained by an overburden of resistant material, they should be anchored using rock anchors, bolts, dowels, keys, benching, or other suitable means. Shallow keys or benching of large footing areas should not be provided where rock removal may require blasting.

Eccentricity. In order to keep the footing pressure as uniform as possible, AASHTO stipulates that the location of resultant of pressure R on the base of the footing should be maintained preferably within $x/6$ of the footing dimension x in any direction. This criterion does not relate to the bearing capacity of the soil, but is rather intended to ensure as uniform a settlement as possible.

Factors of safety. Spread footings on soil should be designed for Group I (ASD) loading with a minimum factor of safety of 3.0 against a bearing capacity failure. The same criterion applies for spread footing on rock.

Dynamic ground stability. AASHTO articulates the requirements of design for dynamic ground stability by referring to the specifications for seismic analysis.

Footings on rock. Spread footings on rock should be designed to support the design loads with adequate bearing and tolerable settlement. The location of the resultant pressure R on the base of the footing should preferably be within $B/4$ of the center of the footing.

LRFD Specifications

Service limit states. Service limit states for foundation design include (a) settlements, (b) lateral displacements, and (c) bearing resistance estimates from presumptive bearing pressures. The limit state for settlement should be based on rideability and economy, where the cost of limiting foundation movement is compared to the cost of designing the superstructure so that it can tolerate larger movement, or to the cost of correcting the consequences of movement through maintenance.

Strength limit states. These include (1) bearing resistance failure, (2) excessive loss of contact, (3) sliding at the base of footing, (4) loss of overall stability, (5) structural capacity, and (6) loss of lateral support.

Foundations should be proportioned such that the factored resistance is not less than the effects of factored loads specified in other sections (see also Tables 2–18 and 2–19). For expediency, we repeat the design equation for LRFD as follows:

$$\phi R_n \geq \sum_i Q_i \quad (8-17)$$

It should be noted that the tables for load factors do not list recommended values for γ or β for water pressure. If the water pressure is evaluated for the worst possible water level, it seems reasonable to use unfactored water calculations in LRFD analyses.

At present, load factor (strength design) methods for foundation analysis and design are not provided for in the standard AASHTO specifications. Although this excludes direct correlation between the two documents, the LRFD load and resistance factor approach may be used in conjunction with AASHTO loads and loading groups.

Resistance factors. Resistance factors for shallow foundations (footings) at both strength and service limit states are given in Table 8–7. Where statistical information was available, reliability theory combined with judgment was used to derive these values. In cases where there was insufficient information for calibration using reliability theory, values of resistance factors were chosen based on judgment so that design based on LRFD can be consistent with ASD procedures.

Table 8–7 Resistance Factors for Strength Limit State for Shallow Foundations, LRFD Specifications

	Method/Soil/Condition	Resistance Factor
Bearing Capacity and Passive Pressure	Sand <ul style="list-style-type: none"> – Semi-empirical procedure using SPT data – Semi-empirical procedure using CPT data – Rational Method— <ul style="list-style-type: none"> using ϕ_f estimated from SPT data using ϕ_f estimated from CPT data 	0.45 0.55 0.35 0.45
	Clay <ul style="list-style-type: none"> – Semi-empirical procedure using CPT data – Rational Method <ul style="list-style-type: none"> using shear resistance measured in lab tests using shear resistance measured in field vane tests using shear resistance estimated from CPT data 	0.50 0.60 0.60 0.50
	Rock <ul style="list-style-type: none"> – Semi-empirical procedure, Carter and Kulhawy (1988) 	0.60
	Plate Load Test	0.55
Sliding	Precast concrete placed on sand <ul style="list-style-type: none"> using ϕ_f estimated from SPT data using ϕ_f estimated from CPT data 	0.90 0.90
	Concrete cast-in-place on sand <ul style="list-style-type: none"> using ϕ_f estimated from SPT data using ϕ_f estimated from CPT data 	0.80 0.80
	Sliding on clay is controlled by the strength of the clay when the clay shear is less than 0.5 times the normal stress, and is controlled by the normal stress when the clay shear strength is greater than 0.5 times the normal stress (see Figure 1, which is developed for the case in which there is at least 6.0 IN of compacted granular material below the footing).	
	Clay (where shear resistance is less than 0.5 times normal pressure) <ul style="list-style-type: none"> using shear resistance measured in lab tests using shear resistance measured in field tests using shear resistance estimated from CPT data 	0.85 0.85 0.80 0.85
	Clay (where the resistance is greater than 0.5 times normal pressure)	
	Soil on soil	1.0
	Passive earth pressure component of sliding resistance	0.50
Overall Stability	Where soil or rock properties and groundwater levels are based on laboratory or in-situ testing, shallow foundations on or near a slope evaluated for overall stability and resistance to a deep-seated failure mode	0.85

8.9 SETTLEMENT OF FOOTINGS IN SOIL, METHODS OF ANALYSIS

The Settlement Problem

The settlement of bridge foundations is particularly relevant since it will affect function and rideability as well as structural performance. The design of footings must, therefore, address two issues: (1) estimate the amount of settlement that the structure can tolerate, and (2) predict the amount of settlement that the footing will undergo as a result of loading the soil.

Soil settlement computations are, with the exception of occasional successful predictions, only best estimates of deformation expected to occur when the loads are applied. During the settlement process, the soil undergoes a transition from its initial body to a new state of stress under the additional load. The stress increment Δq produces a time-dependent accumulation of particle rolling, sliding, crushing, and elastic distortions in the soil system within a limited influence zone beneath the loaded area.

The principal components of the vertical movement are particle rolling and sliding producing a change in the void ratio, crushing that alters the material, and elastic deformation (usually a small fraction). As a result, if the applied stress is removed, only a little portion of the settlement will be recovered as elastic rebound. It is however, convenient to treat the soil as a pseudoelastic material to estimate settlements, an approach that appears reasonable since larger stress changes produce larger settlements.

Settlements may be classified as (1) immediate, or those that take place as the load is applied or shortly thereafter; and (2) consolidation, that occurs as time dependent over a period of months or years. Alternatively, and for the purpose of analysis, the total settlement may be considered as the sum of elastic, consolidation, and secondary components, and may be determined from

$$S_t = S_e + S_c + S_s \quad (8-18)$$

where S denotes settlement and the subscripts t , e , c , and s denote total, elastic, consolidation and secondary, respectively. Note the Equation (8-18) is also AASHTO Eq. (4.4.7.2-1).

Elastic settlement should be determined using the unfactored dead load plus the unfactored live and impact load assumed to extend to the footing level. Consolidation and secondary settlement may be estimated using the unfactored dead load only.

Approximate stress distribution in soil mass. Figure 8-11 shows an assumed pressure distribution due to the load Q introduced by a footing. The notation corresponds to the same symbols shown in Figure 8-5. There are several methods currently used to estimate the increased pressure at some depth below the loaded area, and a simple procedure is to assume the 2:1 slope as shown in Figure 8-11. If the stress zone is defined in this manner the pressure increase $q_u = \Delta q$ at depth z due to load Q is

$$q_u = \frac{Q}{(B+z)(L+z)} \quad (8-19)$$

which for a square footing is reduced to

$$q_u = \frac{Q}{(B+z)^2} \quad (8-20)$$

This approximation will give satisfactory comparisons with theoretical predictions from $z = B$ to about $4B$, but should not be used in the depth zone $z = 0$ to B .

Settlement of Footings in Sand from Standard Penetration Tests

Terzaghi and Peck procedure. This method, developed by Terzaghi and Peck (1967) has been widely used but is considered conservative in the sense that it often overestimates settlement. Recent studies by Tan and Duncan (1991) show that in many instances settlements estimated using the Terzaghi-Peck method are larger than the ac-

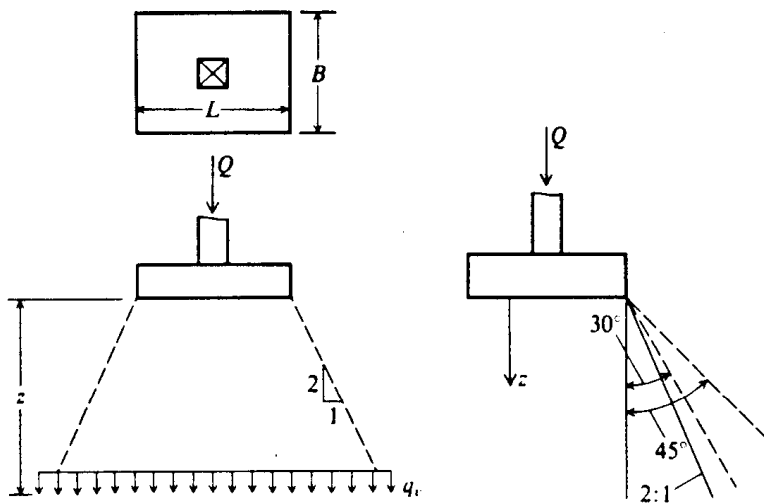


Figure 8-11 Approximate methods of obtaining the stress increase q_r in the soil at a depth z beneath the footing.

tual settlements. It appears that this method is reliable in the sense that it seldom underestimates settlement, but at the same time the results are not highly accurate. Since settlements of footing in sand are usually erratic, it follows that procedures that seldom underestimate settlements will tend to give overestimations. This approach, however, is often taken as a convenient compromise between accuracy and reliability.

The Terzaghi-Peck method may be used in the graphical form shown in Figure 8-12. The graphs are derived from the assumption of 1-in tolerable settlement. For a given width of footing and SPT blow count, the bearing pressure is obtained directly from the charts, and corresponds to 1-in settlement. If settlements other than 1-in provide the design criterion, the corresponding bearing pressures can be estimated by noting that settlements are very nearly proportioned to bearing pressures.

The value of N used in estimating the bearing pressure from these graphs should be the average value measured in all borings, within the range of depth from the footing base equal to B = footing width. Figure 8-12 can be used directly when the groundwater table is at a depth below the bottom of footing at least $2B$. For higher groundwater levels, the bearing pressure obtained from Figure 8-12 should be reduced as follows: (1) for shallow foundations with $D_f/B < \frac{1}{2}$, the pressures should be reduced by 50 percent; (2) for deeper foundations with $D_f/B = 1$, the pressures should be reduced by 30 percent.

If the groundwater level is between a depth $2B$ and the ground surface, the bearing pressure should be reduced by an amount between zero and 50 percent for shallow footings ($D_f/B < \frac{1}{2}$); for deeper foundations ($D_f/B \approx 1$) the bearing pressure should be reduced by an amount between zero and 30 percent.

According to Bazaraa (1967), the relationship between bearing pressure p_q , footing width B and N values may be expressed analytically as

$$p_q = p_s \frac{N}{3} \left(\frac{B+1}{2B} \right)^2 \quad (8-21)$$

where p_q = bearing pressure corresponding to a given magnitude of settlement; p_s = settlement (in), and B = footing width (ft). Pressures calculated from Equation (8-21) should likewise be reduced for groundwater effects.

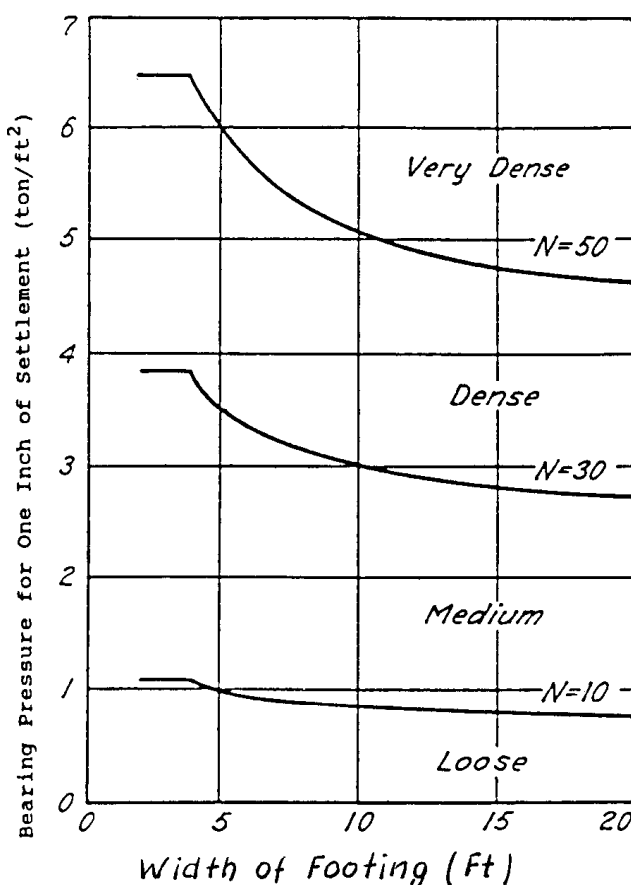


Figure 8-12 Bearing pressure for one inch of settlement of footings on sands (from Terzaghi and Peck, 1967).

Example. The minimum average N at a bridge site is 12. For a column footing with $B = 11$ feet, the bearing pressure corresponding to one-inch settlement is found graphically from Figure 8-12 as 1.0 ton/ft² if groundwater effects are absent. If the groundwater table can rise to the ground surface and the footing is shallow ($D_f < 5.5$ ft), the bearing pressure corresponding to one-inch settlement is 50 percent less, or 0.5 ton/ft². The bearing pressure causing a three-inch settlement should be about 2.0 tons/ft² if groundwater effects are not present, and about 1.0 ton/ft² with the water table at the surface.

D'Appolonia method. This method (D'Appolonia, D'Appolonia, and Brisette, 1970) uses the SPT blow count, but it is also based on elastic theory. The N values are used to estimate in situ soil compressibility. For footings on sand, the settlement is found from

$$p_s = \mu_0 \mu_1 \frac{p_a B}{M} \quad (8-22)$$

where p_s = settlement of footing (same length units as B); μ_0, μ_1 = settlement influence factors that depend on footing geometry, embedment depth, and depth to the relatively incompressible layer (dimensionless); p_a = average applied pressure under service loads; B = footing width; and M = modulus of compressibility.

Values of μ_0 and μ_1 are given in Figure 8-13. The modulus of compressibility M and the average SPT blow count may be correlated by referring to Figure 8-14. The value of SPT blow count used to estimate M is the average value within the range of

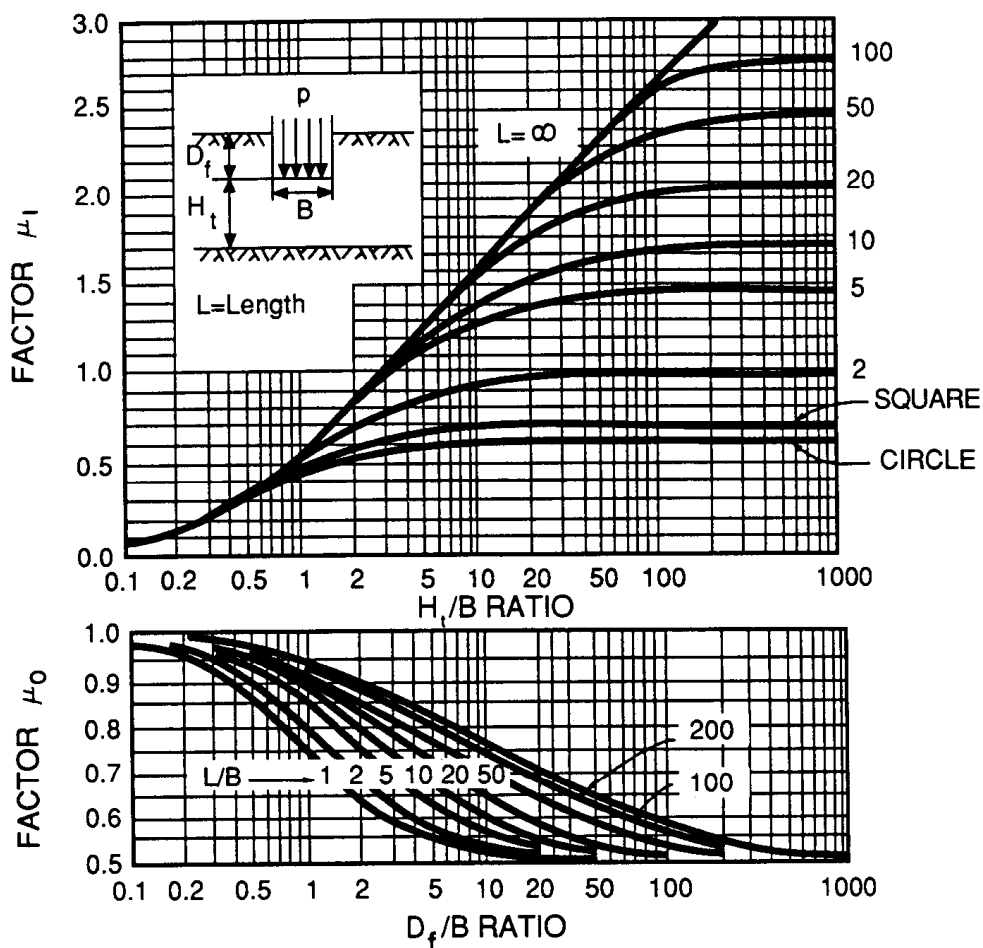


Figure 8-13 Settlement influence factors μ_0 and μ_1 for the D'Appolonia procedure (from D'Appolonia et al., 1970).

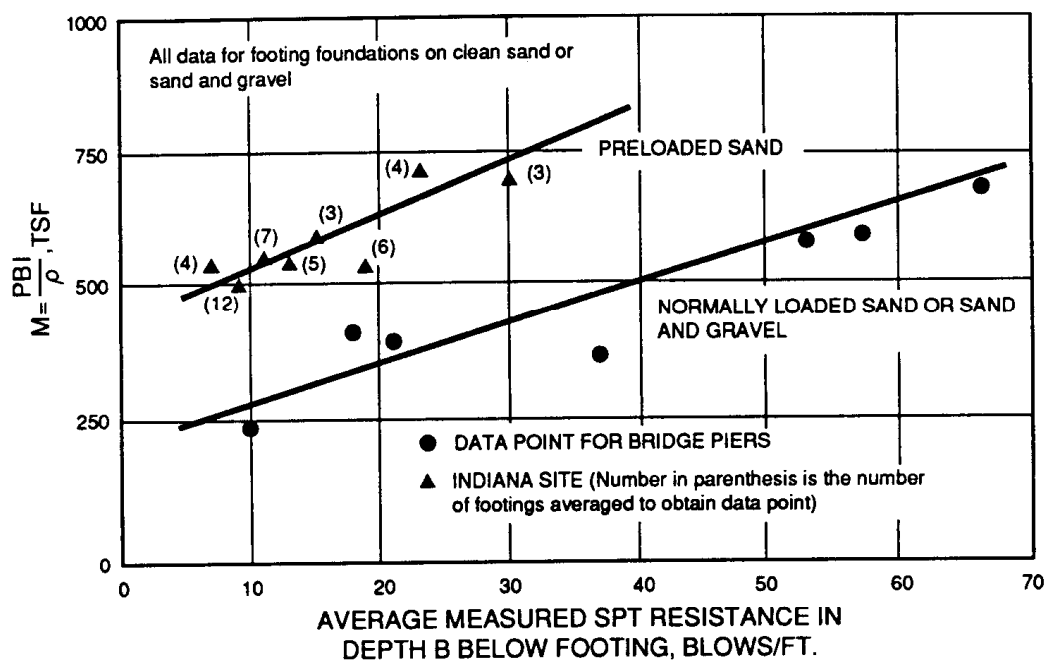


Figure 8-14 Correlation between modulus of compressibility and average value SPT blow count (from D'Appolonia et al., 1970).

depth from the footing level to depth B below that level. These investigators tend to agree with Meyerhof (1953, 1956, 1957) that the effect groundwater presence on soil modulus is reflected in the measured SPT blow count, hence no correction for groundwater effect is necessary.

Equation (8–22) can be rearranged to give the bearing pressure p_a in terms of a given settlement p_s , or

$$p_a = \frac{1}{\mu_0 \mu_1} \frac{p_s M}{B} \quad (8-23)$$

where all symbols are as previously.

The validity of the D'Appolonia method appears to be confirmed in studies reported by Tan and Duncan (1991), particularly with respect to the level of accuracy provided. More explicitly, the average settlements estimated using this method were about equal to the average values of actual settlements observed for a large number of footings.

Settlement of Footings in Sand from Cone Penetration Tests

Estimates of settlements of footings in sand using cone penetration test results may be made as proposed by Schmertmann (1970, 1977) who has also developed methods for computing elastic settlements. The CPT method has a rational basis, and uses the cone penetration resistance q_c as a measure of in situ soil compressibility.

The expression for calculating settlement of footings in sand is

$$p_s = C_p C_t \Delta p \Sigma \left(\frac{I_z}{E_s} \Delta Z \right) \quad (8-24)$$

where p_s = settlement; C_p = pressure change correction factor for initial overburden pressure (Table 8–8); C_t = time rate factor (or creep correlation factor), from Table 8–9; Δp = net increase in bearing pressure at foundation level; I_z = settlement influence factor that varies with depth and L/B ratio (from Figure 8–15 and Table 8–10); E_s = in situ soil modulus; and ΔZ = thickness of sublayer. The in situ modulus can be correlated with the value of cone resistance q_c .

Figure 8–15 shows the variation of settlement influence factor I_z with depth. The

Table 8–8 Pressure Change Correction Factor, C_p

$\frac{\sigma_{vo}'}{\Delta p}$	C_p
0.0	1.0
0.2	0.9
0.4	0.8
0.6	0.7
0.8	0.6
≥ 1.0	0.5

Note: σ_{vo}' = initial vertical pressure at level of bottom of footing (in pressure units)

Δp = average net bearing pressure at foundation level (same pressure units as σ_{vo}')

Table 8-9 Time Rate Factor, C_t for Settlements of Cohesionless Soils

Time	c_t
1 month	1.0
4 months	1.1
1 year	1.2
3 years	1.3
10 years	1.4
30 years	1.5

values of the parameters that define the dimensions of the settlement influence diagrams are given in Table 8-10.

For square footings, the in situ soil modulus E_s may be estimated from the expression

$$E_s = 2.5 q_c \quad (8-25)$$

where q_c = cone penetrating resistance

For footings with $L/B \geq 10$ the soil deforms in a condition closer to plane strain, and the soil is stiffer because of the increased confinement. For these long footings the expression for estimating E_s is

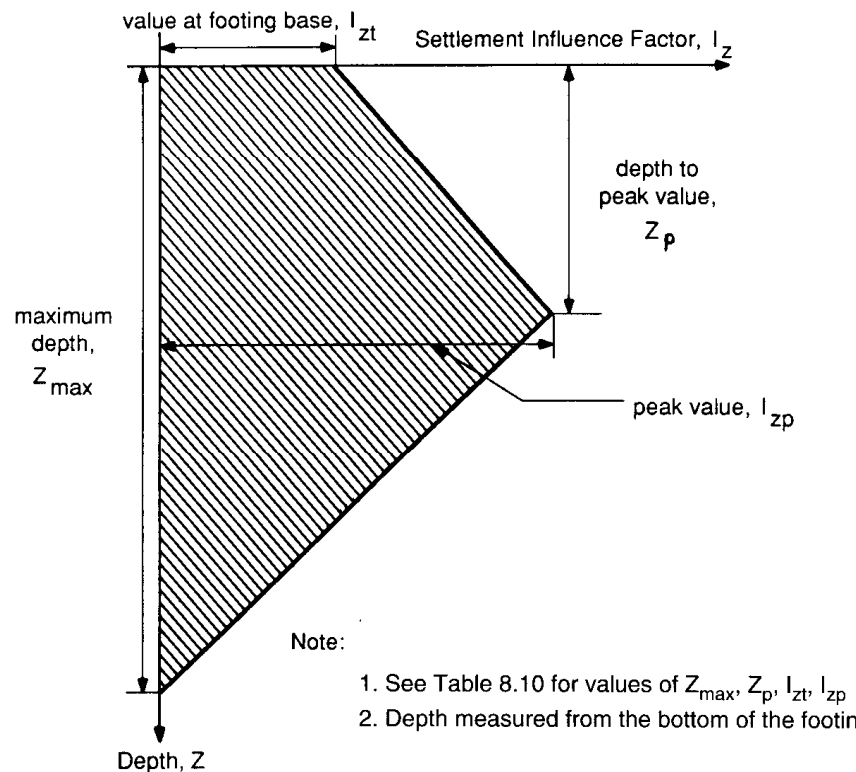


Figure 8-15 Variation of Schmertmann's improved settlement influence factors with depth (from Schmertmann et al., 1977).

Table 8–10 Coefficients to Define the Dimensions of Schmertmann's Improved Settlement Influence Factor Diagram in Figure 8–15

L/B	Max. Depth of Influence Z_{max}/B	Depth to Peak Value Z_p/B	Value of I_Z at top I_{Zt}	Peak Value of Stress Influence Factor I_{Zp}			
				$\frac{\Delta p}{\sigma_{vp}} = 1$	$\frac{\Delta p}{\sigma_{vp}} = 2$	$\frac{\Delta p}{\sigma_{vp}} = 4$	$\frac{\Delta p}{\sigma_{vp}} = 10$
1	2.00	0.50	0.10	0.60	0.64	0.70	0.82
2	2.20	0.55	0.11	0.60	0.64	0.70	0.82
4	2.65	0.65	0.13	0.60	0.64	0.70	0.82
8	3.55	0.90	0.18	0.60	0.64	0.70	0.82
≥ 10	4.00	1.00	0.20	0.60	0.64	0.70	0.82

Note: B = footing width

L = footing length

$\Delta p = \sigma_{vf}' - \sigma_{vo}'$ = net bearing pressure

σ_{vf}' = final vertical pressure at level of bottom of footing

σ_{vo}' = initial vertical pressure at level of bottom of footing

σ_{vp} = initial vertical pressure at depth of peak influence

(From Schmertmann, et al., 1977).

$$E_s = 3.5 q_c \quad (8-26)$$

For footings with L/B ratios between 1 and 10, the $E_s - q_c$ relationship may be estimated by interpolation.

The foregoing method can account for the variation in sand density and compressibility with depth. If the ground stratigraphy is heavily layered, the soil beneath the foundation level is divided into several sublayers, chosen so that the values of cone resistance within each sublayer are essentially constant. The value of the settlement influence factor for each sublayer is evaluated at midheight of the sublayer. Since the value of settlement influences factor peaks at some depth below the foundation level Z_p , it is necessary that a sublayer boundary occurs at Z_p .

The computational procedure is rather lengthy and warranted only when the site is characterized by extensive layering. If the soil profile shows sand layers of limited thickness overlying firm soil or rock, the influence diagram is terminated at the top of the firm layer. For homogeneous soil, the process is simplified since it is not necessary to divide the soil profile into sublayers. For homogeneous conditions, the settlement may be computed as follows

$$p_s = I' C_p C_t \left(\frac{\Delta p}{q_c} \right) B \quad (8-27)$$

where I' = equivalent settlement influence factor from Table 8–11, and other terms are as previously.

By rearranging Equation (8–27), we can obtain an expression for estimating the pressure required to cause a given settlement, or

$$\Delta p = p_s \frac{q_c}{BI'} \frac{1}{C_p C_t} \quad (8-28)$$

This expression is convenient if the tolerable settlement is known and it is necessary to estimate the corresponding bearing pressure.

Table 8–11 Values of Equivalent Settlement Influence Factor

L/B	Equivalent Settlement Influence Factor, I'			
	$\frac{\Delta p}{\sigma_{vp}} = 1$	$\frac{\Delta p}{\sigma_{vp}} = 2$	$\frac{\Delta p}{\sigma_{vp}} = 4$	$\frac{\Delta p}{\sigma_{vp}} = 10$
1	0.25	0.27	0.29	0.34
2	0.27	0.28	0.31	0.36
4	0.30	0.32	0.35	0.40
8	0.35	0.37	0.40	0.46
≥ 10	0.37			

The Tangent Modulus (Janbu) Method for Settlement of Footings in Sand, Silt, and Clay

Janbu (1963, 1967) has developed an approach for estimating settlement of footings in soils using tangent modulus values to articulate soil compressibility. The soil beneath the footing is divided into a number of sublayers, each characterized by a value of constraint tangent modulus M_t . The settlement is estimated as the sum of reductions in thickness of each of the sublayers, and is expressed as

$$p_s = \Sigma \left(\frac{\Delta \sigma' v}{M_t} \cdot \Delta Z \right) \quad (8-29)$$

where p_s = settlement; $\Delta \sigma'_v$ = increase in effective stress with the sublayer due to footing load; M_t = tangent value of constrained modulus of the soil; and ΔZ = sublayer thickness.

The constrained tangent modulus will vary with the soil type, its density, whether it is normally consolidated or overconsolidated, and the stress history before and after the load is applied. Values of M_t can be obtained in conventional laboratory tests (Tan and Duncan, 1991). The pressures used in these tests should cover the range from the initial pressure (before the load is applied) to the final pressure (with the load applied). The parameter M_t is determined by dividing the stress increment in the sublayer, $\Delta \sigma'_v = \sigma'_{vf} - \sigma'_{vo}$, by the corresponding strain $\Delta \epsilon'_v$, as shown in Figure 8–16. When laboratory tests are not contemplated for estimating M_t , good values may be obtained from Table 8–12 in conjunction with the following expressions:

For sands and silts, values of M_t may be estimated from

$$M_t = mp_{at} \left(\frac{\sigma'_{va}}{p_{at}} \right)^{0.5} \quad (8-30)$$

where m = dimensionless modulus number shown in Table 8–12; σ'_{va} = average vertical stress = $1/2(\sigma'_{vo} + \sigma'_{vf})$; and p_{at} = atmospheric pressure.

For normally consolidated clays, values of M_t may be estimated from

$$M_t = m\sigma'_{va} \quad (8-30a)$$

where m = dimensionless modulus number shown in Table 8–12, and σ'_{va} = average vertical stress as previously.

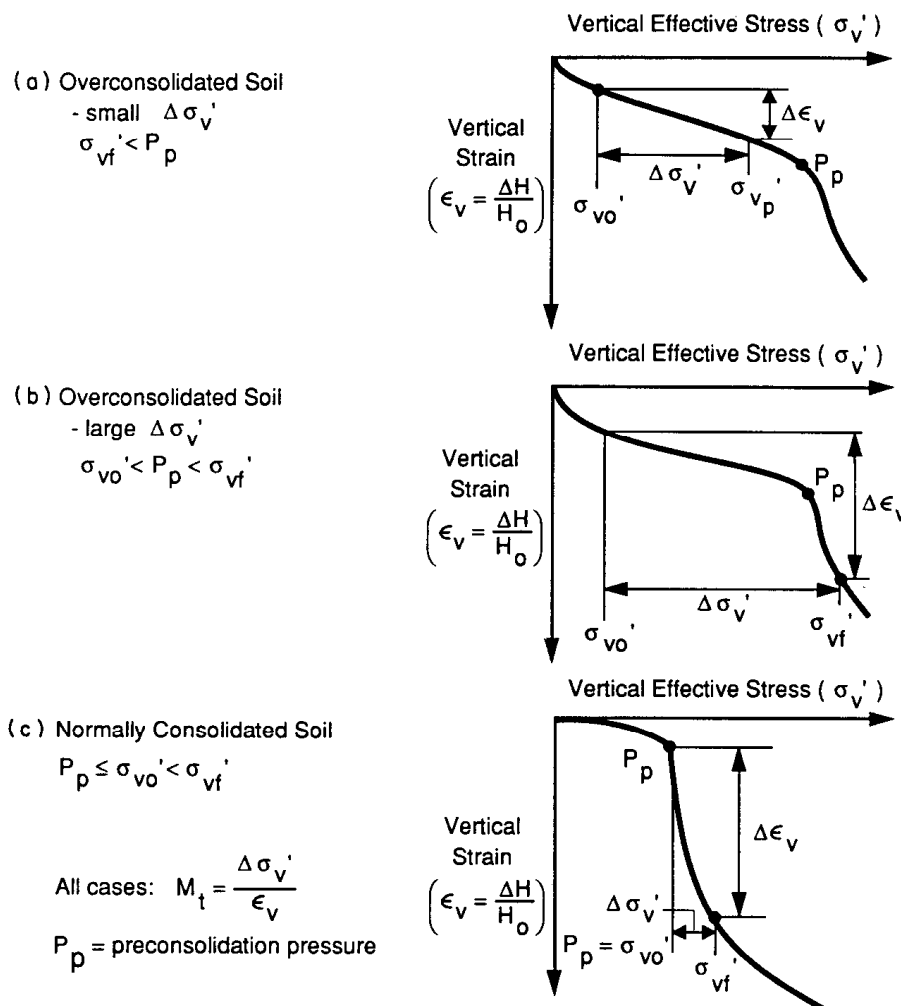


Figure 8-16 Determination of M_t from results of laboratory consolidation tests.

From Figure 8-16 and Table 8-12 it is apparent that values of M_t are higher for overconsolidated soils ($p_p > \sigma_{vo}'$). When the final pressures do not exceed the preconsolidation pressure ($\sigma_{vf}' < p_p$), the soil is being reloaded and the value of M_t is higher than where $\sigma_{vf}' < p_p$.

Settlement of Footings in Soil By Elastic Methods

Since the elastic settlement is essentially

$$\Delta H = \int_0^H \epsilon_i (dh) = \sum_{i=1}^n \epsilon_i H_i \quad (8-31a)$$

where ϵ_i = strain at layer H_i , any method that gives the strain in the appropriate sub-layer may be used to estimate settlement.

Steinbrenner (1934) and Giroud (1972) have proposed the following equation for estimating settlement

Table 8-12 Values of Modulus Number, m, for Sands, Silts, and Clays

Sand	Relative Density (Dr)	Value of m		
		$\sigma_{vo}' = p_p$	$\sigma_{vo}' < p_p < \sigma_{vf}'$	$\sigma_{vf}' < p_p$
	30% (Loose)	80–160	120–300	240–500
	50% (Medium)	120–240	200–400	350–700
	70% (Dense)	200–400	300–700	600–1200
Silt	Porosity (N)	Values of m		
		$\sigma_{vo}' = p_p$	$\sigma_{vo}' < p_p < \sigma_{vf}'$	$\sigma_{vf}' < p_p$
	50%	25–50	40–200	120–240
	40%	60–120	80–400	300–600
	30%	100–200	150–700	500–1000
Clay	In Situ Water Content	Value of m		
		$\sigma_{vo}' = p_p$	$\sigma_{vo}' < p_p < \sigma_{vf}'$	$\sigma_{vf}' < p_p$
	70%	6–12	10–80	60–120
	50%	9–18	15–120	90–180
	30%	15–35	25–200	150–350

p_p = preconsolidation pressure = highest pressure to which the soil has been subjected in the past.

(From Janbu, 1985).

$$p_f = \frac{p_b B}{E_s} I_p \quad (8-32)$$

where p_f = final (elastic) settlement; p_b = average bearing pressure; E_s = in situ soil modulus; I_p = dimensionless settlement influence factor depending on footing geometry, thickness of compressible layer, and Poisson's ratio; and B = width of footing. For estimating settlement of footings in sand and clay for drained conditions, Poisson's ratio ν may be taken as 0.3. In this case values of I_p for $\nu = 0.3$ may be taken from the graphs of Figure 8-17. The accuracy of this method depends on the accuracy with which the soil modulus is estimated. If settlement observations on similar soils are available, the soil modulus can be back-calculated from these data.

Another method is proposed by Schmertmann (1970) where the change in the Boussinesq pressure bulb (see AASHTO Fig. 4.4.7.2.1A) is interpreted as related to strain. Since the pressure bulb changes more rapidly from about 0.4 to 0.6B, this depth range is interpreted to have the largest strains. The same investigator also proposed using a triangular relative-strain diagram to model this strain distribution with ordinates 0.06 and 0 at B , $0.5B$, and $2B$. The area of the diagram is correlated with the settlement, and for constant E_s the settlement may be computed directly as the area of the triangle times the strain, or

$$\Delta H = 0.6B \frac{\Delta q}{E_s} = 0.6B \epsilon \quad (8-33)$$

where all symbols correspond to the notation of Equation (8-31). Schmertmann also incorporated two correction factors for embedment depth and time.

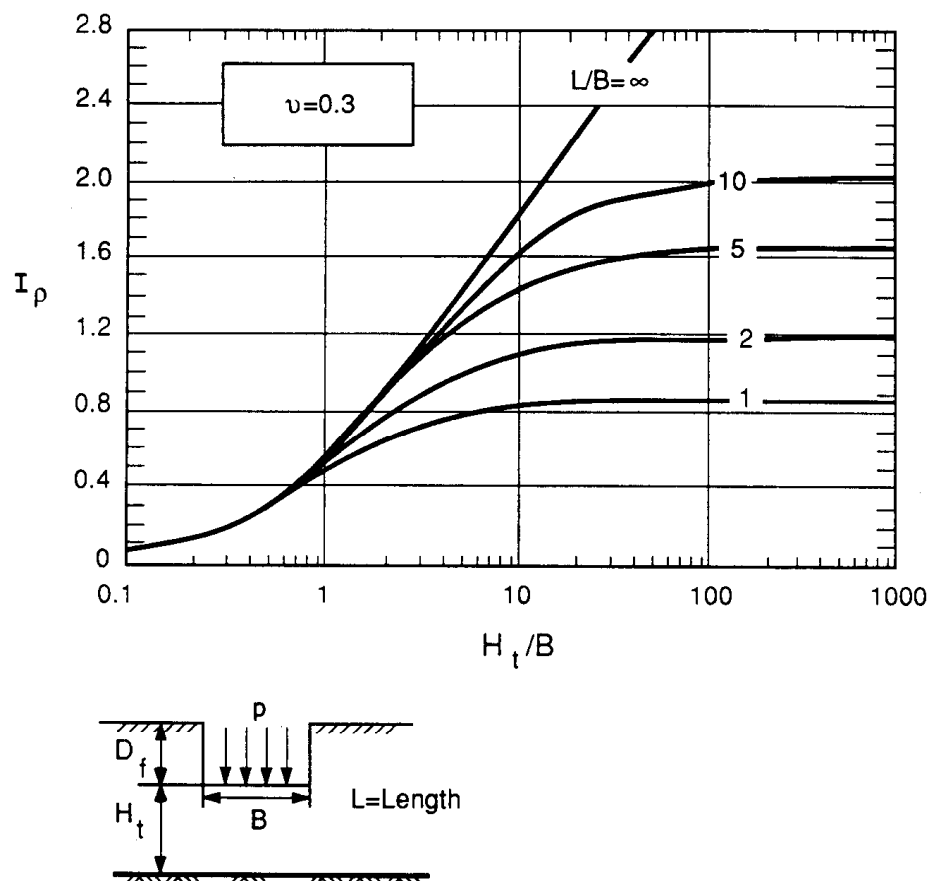


Figure 8-17 Settlement influence factor from Steinbrenner's approximation for $v = 0.3$ (from Taylor and Matyas, 1983).

Consolidation Settlement

Clays. Settlements resulting from consolidation of normally consolidated and lightly overconsolidated clays can be considerable. For fine-grained, saturated cohesive soils the settlement is time dependent; where such soils are loaded by fills, settlements as large as several feet may occur. Highly compressible clays are rarely suitable for bridge foundations since the tolerable settlement is usually limited to a small fraction of the anticipated settlement.

When consolidation theory is used to estimate settlement in clays, the following factors must be considered: (1) whether the clay is normally consolidated or preconsolidated ($OCR > 1$); (2) obtaining the in situ void ratio e_o and sufficient compression indices to profile the clay layers; and (3) estimating the average stress increase Δq in a layer of thickness H . These considerations are refined in the current AASHTO procedures for estimating settlement of footings on saturated or nearly saturated cohesive soils, and address initially overconsolidated soils, or initially normally consolidated soils. A distinction is also made between laboratory test results expressed in terms of the void ratio, or in terms of vertical strain.

Time dependent settlement in sand. Footings in sand continue to settle but at a slow and decreasing rate. The time rate factor is included in Schmertmann's method, and is

identified in Equations (8–24) and (8–27). A similar allowance for increased settlement with time may be used with other methods. A general expression in this case is

$$p_{st} = p_{si}C_t \quad (8-34)$$

where p_{st} = settlement at time t ; p_{si} = settlement initially computed; and C_t = time rate factor obtained from Table 8–9.

Secondary Settlement

Footings in clay continue to settle at a slow and decreasing rate after the clay undergoes its initial compression. This process is termed secondary compression, and the associated settlement may be computed from

$$p_{sc} = C_a H_t \log \frac{t_{sc}}{t_p} \quad (8-35)$$

where p_{sc} = settlement due to secondary compression; C_a = coefficient of secondary compression (obtained from Table 8–13); H_t = total thickness of layer undergoing secondary compression; t_{sc} = time for which secondary compression is calculated; and t_p = time for primary compression (not less than one year). Equation (8–35) is essentially the same as AASHTO Eq. (4.4.7.2.4–1) but with a different notation.

Reliability of Settlement Analysis

The methods presented for estimating immediate (elastic) settlement of footings in soil may be used independently or as an adjunct to the procedures recommended by AASHTO. Factors that may influence settlement are embankment loading, lateral or eccentric loading, vibration loading from dynamic live loads or earthquakes, and so on.

For design purposes, consideration should be given to the total settlement expressed in Equation (8–18), and made up of elastic (immediate), consolidation, and secondary compression components. In cohesionless soils and unsaturated clays the immediate settlement predominates with perhaps some creep (secondary compression). Results of computations of immediate settlement may vary, but with some judgment these can converge to reasonably satisfactory predictions. Consolidation theory tends to predict settlement rather well, provided that representative soil samples are obtainable. However, the time rate for consolidation settlement is not well predicted, and this is because the coefficient of permeability is a significant factor.

Studies by Tan and Duncan (1991) have compared measured settlement with settlement calculated using the various procedures reviewed in the foregoing sections. These show that methods that result in settlements close to the average of measured

Table 8–13 Values of C_a for Clays

Natural Water Content of Clay	Value of C_a	
	For $OCR = 1$	For $OCR \geq 5$
10%	0.001	0.0003 to 0.0005
20%	0.002	0.0006 to 0.0010
40%	0.004	0.0012 to 0.0020
80%	0.008	0.0025 to 0.0040

Table 8-14 Values of Adjustment Factor for 50 Percent and 90 Percent Reliability in Displacement Estimates

Method	Soil Type	Adjustment Factor	
		For 50% Reliability	For 90% Reliability
Terzaghi and Peck	Sand	0.45	1.05
Schmertmann	Sand	0.60	1.25
D'Appolonia, et al.	Sand	1.00	2.00

(From Tan and Duncan, 1991).

values tend to underestimate settlements half the time and overestimate them half the time. Methods that are more conservative (namely the Terzaghi and Peck method) tend to overestimate settlements more than half the time and to underestimate them rather infrequently.

A relatively accurate method may be considered as one that results in estimated settlement about equal to the average settlement for a group of footings. A reliable method is one that predicts settlements that are greater than or equal to the actual settlement most of the time (Tan and Duncan, 1991). An analysis shows that any method for estimating settlements of footings on sand can be modified by applying an adjustment factor to yield about the same combination of accuracy and reliability as any other method.

Adjustment factors for 50 percent and 90 percent reliability in calculated values of settlement are given in Table 8-14 for the three methods reviewed in the foregoing sections. As an example, to ensure that the D'Appolonia method (that predicts settlements about equal to the average value of actual settlements and underestimating settlements half the time) gives values that are equal or exceed the measured settlement about 90 percent of the time, the computed settlements should be multiplied by a factor of 2. This adjustment would increase the reliability from about 50 percent to 90 percent.

8.10 SETTLEMENT OF FOOTINGS IN ROCK

Competent rock. If footings are founded on competent rock, the settlement would not be large enough to cause problems, generally of the order of one-half inch or less. Where elastic settlements of this magnitude cannot be tolerated, or where very large loads are to be applied, such as at abutments for arch bridges or very tall piers, an analysis of settlement considering the rock characteristics is indicated. For rock masses with time-dependent settlement behavior, the procedures used for footings in soil may be used.

Broken or jointed rock. In rock masses with seams or soft material, consolidation and secondary settlements may occur. For most other rock masses, the settlement will occur immediately, and its magnitude may be estimated from elastic theory. A general expression of the elastic settlement of footing on broken or jointed rock is

$$p_m = \frac{P(1 - v_m^2)}{\beta_2 E_m A^{0.5}} \quad (8-36)$$

where p_m = settlement of rock mass; P = applied load; v_m = Poisson's ratio for rock

mass; β_2 = shape and rigidity factor; E_m = Young's modulus for rock mass; and A = footing area. Using typical values of v_m and β_2 , Kulhawy (1978) proposed that for circular, square, and rectangular footings ($L/B \leq 3$), Equation (8-36) may be modified as follows:

$$p_m = \frac{0.9P}{E_m A^{0.5}} \quad (8-37)$$

When $L/B \geq 10$, Equation (8-36) becomes approximately

$$p_m = \frac{0.7P}{E_m A^{0.5}} \quad (8-38)$$

If P is expressed in terms of q_o and A ($P = q_o A = q_o BL$) and $A = BL$, Equation (8-36) is reduced to AASHTO Eq. (4.4.8.2.2-2). For rectangular footings with $3 \leq L/B \leq 10$, the settlement may be estimated by interpolation.

The accuracy of settlement predictions using elastic theory depends on the accuracy with which the parameter E_m is obtained. For unusual or poor rock conditions, it may be necessary to determine the modulus from in situ tests, such as plate loading and pressuremeter tests. The presence of rock fractures tends to give a smaller rock mass modulus than for intact rock. This difference is associated with the discontinuity spacing, which in turn can be correlated with RQD, as shown in Table 8-15. In order to use these data, the values of E_r (Young modulus of rock core sample) and K_n (normal stiffness of discontinuities) are determined from laboratory tests. Typical values of E_r/K_n ranging from 0.2 to 4.2 meters, with an average of 1.2 meters, may be used for preliminary purposes.

Special problems. Special problems may arise in conditions such as weathering of rock, solution cavities, swelling of rock, creep, and mining subsidence. These problems call for special design considerations or foundation treatment. In some instances, the

Table 8-15 Values of Modulus Reduction Factor, $a_E = E_m/E_r$

RQD (%)	Value of a_E for E_r/K_n *		
	0.1m	0.5m	1.0m
<10	0.22	0.06	0.03
20	0.35	0.10	0.05
30	0.40	0.13	0.06
40	0.44	0.15	0.08
50	0.46	0.16	0.09
60	0.50	0.18	0.11
70	0.53	0.20	0.12
80	0.56	0.22	0.14
90	0.70	0.30	0.18
100	0.92	0.75	0.60

*Note: E_r/K_n is in meters; and
 - E_r = Young's modulus for rock core sample
 - K_n = Normal stiffness for discontinuities
 - E_m = Young's modulus for rock mass
 - For $E_r/K_n \geq 10$, use equivalent soil modulus for analysis.

(From Kulhawy, 1978).

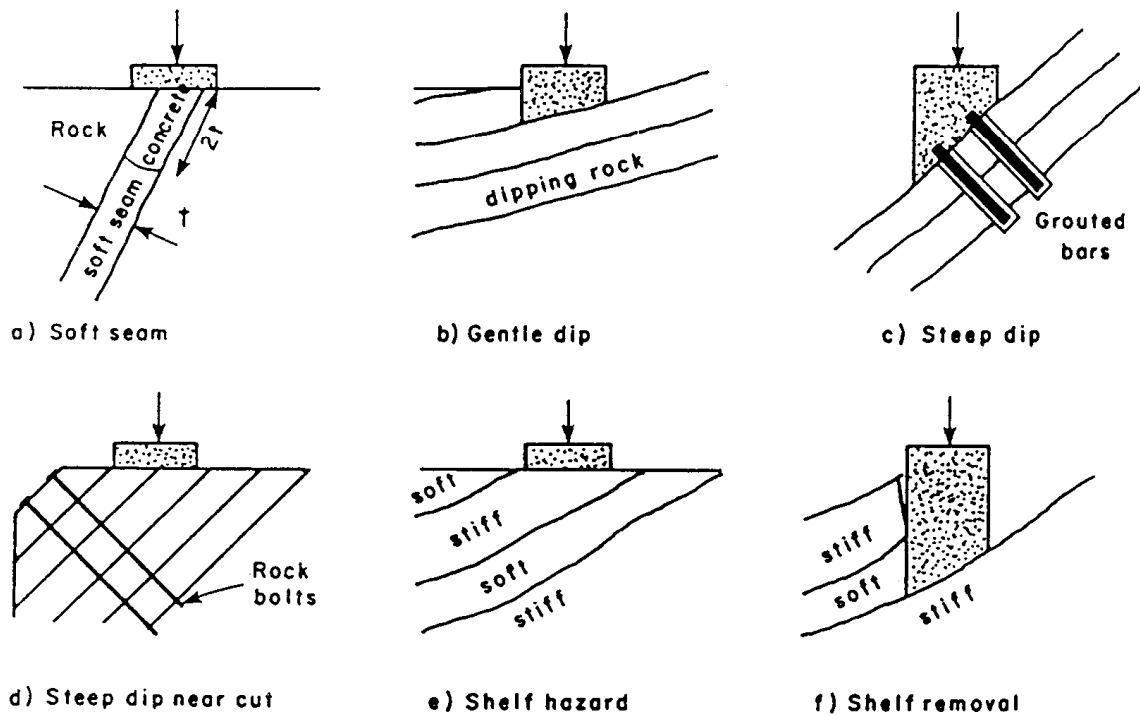


Figure 8-18 Rock foundation contact problems (*from Sowers, 1979*).

presence of sink holes in limestone make footing foundations impractical. A comprehensive review of these problems is given by Peck (1976).

Practical concerns relating to construction of footings in rock are:

1. Good contact between rock mass and foundation. If local defects are present, they may create special problems that will require special treatment. Typical contact problems with suggested solutions are shown in Figure 8-18. They include filling a narrow soft seam with dental concrete, anchoring footing on dipping rock surfaces with anchors or bolts, and avoiding obvious structural hazards by placing the foundation on the stiffer rock layer.
2. Effect of excavation on rock quality. Blasting often results in overbreak and fractures or opening of joints in the rock mass. Potential settlement problems can be avoided if the rock surface is properly cleaned, and fractured rock below the foundation is replaced with lean concrete or well-compacted gravel.

8.11 STRUCTURAL ACTION OF FOOTINGS

Gross and Net Soil Pressure

Figure 8-5 shows the design terminology for footing foundations, and the loads acting on the footing. If the footing thickness is t , the weight of soil above the footing is $\gamma(D_f - t)$ per unit area. With no column load, the only downward load is the weight of soil above the footing and the weight of the footing. This causes a soil pressure balanced by an equal and opposite upward reaction pressure of the same intensity. As a result,

the net effect on the concrete footing is zero. There are no moments or shears in the footing at this loading stage.

When a column load Q is added, the pressure under the footing increases by $q_n = Q/LB$. The total pressure now is the initial plus q_n . For calculating moments and shears in the footing, the initial pressure and its reactions are canceled out, leaving only the net pressure q_n to cause internal force effects in the footing.

Structural Requirements, Spread Footings

The design of a footing usually must consider bending, shear, development of reinforcement, and the transfer of load from a column or wall to the footing.

Flexure. Consider the square footing supporting a single given column shown in Figure 8–19. External moment on section A-A, taken at the face of the column, is caused by the net pressure q_n acting on an area bf . This is also the critical section for bending. If the column is now square or rectangular, the critical section should be taken at the face of the concentric square of equivalent area. If the footing is under a metallic column base, the critical section should be taken halfway between the column base and the edge of metallic plate.

Referring to Figure 8–19(a), the entire moment acting along section A-A is

$$M = (q_n bf) \frac{f}{2} \quad (8-39)$$

where $q_n bf$ is the resultant of the soil pressure on the hatched area and $f/2$ is the moment arm. This moment must be resisted by reinforcement placed at the bottom of the footing as shown in Figure 8–19(b).

In a similar manner, the soil pressure under the portion perpendicular to the direction A-A will cause a critical moment at the face of the column. This must be resisted by flexural reinforcement placed in a perpendicular direction at the bottom of the footing, resulting in two layers of steel, one each way. This reinforcement is distributed uniformly across the entire width of footing.

Consider now the rectangular footing shown in Figure 8–20 with dimensions b and l supporting a rectangular column as shown. The footing is under the action of a uniform net soil pressure q_n . In the long direction l , the moment due to q_n is taken along section B-B. This moment is

$$M_B = (q_n bf_b) \frac{f_b}{2} \quad (8-40)$$

The reinforcement in the bottom of the footing necessary to resist M_B is distributed uniformly across the entire width b . In the short direction b , the moment is taken along section A-A, and is

$$M_A = (q_n lf_a) \frac{f_a}{2} \quad (8-41)$$

The total reinforcement A_{st} required to resist M_A is distributed along the length l as follows:

Over a band width, centered on the center line of the column, equal to the length of the short side of the footing (width b), the portion of the reinforcement is

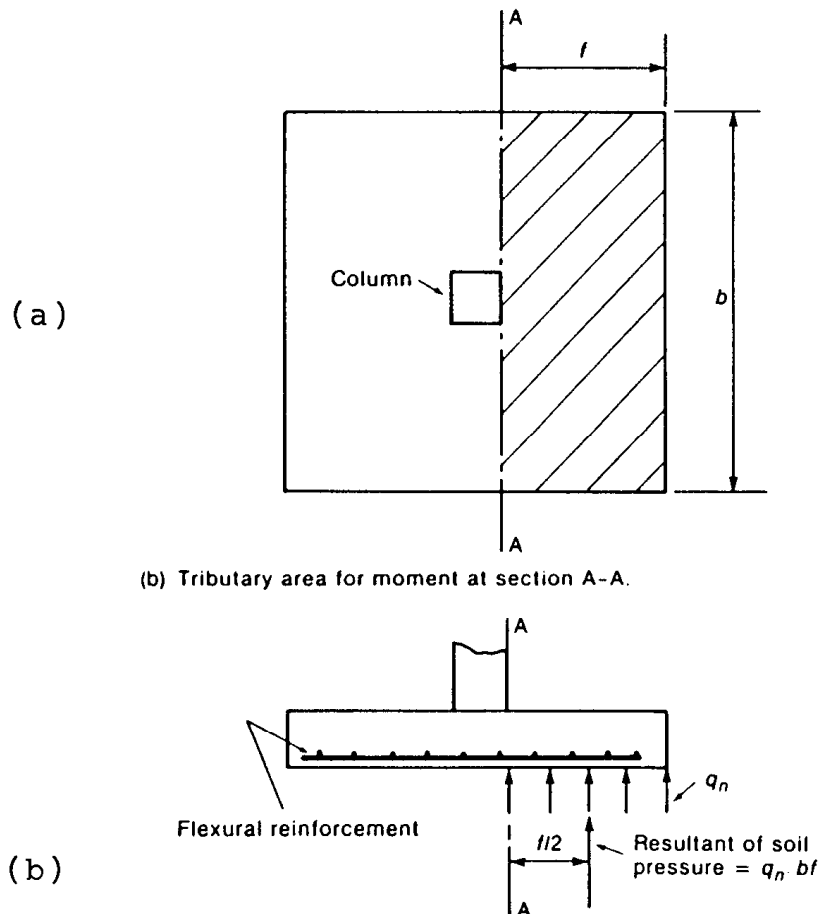


Figure 8-19 Flexural action of a spread footing. (a) Tributary area for moment at section A-A; (b) moment about section A-A.

$$A_1 = \frac{2A_{st}}{(B + 1)} \quad (8-42)$$

where $B = \text{ratio } l/b$. The remainder of reinforcement ($A_{st} - A_1$) required in the short direction is distributed uniformly outside the center band width of the footing.

Two-way shear. Referring to Figures 8-19 and 8-20, the footing is subjected to two-way or punching shear. The footing in this case may undergo shear failure, occurring suddenly with little, if any, warning. Once such a failure has taken place, the column may slide down the footing, with the reinforcing steel ripping out of its place, leaving no physical connection between the footing and the column. Thus, while a two-way footing possesses great ductility if it fails in flexure, it has no extra defense if it fails in shear. Quite frequently shear controls the footing thickness in bridge foundations.

Based on extensive tests, Moe (1961) concluded that the critical section for two-way shear is at the surface of the column. The ACI accepted this conclusion, but showed that a much simpler design equation could be derived by considering the critical section to be located at $d/2$ from the face of the column, where d is the effective depth. This simplification has been incorporated in the ACI Code and in the AASHTO specifications.

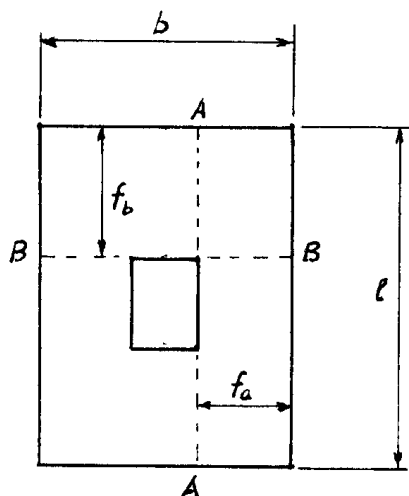


Figure 8-20 Flexural action in rectangular footing.

Thus, for the footings of Figures 8-19 and 8-20, the shear capacity is governed by two-way action, with a critical section located so that the perimeter b_o is a minimum, but not closer than $d/2$ to the perimeter of the concentrated load (i.e., face of column). This procedure is illustrated in Figure 8-21.

Design Shear Stress, Allowable Stress Design. The design shear stress may be computed from

$$v = \frac{v}{b_o d} \quad (8-43)$$

where v is the shear at the critical perimeter b_o , resulting from the net soil pressure on the portion shaded in Figure 8-22(a). The design shear stress v computed from Equation (8-43) should not exceed v_c given by

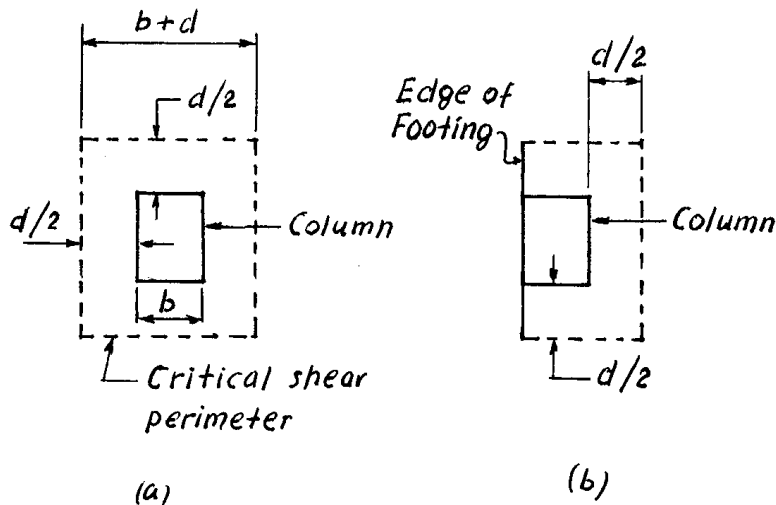


Figure 8-21 Location of critical shear perimeter; (a) interior column;
(b) exterior column.